USGS
science for a changing world

Heat as a tool for studying the movement of ground water near streams

Circular 1260

U.S. Department of the Interior
U.S. Geological Survey

Confluence of Case Creek with Champoeg Creek in the Willamette lowland of Oregon. Temperatures in sediments beneath channels like these provide information on losses and gains of surface water to and from ground water. Case Creek is one of six study sites in the Willamette Basin where thermal techniques were used to produce estimates of seepage losses to ground water (see Chapter 5).

Heat as a Tool for Studying the Movement of Ground Water Near Streams

EDITED BY

David A. Stonestrom

Jim Constantz

Circular 1260

U.S. Department of the Interior
U.S. Geological Survey

U.S. Department of the Interior
Gale A. Norton, Secretary

U.S. Geological Survey
Charles G. Groat, Director

U.S. Geological Survey,
Reston, Virginia: 2003

Available from U.S. Geological Survey, Information Services
Box 25286, Denver Federal Center
Denver, CO 80225
or
World Wide Web: http://pubs.water.usgs.gov/circ1260/

For more information about the USGS and its products:
Telephone: 1-888-ASK-USGS
World Wide Web: http://www.usgs.gov/

SBN 0-607-94071-9

Contents

Acknowledgments

The U.S. Geological Survey (USGS) Office of Ground Water and Water Resources Discipline's National Research Program provided major funding for both the circular as well as the studies on which it is based. Studies also received matching support from state and local water agencies in Oregon, California, Nevada, Arizona, and New Mexico, and from the private sector. We especially thank Paul Pettit and Patricia Cannon of Newmont Mining (Carlin, Nevada), Douglas McGibbon and John Barber of Glamis Marigold Mining (Valmy, Nevada), and Karl Wozniak of Oregon Water Resources (Salem) for encouragement and support of specific studies within their purview. Many USGS colleagues contributed to this circular by providing technical assistance and critical reviews of draft chapters. They include John Callahan (Arizona), Fredrick Gebhardt (New Mexico), Stephanie Moore (New Mexico), Donita Parker (Oregon), Nye Pennington (Nevada), Russell Plume (Nevada), and John C. Stone (Nevada). David R. Jones (Menlo Park, California) designed the layout and provided graphical support. Keith G. Kirk (Menlo Park, California) provided overall editorial supervision, work-flow and production support.

Conversion factors and abbreviations

Multiply	By	To obtain
	Length	
centimeter (cm)	0.3937	inch (in.)
millimeter (mm)	0.03937	inch (in.)
meter (m)	3.281	foot (ft)
kilometer (km)	0.6214	mile (mi)
meter (m)	1.094	yard (yd)
	Area	
square meter (m^2)	0.0002471	acre
hectare (ha)	2.471	acre
square centimeter (cm^2)	0.001076	square foot (ft^2)
square meter (m^2)	10.76	square foot (ft^2)
square centimeter (cm^2)	0.1550	square inch (ft^2)
hectare (ha)	0.003861	square mile (mi^2)
square kilometer (km^2)	0.3861	square mile (mi^2)
	Volume	
liter (L)	33.81	ounce, fluid (fl. oz)
liter (L)	2.113	pint (pt)
liter (L)	1.057	quart (qt)
liter (L)	0.2642	gallon (gal)
cubic meter (m^3)	264.2	gallon (gal)
cubic centimeter (cm^3)	0.06102	cubic inch (in^3)
cubic decimeter (dm^3)	61.02	cubic inch (in^3)
liter (L)	61.02	cubic inch (in^3)
cubic meter (m^3)	35.31	cubic foot (ft^3)
cubic meter (m^3)	1.308	cubic yard (yd^3)
cubic kilometer (km^3)	0.2399	cubic mile (mi^3)
cubic meter (m^3)	0.0008107	acre-foot (acre-ft)
	Flow rate	
cubic meter per second (m^3/s)	70.21	acre-foot per day (acre-ft/d)
meter per second (m/s)	3.281	foot per second (ft/s)
cubic meter per second (m^3/s)	35.31	cubic foot per second (ft^3/s)
liter per second (L/s)	15.85	gallon per minute (gal/min)
	Pressure	
kilopascal (kPa)	0.009869	atmosphere, standard (atm)
kilopascal (kPa)	0.01	bar
	Density	
kilogram per cubic meter (kg/m^3)	0.06242	pound per cubic foot (lb/ft^3)
	Energy	
joule (J)	0.2778×10^{-6}	kilowatthour (kWh)
	Hydraulic conductivity	
meter per second (m/s)	3.281	foot per second (ft/s)

Temperature in degrees Celsius (°C) may be converted to degrees Fahrenheit (°F) as follows:

$$°F=(1.8\times°C)+32$$

Chapter 1

Heat as a tracer of water movement near streams

Jim Constantz and David A. Stonestrom

Introduction

Stream temperature has long been recognized as an important water quality parameter. Temperature plays a key role in the health of a stream's aquatic life, both in the water column and in the benthic habitat of streambed sediments. Many fish are sensitive to temperature. For example, anadromous salmon require specific temperature ranges to successfully develop, migrate, and spawn [see Halupka and others, 2000]. Metabolic rates, oxygen requirements and availability, predation patterns, and susceptibility of organisms to contaminants are but a few of the many environmental responses regulated by temperature.

Hydrologists traditionally treated streams and ground water as distinct, independent resources to be utilized and managed separately. With increasing demands on water supplies, however, hydrologists realized that streams and ground water are parts of a single, interconnected resource [see Winter and others, 1998]. Attempts to distinguish these resources for analytical or regulatory purposes are fraught with difficulty because each domain can supply (or drain) the other, with attendant possibilities for contamination exchange. Sustained depletion of one resource usually results in depletion of the other, propagating adverse effects within the watershed.

An understanding of the interconnections between surface water and ground water is therefore essential. This understanding is still incomplete, but receiving growing attention from the research community. Exchanges between streams and shallow ground-water systems play a key role in controlling temperatures not only in streams, but also in their underlying sediments. As a result, analyses of subsurface temperature patterns provide information about surface-water/ground-water interactions.

Chemical tracers are commonly used for tracing flow between streams and ground water. Introduction of chemical tracers in near-stream environments is, however, limited by real and perceived issues regarding introduced contamination and practical constraints. As an alternative, naturally occurring variations in temperature can be used to track (or trace) the heat carried by flowing water. The hydraulic transport of heat enables its use as a tracer.

Differences between temperatures in the stream and surrounding sediments are now being analyzed to trace the movement of ground water to and from streams. As shown in the subsequent chapters of this circular, tracing the transport of heat leads to a better understanding of the magnitudes and mechanisms of stream/ground-water exchanges, and helps quantify the resulting effects on stream and streambed temperatures.

Chapter 1 describes the general principals and procedures by which the natural transport of heat can be utilized to infer the movement of subsurface water near streams. This information sets the foundation for understanding the advanced applications in chapters 2 through 8. Each of these chapters provides a case study, using heat tracing as a tool, of interactions between surface water and ground water for a different location in the western United States. Technical details of the use of heat as an environmental tracer appear in appendices.

What causes exchanges of water between streams and ground water?

Water in the subsurface flows from higher to lower total head, where *total head* is the sum of water elevation and water pressure (expressed as a head). The *pressure head* is zero (with respect to atmospheric pressure) at the stream surface and at all points on the water table. Therefore, the elevation of the water table relative to the stream surface indicates the direction of subsurface flow between streams and nearby ground water. The resistance to flow presented by sediments, as well as the gradient in head, governs the *rate* at which water moves between surface-water and ground-water systems [see Freeze and Cherry, 1979].

As water passes through streambed sediments, chemical reactions occur that change its composition and thus affect water quality. Dissolved materials increase due to mineral dissolution. Exchange and other reactions change the relative abundance of materials in solution. Changes in water chemistry can increase towards saturation as water continues to flow through geologic strata. If ground water enters the stream, the stream's chemical composition is affected. Exchanges of water can sometimes be tracked by monitoring the chemistry of water along flow paths. Flow paths can be traced at watershed scales or at the smaller scales of stream banks, sand bars, and local reaches of a stream [see Bencala and others, 1984]. Local-scale exchanges may be separately inconsequential but collectively important. Multiple exchanges of surface and ground water can strongly influence the quality of surface-water resources. Heat is especially well suited for delineating these small-scale flow paths. Naturally

occurring changes in temperature in the near-stream environment are often large and rapid, providing a clear thermal signal that is easy to identify and measure.

History of heat as a hydrological tracer

The concept of using heat as a tracer of ground-water movement is not new. By the early 1900s, researchers recognized that heat is transferred during the course of water movement through sediments and other porous materials [Bouyoucos, 1915]. In the middle of the last century, groundwater hydrologists explored the possibility of using temperature measurements to estimate the rate at which water travels from the surface to great depths [for example, see Rorabough, 1954; and Stallman, 1963]. Since then, temperature patterns have been exploited to study subsurface flow systems ranging from irrigation water in rice paddies to geothermal water beneath volcanoes [Suzuki, 1960; Sorey, 1971]. Heat as a tracer of ground-water movement had many more theoretical than practical applications due to measurement and computational limitations. Recently, however, the measurement and modeling of heat and water transport have benefited from significant improvements in data-acquisition and computational techniques. These advances enable the economical and routine application of heat as a hydrologic tracer.

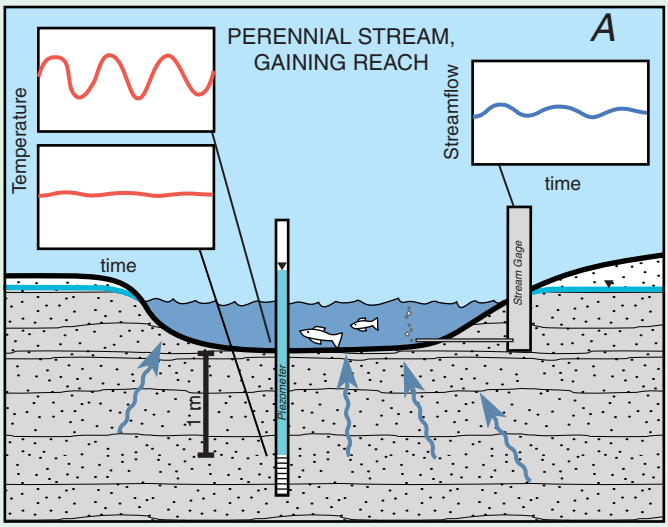

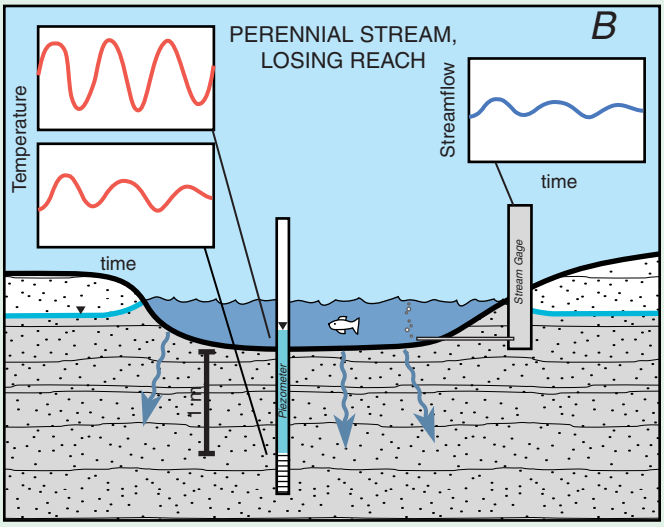

For the case of a gaining stream (panel A), the hydraulic gradient is upward *(higher total head beneath the stream than in the stream)* as indicated by the higher altitude of water in the *piezometer* (observation well) than in the stream stage (measured by the stream gage). The stream has a large diurnal variation in water temperature. The sediment beneath the streambed has only a slight diurnal variation, because water is flowing up from depths where temperatures are constant on diurnal time scales. The variation in sediment temperature beneath the streambed reflects the balance between the oscillating transport of heat via conduction *(transfer of heat through a substance from warm areas to cool areas without movement of the substance)* and upward transport of heat via advection *(transport of heat by a moving fluid)*. At any given depth beneath the streambed, higher flows of ground water to the stream lead to smaller variations in sediment temperature while smaller flows lead to larger variations *(which become increasingly damped with depth)*. Consequently, shallow installation of temperature equipment *(inside the piezometer or directly in the streambed sediments)* is necessary to characterize gaining stream reaches, in order to detect significant temperature variations.

For the case of a losing stream (panel B), the hydraulic gradient is downward *(lower total head beneath the stream than in the stream)*. The downward flow of water transports heat from the stream into the sediments. The downward advection of heat results in large diurnal fluctuations in sediment temperature. In addition, since regional groundwater is not flowing into the stream, temperatures vary more in losing streams than in gaining streams [Constantz, 1998]. Consequently, deeper installation of temperature equipment (inside the piezometer or beneath the streambed) is necessary for characterizing losing streams.

Using heat to follow water flow near streams

Whenever a difference in temperature exists between two points along a flow path, heat will flow between them by transport in the flowing water *(advective heat flow)*. This heat movement is in addition to thermal conduction through the non-moving solids and fluids *(conductive heat flow)*. Typically, heat movement is traced by continuous monitoring of temperature patterns in the stream and streambed, followed by interpretation using numerical models. Even before modeling, temperature patterns can immediately indicate the general character of the flow regime. For example, reaches of the channel in which sediment-temperature fluctuations are highly damped relative to in-stream fluctuations indicate high rates of ground-water discharge to the stream (that is, *ground-water discharge to a strongly gaining reach*). Conversely, segments of the stream channel where fluctuations in streambed temperatures closely follow in-stream fluctuations indicate high rates of water loss through streambed sediments (that is, *ground-water recharge from a losing reach*). To quantify the rates, location, and timing of stream-flow gains and losses, an array of temperature sensors is deployed in the stream and adjacent sediments.

The use of heat as a hydrologic tracer has several distinct advantages over applied chemical tracers. The signal arrives naturally. The primary measurement is of temperature, which is a robust and relatively inexpensive parameter to measure. In contrast to chemical tracers, which often require laboratory

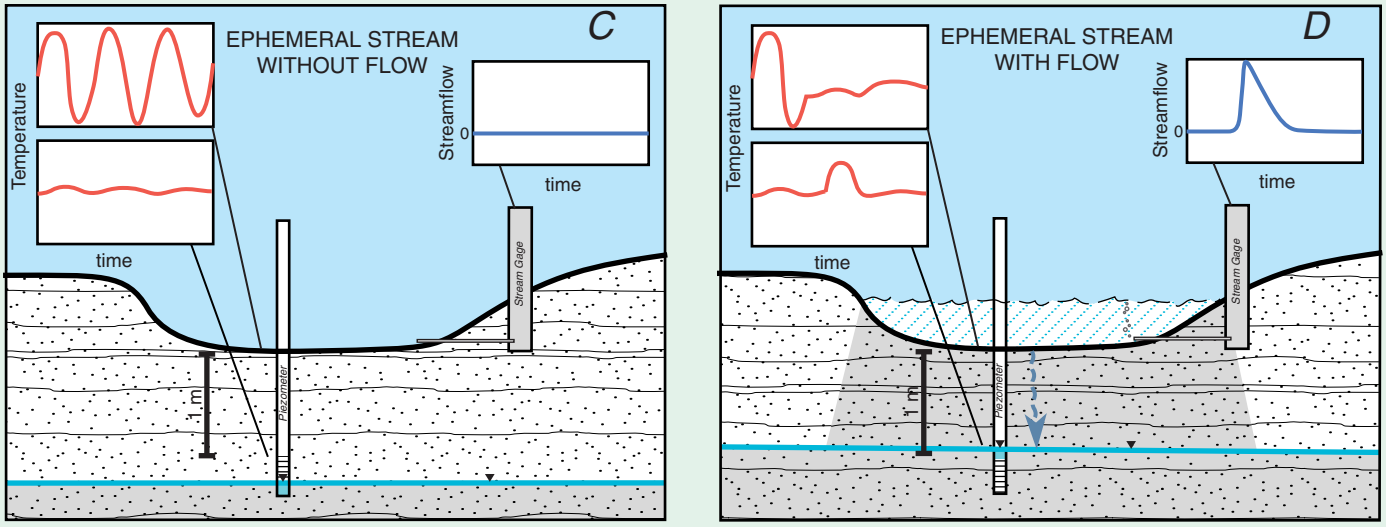

For the case of a dry streambed (panel C), pore-water pressures in channel sediments are negative relative to atmospheric, and not measurable with a piezometer. (Negative pore water pressures exist in materials that are not fully saturated, such as a damp sponge or towel. Significant amounts of water my be present but will not occupy a piezometer; instead, atmospheric air pressure pushes subatmospheric water from the tube.) The streambed has high diurnal variations in temperature from daytime heating and nighttime cooling. The ability of dry material to transport heat is lower than that of wet material, damping diurnal variations in sediment temperatures at relatively shallow depths.

For the case of a channel that conveys ephemeral stream flow (panel D), a distinct temperature signal almost always marks the initiation of flow. The piezometer will register only if the screened interval is below the water table (*at which point it will register the water-table elevation*). High rates of infiltration at the onset of ephemeral flow produce rapid thermal responses in the streambed, as seen in the abruptly arriving signal in the streambed thermograph.

Figure 1. Idealized stream channel for four possible interactions with ground water—a perennial stream gaining water from the underlying sediments, a perennial stream losing water to the underlying sediments, an ephemeral stream without flow, and an ephemeral stream with flow. Inset graphs show stream-flow hydrographs and corresponding streambed thermographs in each case.

analyses before interpretation is possible, temperature data are immediately available for inspection and interpretation.

Figure 1 provides a series of graphics portraying thermal and hydraulic responses to four possible streambed conditions. Panels A and B show gaining and losing perennial streams that are connected to the local ground-water system. Panels C and D show dry and flowing ephemeral streams that are separated from the local ground-water system by an intervening unsaturated zone. Ephemeral channels lose water when flowing. The panels provide graphical depictions relevant to installation of monitoring equipment by illustrating the unique thermal signature for each stream condition. The inset hydrograph (on the right of each panel) shows stream flow. The inset thermographs (on the left of each panel) show temperature histories corresponding to the hydrographs. The thermographs show diurnal (daily) patterns of temperature at the surface of the channel and beneath the channel. A *piezometer* (instrument for measuring pressure head) shows pressure within the streambed. As noted above, the thermographs by themselves (even without the pressure data) permit identification of strongly gaining or strongly losing conditions.

Computer simulations to estimate water movement below the streambed

Computer simulations are based on a set of mathematical expressions that represent the physical and chemical processes known to occur in the system. Computer simulations are useful for analyzing portions of the hydrological cycle that can be accurately described by algebraic and differential equations. Simulation of water exchange between streams and surrounding sediments requires knowledge of the thermal and hydraulic parameters used as input values. *Hydraulic conductivity*, which quantifies the resistance of a porous material to water flow, can vary by orders of magnitude from one streambed to another. In contrast, *thermal conductivity*, which quantifies the resistance of the material to heat flow, varies little from one streambed to another. Figure 2 shows the relative sensitivity of hydraulic and thermal conductivities to texture. Note that thermal conductivity is virtually independent of texture, while hydraulic conductivity is highly dependent on texture. This is because heat travels in a direct path through the entire cross-section of solids and pore-filling fluids, whereas fluid flow is confined to a tortuous path through interconnected pores. Fluid flow is the product of hydraulic conductivity and *hydraulic gradient* (Darcy's law). Analogously, conductive heat flow is the product of thermal conductivity and *temperature gradient* (Fourier's law).

Continuous monitoring of streambed temperatures provide a *time-series* of profiles (temperature versus depth curves) that document changes in water flux into and out of the stream. Figure 3 shows hypothetical streambed temperature profiles for a *losing stream* (downward water flux) versus a *gaining stream* (upward water flux) over a natural thermal

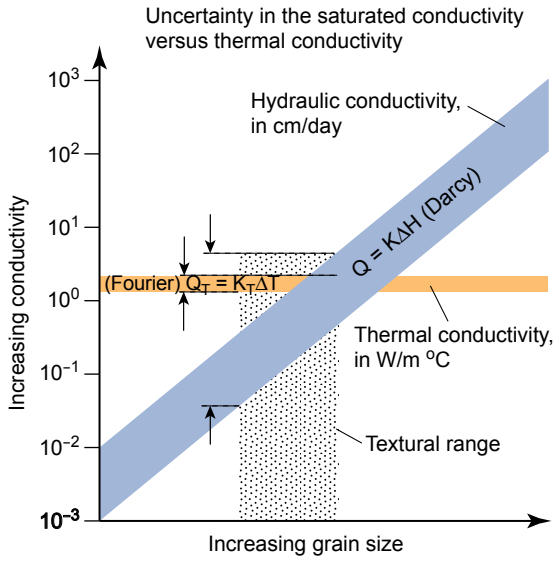

Figure 2. The hydraulic conductivity of saturated sediments (blue band) is strongly dependent on sediment texture (represented here by grain size), whereas the thermal conductivity (tan band) is almost independent of texture. The vertical width of the hydraulic and thermal-conductivity bands gives an approximate range of the respective parameter for a given texture. Arrows show the degree to which the two conductivities will vary for a given range in textures (stippled band).

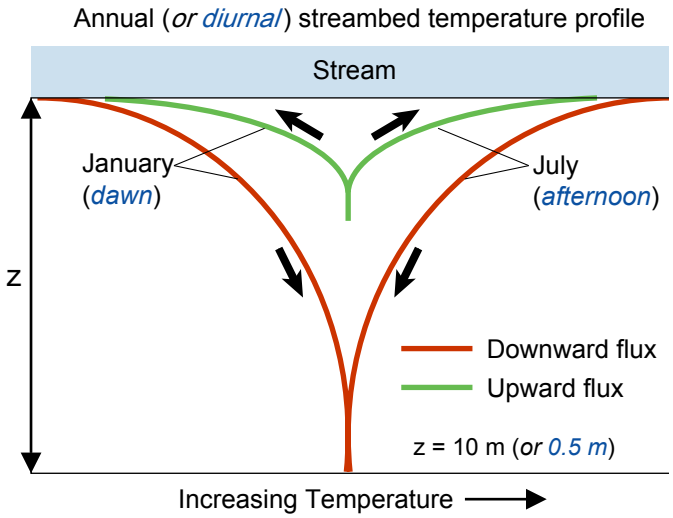

Figure 3. Ranges of sediment temperatures versus depth, Z, for gaining conditions (green lines) compared with losing conditions (red lines), over daily or annual cycles. The depth at which the temperature becomes constant depends upon the upward or downward flow of water through the sediments. For annual profiles, this depth may be 10 meters or more for downward flow versus less than a few meters for upward flow. For diurnal cycles, the depths at which temperatures become constant are shallower by the square root of (365/1) for a neutral flux (see Appendix A).

cycle (either one day or one year). The penetration of cyclic temperature changes is greater for the case of downward water movement because the downward-moving water has been heated and cooled at the land surface. Conversely, the penetration of cyclic temperature changes is less for the case of upward water movement because the upward-moving ground water comes from depths that are buffered from temperature fluctuations at the land surface. This water has a relatively constant temperature close to the cyclical average. Maximum and minimum temperatures during a complete cycle (annual or daily) form a 'temperature envelope' for a particular site, within which all measured temperature profiles reside. For the annual cycle, January and July profiles typically approximate the bounds of the envelope. When ground water is flowing into a gaining stream, the annual envelope collapses toward the streambed surface. When the stream is losing water to underlying sediments, the envelope expands downward. The same thing happens on a smaller scale over the daily cycle, with dawn and afternoon profiles approximating the daily temperature envelope (in which all other, for example hourly, temperature profiles reside).

Figure 4 depicts measured temperatures beneath the Rio Grande at Albuquerque, New Mexico together with simulated temperatures produced by various combinations of hydraulic conductivity and hydraulic gradient [Bartolino and Niswonger, 1999]. The figure shows that a hydraulic conductivity of 6.7 x 10^{-6} m/s (0.0000067 meters per second, or about 58 centimeters per day) results in simulated temperatures that closely match the measured profile. From Darcy's Law, the temperature-based estimate of hydraulic conductivity times the measured hydraulic gradient provides a robust estimate of the water flux. A typical hydraulic gradient is less than 10% (less than a 0.1-m decrease in head per meter of travel). Rates of ground-water movement are usually a small fraction of the hydraulic conductivity. Changing the hydraulic conductivity (or hydraulic gradient) results in significant changes to the predicted temperature profile (fig. 4). The large sensitivity of streambed temperatures to hydraulic conditions is readily apparent, and makes heat a versatile tracer of ground-water movement. The technical details of applying thermal tracing techniques are given in the appendices. Appendix A describes the procurement of data (temperature, heat capacity and thermal conductivity) required to measure and interpret dynamic thermal profiles. Appendix B describes how simulation models are constructed and applied to observed measurements, with specific attention on publicly available computer codes for simulating the coupled transport of heat and ground water near streams.

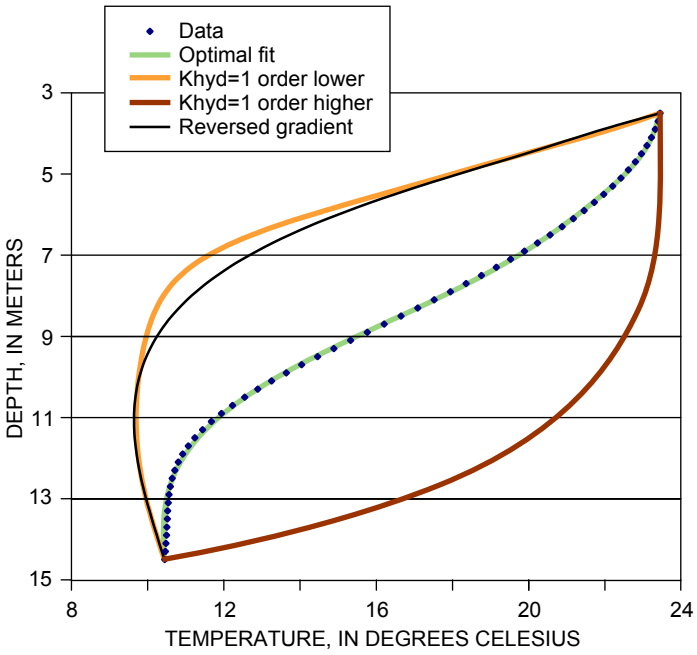

Figure 4. Measured and modelled temperatures in sediments beneath the Rio Grande. Observed temperature data (dots) are compared with results of computer simulations (lines) for different theoretical values of hydraulic conductivity (Khyd) and hydraulic gradient. These results show the large sensitivity of modeled sediment temperatures to hydraulic parameters.

A preview

Protecting stream environments and water supplies requires an adequate understanding of the interactions between streams and their underlying ground water. The body of this circular comprises seven chapters describing the manner in which heat has been used to study these interactions in the western United States.

As described in chapter 2, the Rio Grande is a narrow ribbon of water flowing through the parched New Mexico landscape. The prosperity of the region has depended on the Rio Grande since prehistoric times. Current demands on the river have become so severe that citizens of New Mexico are considering their long ignored rights to the Colorado River.

The alluvial aquifer beneath the Russian River in northern California is the primary source of water for residents of Sonoma and northern Marin Counties (chapter 3). Three fish species are currently listed as endangered, so impacts of water-resources utilization must be carefully monitored (see fig. 5).

The Santa Clara River in southern California is the last natural stream in Los Angeles County (chapter 4). Maintenance of a healthy river depends intimately on the inter-connectivity of the stream with the adjacent flood plain, which broadens westward from the base of the San Gabriel Mountains towards the Pacific Ocean.

Tributaries of the Willamette River south of Portland, Oregon, represent spawning habitats for a number of endangered and seagoing fish species. Agriculture in the Willamette Valley has shifted from non-irrigated grains to irrigated orchards, vineyards, and other crops (chapter 5). Changes in stream-water temperature and availability associated with

Figure 5. Pontoon rafts with fish counting wheels operating along the Russian River in coastal northern California. Particular attention to fishery habitat is needed when ground water is pumped near streams.

ground-water extraction affect fish populations. Recognition of these effects has placed new emphasis on quantifying the impacts of irrigation withdrawals on fish habitats.

Trout Creek, California, flows into the southern end of Lake Tahoe, presenting the opportunity to study how stream interactions with ground water are affected by a lake (chapter 6). The exchanges between Trout Creek and shallow ground water are strongly affected by lake level. Seasonally rising and falling lake levels create a drastic change in streambed thermal patterns that, in turn, affect stream ecology.

Rillito Creek flows through Tucson, Arizona, providing a main source of recharge to the underlying ground-water system. Where and when recharge occurs beneath this rapidly growing city is an important uncertainty that affects the region's urban planning (chapter 7).

Trout Creek in central Nevada is a small stream that flows down the north side of Battle Mountain (chapter 8). The stream is typical of thousands of similar streams throughout the vast basin and range province. Trout Creek provides an excellent example for exploring the cumulative importance of mountain-front streams in providing recharge to regional aquifers. An understanding of mountain-front recharge is essential for managing water resources in rugged deserts throughout the world.

As a set, these chapters provide a detailed assessment of interactions between surface water and ground water, using temperature patterns and their interpretation as a hydrologic tool. They also show the manner in which this information may be used to better understand and manage biological and water resources.

Chapter 2

The Rio Grande—competing demands for a desert river

James R. Bartolino

Introduction

The Middle Rio Grande Basin covers approximately 7,900 square kilometers in central New Mexico, encompassing parts of Santa Fe, Sandoval, Bernalillo, Valencia, Socorro, Torrance, and Cibola Counties ("Middle Rio Grande Basin" here refers to the geologic basin defined by the extent of deposits of Cenozoic age along the Rio Grande from about Cochiti Dam to about San Acacia). The basin lies in an asymmetric elongated valley along the Rio Grande. The basin encompasses the inner valley, or floodplain, of the Rio Grande and the surrounding terrain that slopes from surface-drainage divides toward the river. As in the rest of the Southwest, the area has grown rapidly since the Second World War; in 2000, the population of the Middle Rio Grande Basin was about 690,000, or about 38 percent of the population of New Mexico (Bartolino and Cole, 2002).

At the current time (2003), essentially the entire population of the basin depends on ground water from the Santa Fe Group aquifer system for their domestic-supply needs. This dependence on ground water, coupled with rapid growth, has led to ground-water-level declines of over 50 meters beneath parts of Albuquerque. Because the interaction between the Rio Grande and the aquifer system has long been recognized by the New Mexico Office of the State Engineer (NMOSE), regulations require major ground-water producers to obtain surface-water rights to compensate for streamflow depletion caused by ground-water pumping. The largest user of ground water in the Middle Rio Grande Basin is the City of Albuquerque and since the 1960s, its water plan has consisted of meeting water demand solely by production from ground water. The scientific understanding of the hydrogeology of the Middle Rio Grande Basin at that time suggested that seepage from the Rio Grande replenished the water in the aquifer withdrawn by pumping. Starting in 1995, a revised understanding of the hydrogeology of the basin suggested that the connection between the Rio Grande and Santa Fe Group aquifer system allowed less ground-water recharge than previously thought (Bartolino and Cole, 2002).

In 1995, the NMOSE declared the Middle Rio Grande Basin a "critical basin"; that is, a ground-water basin faced with rapid economic and population growth for which there is less than adequate technical information about the available water supply. Though the basin had been intensively studied for a number of years, important gaps remained in the understanding of the water resources of the basin. In an effort to fill some of these gaps, the U.S. Geological Survey (USGS) and other Federal, State, and local agencies conducted an intensive effort to improve the understanding of the hydrology, geology, and land-surface characteristics of the Middle Rio Grande Basin (Bartolino and Cole, 2002).

Figure 1. Location of the Middle Rio Grande Basin.

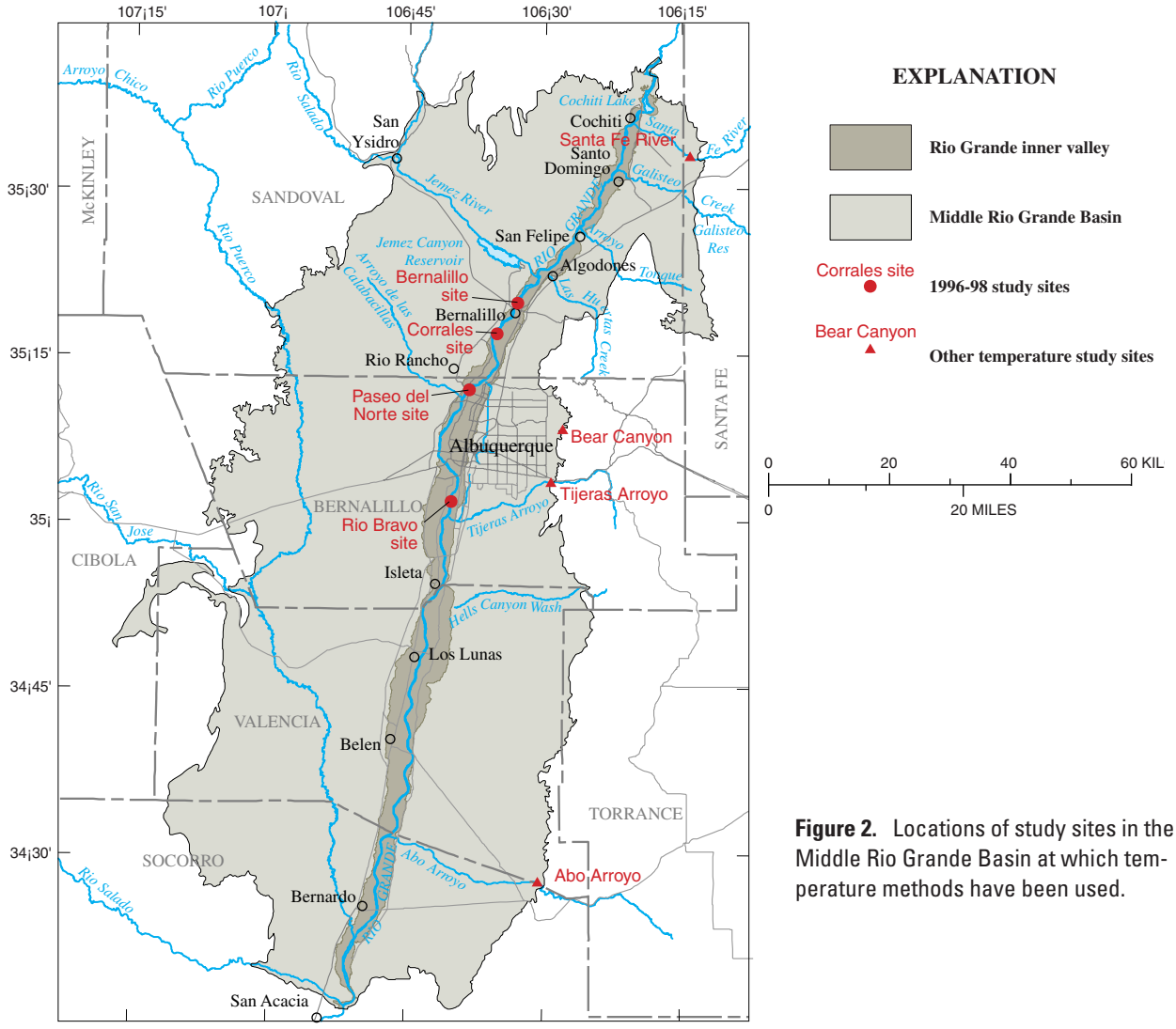

Figure 2. Locations of study sites in the Middle Rio Grande Basin at which temperature methods have been used.

One of the most important gaps in the understanding of the hydrology of the Middle Rio Grande Basin is the rate at which water from the Rio Grande recharges the Santa Fe Group aquifer system. This question is important because ground-water pumping for municipal supplies depletes flow. In addition, the City of Albuquerque is pursuing plans for direct use of their San Juan Chama Project water (a transmountain diversion of Colorado River basin water into the Rio Grande basin upstream from the city) (City of Albuquerque Public Works Department, 1997). Currently (2003), competing demands for river water include agricultural irrigation, endangered species, Rio Grande Compact obligations, and planned direct use of surface water for municipal supplies. An understanding of the complex interactions between the surface- and ground-water systems is necessary for water-resource managers to make scientifically based management decisions.

The Middle Rio Grande Basin

The most prominent hydrologic feature in the Middle Rio Grande Basin is the Rio Grande, which flows through the entire length of the basin, generally from north to south. Though flow in the Rio Grande is currently (2003) regulated by a series of dams and storage reservoirs, the greatest flows tend to occur in late spring as a result of snow melt, and for shorter periods during the summer in response to rainfall. Historically, the Rio Grande has flowed year-round through much of the basin, "except for those periods of severe, extended drought" (Scurlock, 1998).

The inner valley of the Rio Grande contains a complex network of irrigation canals, ditches, and drains that has evolved from the original acequia system. The Middle Rio Grande Conservancy District administers this irrigation system and diverts Rio Grande water at four points in the basin: Cochiti Dam, Angostura (near Algodones), Isleta, and San Acacia (which serves an irrigation area downstream of the basin). During the irrigation season, water is diverted from the river and flows through the Rio Grande inner valley in a series of irrigation canals and smaller ditches for application to fields. This water either recharges to ground water, is lost to evaporation or evapotranspiration by plants, or is intercepted by interior drains and returned to the river (Bullard and Wells, 1992; Kernodle, McAda, and Thorn, 1995; Anderholm, 1997).

The other main component of the inner-valley surface-water system is a system of riverside drains, which are deep canals that parallel the river immediately outside the levees. They are designed to intercept lateral ground-water flow from the river, thus preventing waterlogged conditions in the inner valley. The riverside drains then carry this intercepted lateral ground-water flow back to the Rio Grande. Within the basin, riverside drains and levees are usually present on both banks of the river, except where bluffs adjoin the river.

The riparian vegetation of the bosque has evolved significantly in the last 100 years as a result of the introduction of exotic species and the construction of flood-control and bank-stabilization projects. During the last 60 years, the bosque has developed in an area that was formerly semi-barren floodplain. It is probable that more water is required to maintain the dense vegetation of the bosque today than was required for the isolated stands of cottonwood and willow that existed in the past.

Water movement between the river and aquifer

Several methodologies, including use of the Glover-Balmer equation, flood pulses, and channel permeameters, have been used to quantify the amount and rate at which water moves between the Rio Grande and the Santa Fe Group aquifer system, with sometimes conflicting results. The reader is referred to Bartolino (2002) for a discussion of these studies.

The work described in this chapter uses both ground- and surface-water temperatures and water levels to quantify the direction and rate of ground-water flux between the river and underlying aquifer and to estimate the effective hydraulic conductivity values of the sediments underlying and adjoining the river. Data collected in the field will be interpreted with the use of numerical simulation in order to obtain flux and hydraulic conductivity values (see Appendix B).

Other temperature work in the Middle Rio Grande

Temperature has been used by several authors to quantify the amount and direction of water moving between the surface- and ground-water regimes in the Middle Rio Grande Basin along perennial reaches of the Santa Fe River, Tijeras Arroyo, and the Rio Grande (fig. 2) (Bartolino and Constantz, 2002). However, the use of water temperature as a tracer was expanded into the realm of ephemeral streams at both Bear Canyon and Abo Arroyo (fig. 2) in order to determine the downward movement of water and the downstream extent of flow in the arroyos (Bartolino and Constantz, 2002). (See Constantz and Thomas, 1996; Thomas, Stewart, and Constantz, 2000; Niswonger and Constantz, 2001; Stewart and Constantz, 2001.)

One-dimensional approach

In the first phase of this study, as described in Bartolino and Niswonger (1999), seven sets of nested piezometers were installed during July and August 1996 at four sites along the Rio Grande in the Albuquerque area (fig. 2), though only four of the piezometer nests were simulated one-dimensionally. In downstream order, these four sites are (1) the Bernalillo site, upstream from the U.S. Highway 550 bridge in Bernalillo; (2) the Corrales site, upstream from the Rio Rancho sewage treatment plant in Rio Rancho; (3) the Paseo del Norte site, upstream from the Paseo del Norte bridge in Albuquerque; and (4) the Rio Bravo site, upstream from the Rio Bravo bridge in Albuquerque. All piezometers were completed in the inner-valley alluvium of the Santa Fe Group aquifer system. Ground-water levels and temperatures were measured a total of six times in the four piezometer nests from September 1996 through August 1998. Ground-water temperatures from one of these phase one piezometers at the Paseo del Norte site are shown in figure 3.

A total of four one-dimensional numerical models of heat and water transport in the subsurface were constructed to simulate the field setting for each piezometer nest (see Appendix B). Comparison of the simulated vertical fluxes and estimated vertical hydraulic-conductivity values from this study with values from other investigations in the Middle Rio Grande Basin indicated broad agreement (Bartolino and Niswonger, 1999).

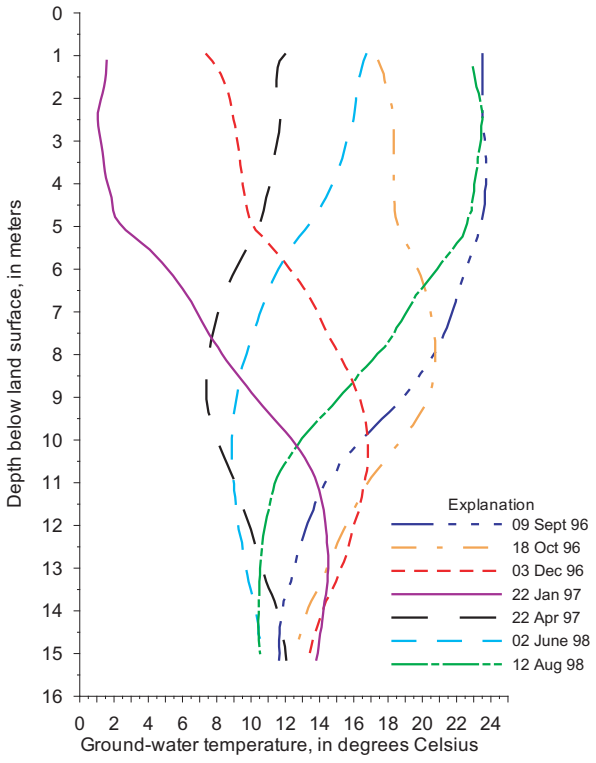

Figure 3. Ground-water temperatures at selected times from September 1996 to August 1998 during the first phase of the study in the PDN01 piezometer. This piezometer is at the Paseo del Norte site and was used only during the first phase of the study.

Table 1. Description of piezometers installed and monitored for this study [m, meters; S, shallow; M, medium; D, deep]

Piezometer nest	Location	Altitude of land surface (m above sea level)	Piezometer	Piezometer depth (m)	Temperature logger	Temperature logger depth (m)
P01	East bank of the Corrales Riverside Drain	1,518.55	S	3.0	A	2
			M	7.6	B	4
			D	12.2	C	6
					D	8
					E	12
P02	Midway between the Corrales Riverside Drain and west bank of the Rio Grande	1,519.55	S	4.0	A	3
			M	7.6	B	4.5
			D	12.2	C	6
					D	8
					E	12
P03	West bank of the Rio Grande at high flow	1,518.93	S	2.1	A	1.5
			M	6.7	B	3
			D	12.2	C	5
					D	8
					E	12
P04	Sandbar in the Rio Grande	1,518.77	S	2.1	A	1.5
			M	6.7	B	3
			D	11.3	C	4.5
					D	7
					E	11
P05	Sandbar in the Rio Grande, west bank of the Rio Grande at low flow	1,518.41	S	2.1	A	1.5
			M	7.6	B	3
			D	11.3	C	4.5
					D	7
					E	11
P06	East bank of the Rio Grande	1,519.43	S	2.4	A	2
			M	6.1	B	4
			D	12.2	C	6
					D	8
					E	12
P07	Midway between the the east bank of the Rio Grande and the Albuquerque Riverside Drain	1,519.32	S	4.9	A	3
			M	6.7	B	4.5
			D	12.2	C	6
					D	8
					E	12
P08	West bank of the Albuquerque Riverside Drain	1,518.39	S	4.0	A	3
			M	6.7	B	4.5
			D	12.2	C	6
					D	8
					E	10

Two-dimensional approach

Despite the general success of the one-dimensional approach to simulate vertical flux and estimate hydraulic conductivity, it was hypothesized that the three sites near riverside drains (with the exception of the Corrales site) had a significant component of horizontal flow. In addition, if the drains intercepted a large proportion of the water infiltrated from the Rio Grande, the volume of ground-water recharge from the river to the Santa Fe Group aquifer system could be overestimated. With these limitations in mind, a second study phase was planned with three major differences: one site would be examined in much greater detail using a cross-sectional approach; temperature data would be collected at fewer depths in a selected well, but with much greater temporal resolution; and more data would be collected on boundary conditions, such as river stage and water temperature in the drains and river.

Site instrumentation and data collection

Eight sets of nested piezometers were installed from January-March 1999 on the north side of the Paseo del Norte bridge

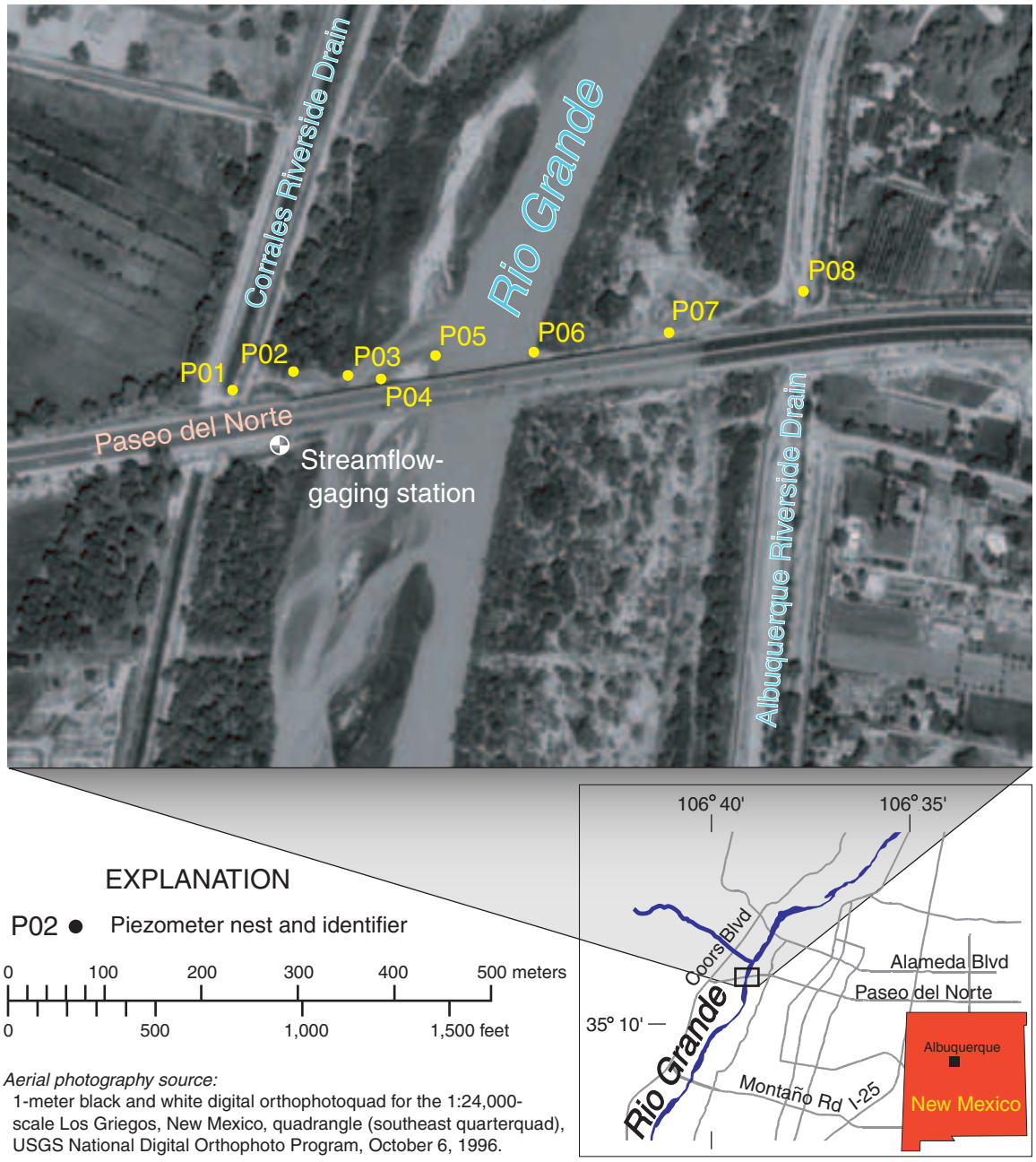

Aerial photography source:
1-meter black and white digital orthophotoquad for the 1:24,000-scale Los Griegos, New Mexico, quadrangle (southeast quarterquad), USGS National Digital Orthophoto Program, October 6, 1996.

Figure 4. The Paseo del Norte bridge study site.

over the Rio Grande in Albuquerque (fig. 4). The piezometer nests were installed from the east bank of the Corrales Riverside drain (P01), across the Rio Grande, to the west bank of the Albuquerque Riverside drain (P08). Three piezometers were installed in each nest at depths ranging from 2.1 to 12.2 m, and all piezometers were completed in the inner-valley alluvium of the Santa Fe Group aquifer system. Piezometer locations and depths are shown in table 1. A core was collected and piezometers were installed at each location using a Geoprobe soil-probing machine, model 8-MU, which is a truck-mounted hydraulic ram/percussion hammer that uses 2.5-cm diameter drill rod.

Ground-water temperatures were measured with single-channel temperature loggers (as described in appendix A). These devices were suspended at five selected depths in the deep piezometer in each of the eight piezometer nests. Ground-water temperatures were measured and recorded at 1-hour intervals from March 1999 to July 2000. The reader is referred to Appendix A for additional information on temperature measurement.

Additional temperature loggers were installed at two locations in each of the surface water bodies at the site: the Corrales Riverside drain, the Rio Grande, and the Albuquerque

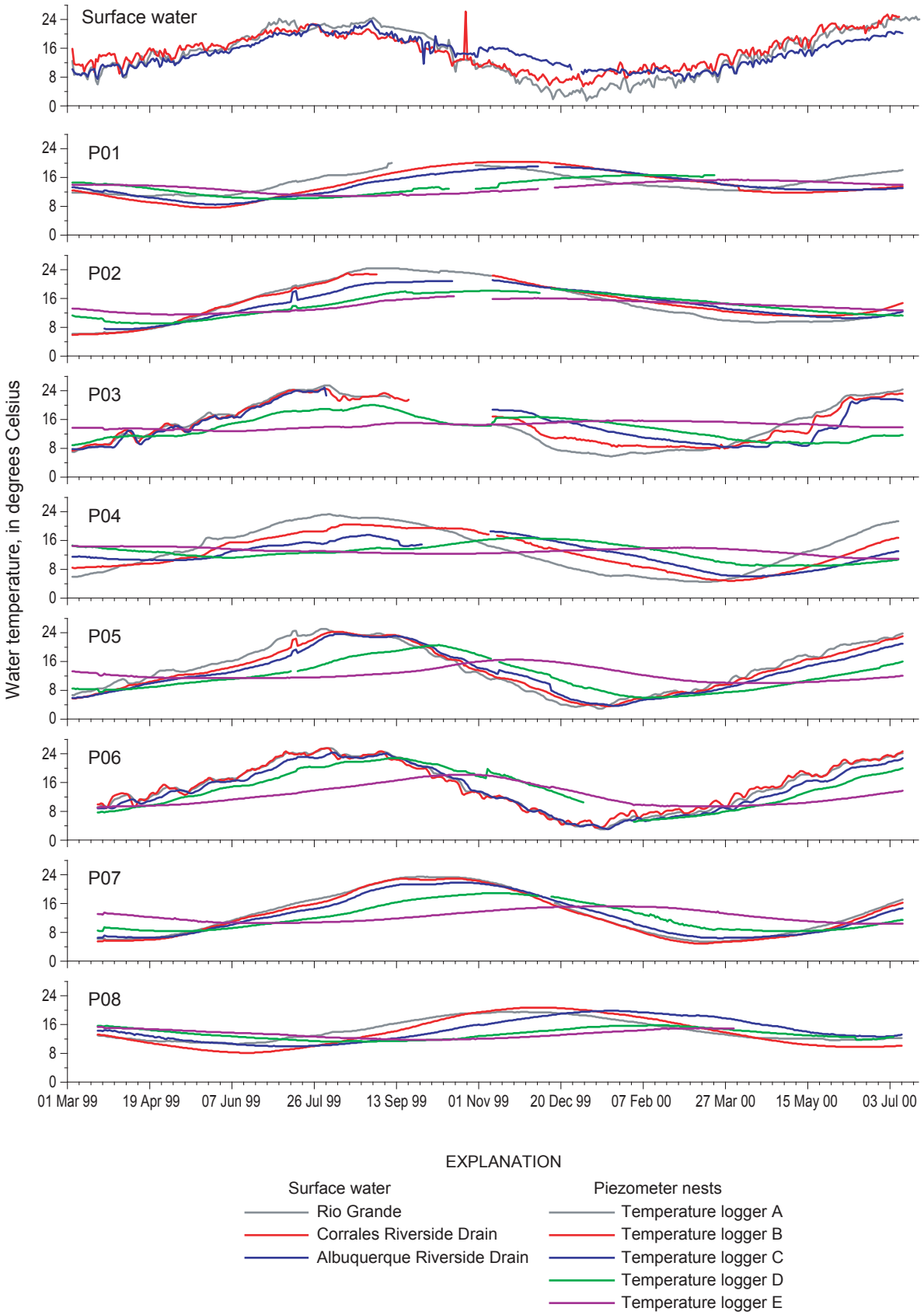

Figure 5. Thermographs showing water temperature in the Rio Grande and piezometer nests at the Paseo del Norte site. See figure 4 and table 1 for location and depth of the temperature measurements.

Riverside drain. Surface-water temperatures were measured and recorded at 1-hour intervals from March 1999 to July 2000.

Ground-water levels were measured in each piezometer at approximately 2-week intervals from March 1999 to July 2000, with the exception of P04 and P05. Because of their location on a sandbar in the channel, these piezometer nests were submerged during high flows in the Rio Grande. Thus, water levels were not measured one time in P04, and five times in P05.

An inactive USGS streamflow-gaging station (Rio Grande near Alameda, New Mexico; 08329928) was reactivated for the study. River-stage data were collected at 15-minute intervals from March 1999 to July 2000. Based on measurements conducted during the survey of the site and the difficulty and expense of instrumenting the drains to collect water levels, water levels in the Corrales and Albuquerque Riverside drains were assumed to be equal to the water levels in the shallow piezometers in the P01 and P08 nests, respectively.

Field observations

Site characteristics

Conditions at the Paseo del Norte site are typical for much of the Rio Grande in the Middle Rio Grande Basin. The channel of the Rio Grande is braided, though the east bank has been stabilized by the installation of Kellner jetties. Levees are present on both sides of the river, with typical bosque vegetation (tamarisk, Russian olive, desert willow, and cottonwood) growing in the area between the river banks and levees. Outside the levees are riverside drains (Corrales on the west, Albuquerque on the east) installed to prevent waterlogging in the inner valley.

The closest long-term gaging station to the Paseo del Norte site is approximately 13 kilometers downstream at the Central Avenue bridge (Rio Grande at Albuquerque, 08330000). From 1974 (when Cochiti Lake began filling) to 2001, flow in the Rio Grande typically peaked in response to spring snowmelt and in response to summer thunderstorms.

During most of the year, Rio Grande flow at the Paseo del Norte site is confined to the main channel, defined as the area between piezometer nests P05 and P06. At river stages greater than approximately 1,520 m, there is also flow in the channel between P03 and P04. At stages greater than approximately 1,521 m, the sandbar on which P04 and P05 are installed is completely submerged.

Temperature

Daily average water-temperature data for all measurement points are shown in figure 5. Several features of the data are readily apparent. First, there is typical large variability apparent in the surface-water temperature measurements ranging from 3°C in the winter to 26°C in the summer. Second, the maximum and minimum water-temperature measurements in each piezometer nest shift with increasing depth. Third, with increasing depth, the measurements in each piezometer nest have less range and variability in water-temperature than shallower measurements.

Water levels

Water-level data for the Paseo del Norte site are shown in figure 6. A good correlation exists between river stage and ground-water levels in the piezometer nests. In addition, ground-water levels decrease away from the river confirming that water flows away from the river toward the riverside drains. The hydrographs in figure 6 indicate there was little vertical movement of ground water during most measurement times at the eight nests.

Lithology

As mentioned previously, continuous core was collected at each piezometer nest. These cores were visually described and detailed lithologic descriptions were developed for each nest. However, for the purpose of developing a numerical ground-water model of the site, these detailed lithologic descriptions were grouped into one of the two main depositional/lithologic classes of the inner valley alluvium: poorly sorted, generally coarse-grained main channel deposits consisting primarily of sand and gravel, and well sorted, generally fine-grained overbank deposits consisting primarily of clay, silt, and fine sand.

Discussion

The riverside drains were constructed to intercept shallow ground-water flow originating in the river, a process confirmed by water-level data. Thus, water temperatures should reflect this movement of water from the river to the riverside drains—as is shown in a subset of the data showing water temperature in the Rio Grande and in ground water at the 6-meter depth in the P06, P07, and P08 piezometer nests on the east side of the river (fig. 7). The P06 piezometer nest is on the east bank of the Rio Grande and consequently the approximate high and low temperatures in the piezometer (shown by red and blue arrows, respectively) occurred roughly at the same time as in the river. Approximately halfway between the river and Albuquerque riverside drain in piezometer nest P07 (146 m from the river), the ground-water maximum and minimum temperatures lag approximately 10 weeks. In addition the temperatures show less short- and long-term variation than in the Rio Grande or P06. Finally, in piezometer nest P08 located on the west bank of the Albuquerque riverside drain (139 m from P07), ground-water maximum and minimum temperatures lag approximately 13 weeks from P07 and water temperature shows increased damping.

Due to the physical properties of heat, it is not possible to treat heat as a conservative tracer and simply estimate hydraulic-conductivity values using the Darcy equation because such properties as dispersivity, thermal conductivity, and heat capacity must be considered.

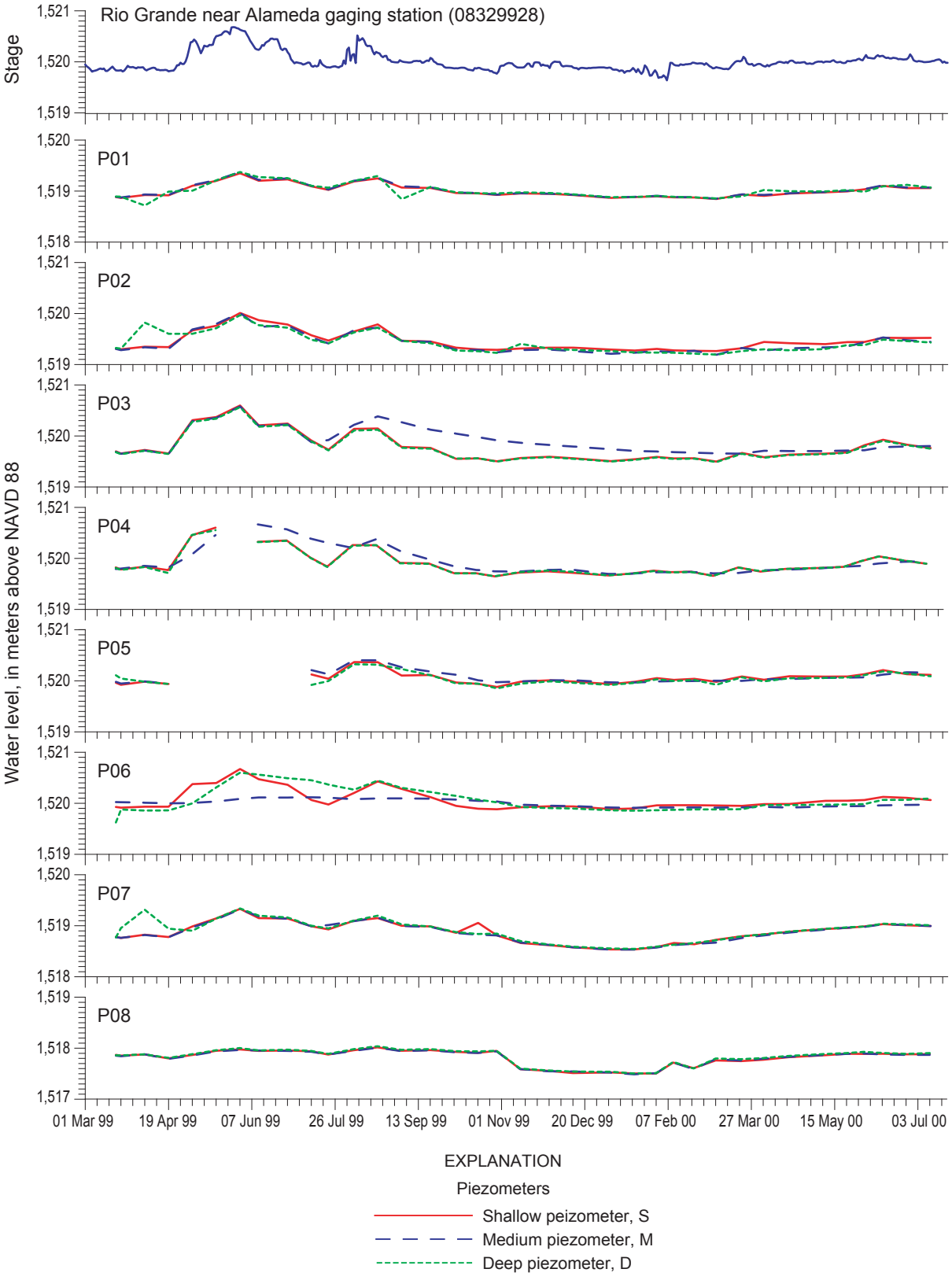

Figure 6. Hydrographs showing stage of the Rio Grande and water levels in the piezometer nests at the Paseo del Norte site.

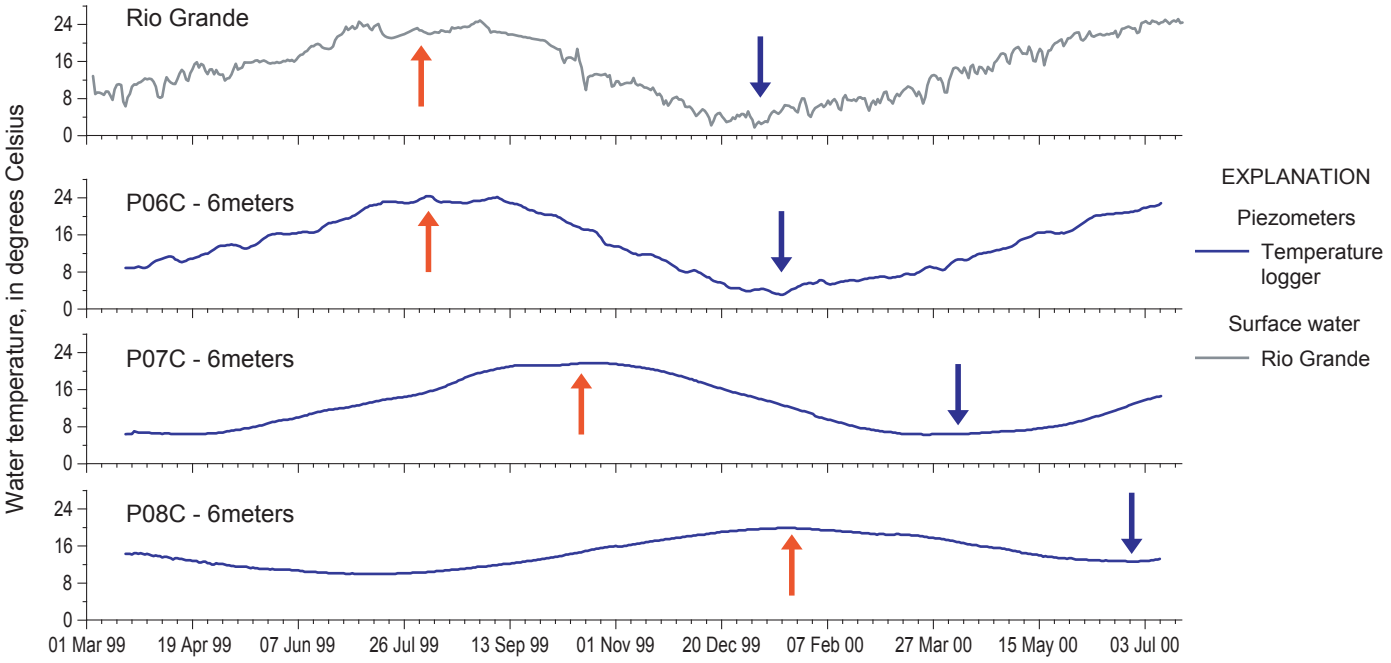

Figure 7. Thermographs showing water temperature in the Rio Grande and at 6 meter depth in the P06, P07, and P08 piezometer nests.

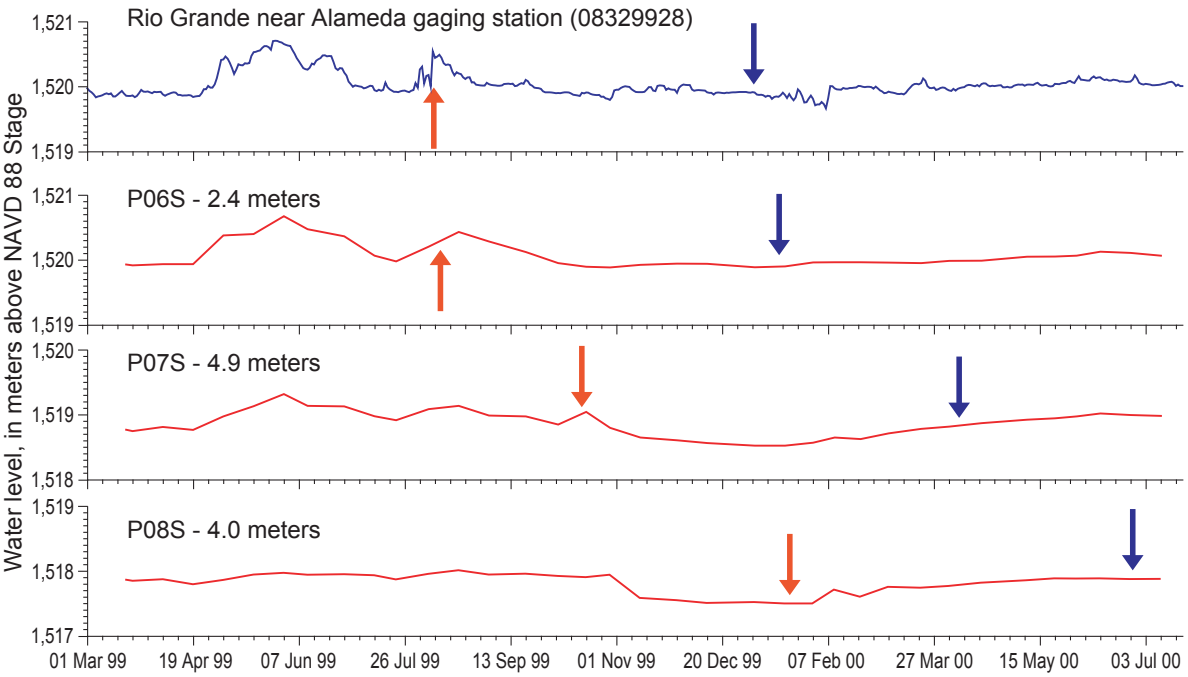

Figure 8. Hydrographs showing stage of the Rio Grande and water levels in the shallow piezometer in the P06, P07, and P08 piezometer nests.

Water-level data for the Rio Grande and shallow piezometer in the P06, P07, and P08 piezometer nests are shown in figure 8. Correspondence between river stage and ground-water level is good in P06, in P07 the shape of the hydrograph is barely discernible, and there is no apparent correlation in P08. In addition, water-level changes in the piezometers do not appear to lag behind changes in the river stage as significantly as temperature, and water levels also decrease away from the river.

A similar analysis of ground-water temperatures on the west bank of the Rio Grande (piezometer nests P01-P05) shows a similar, though more complex pattern. The increased complexity is due to the more gradual slope of the west bank of the Rio Grande. As discussed previously, the west edge of water ranges between P03 and P05, depending on river stage. Thus, at low stages, P05 is at the west edge of water and its water temperatures mimic that of surface water. At high stages, water temperatures in P03, P04, and P05 all mimic surface-water temperature. Therefore, the thermographs for the west bank are more complex than those for the east bank, yet still indicate the seasonal movement of temperature.

Figure 9. The Rio Grande at Paseo del Norte in northern Albuquerque with three piezometers in the foreground used to monitor shallow, intermediate, and deeper water-levels and temperatures.

Summary and Conclusions

One of the most important gaps in the understanding of the hydrology of the Middle Rio Grande Basin is the rate at which water from the Rio Grande recharges the Santa Fe Group aquifer system. This question is important because ground-water pumping for municipal supplies depletes flow in the river. Currently (2003), competing demands for river water include agricultural irrigation, endangered species, Rio Grande Compact obligations, and planned direct use of surface water for municipal supplies. An understanding of the complex interactions between the surface- and ground-water systems is necessary for water-resource managers to make scientifically based management decisions.

Several methodologies, including use of the Glover-Balmer equation, flood pulses, and channel permeameters, have been applied to this problem in the Middle Rio Grande Basin. In this study, ground- and surface-water temperatures and water levels at a site at the Paseo del Norte bridge on the Rio Grande were measured (fig. 9). Initial analysis of the data indicates the conceptual validity of the water-temperature method. Further analysis will utilize a two-dimensional numerical ground-water model of the site and will yield the direction and rate of ground-water flux between the river, riverside drains (fig. 10), and underlying aquifer, as well as the effective hydraulic-conductivity values of the sediments underlying the river.

Figure 10. Riverside drains form part of a complex irrigation network that is intimately linked with the Rio Grande and underlying Santa Fe Group aquifer system.

Chapter 3

Heat tracing in the streambed along the Russian River of northern California

Jim Constantz, James Jasperse[1], Donald Seymour[1], and Grace W. Su[2]

Introduction

The Russian River flows south from headwaters in Northern California through Mendocino County into Sonoma County, as shown in figure 1. About 100 km north of the Golden Gate Bridge, active plate tectonics force the river to the west upon reaching the Santa Rosa Plain. The plain overlies a large alluvial ground-water basin, representing the primary source of water resources for Sonoma and northern Marin Counties. A variety of activities place increased demands on the water resources available beneath the Santa Rosa Plain. This landscape, which once featured oak studded hills with grazing cattle and vast apple orchards stretching across the lowlands, is rapidly following the course of neighboring Napa Valley to the east as an internationally renowned wine-producing region. Vineyard acreage is rapidly increasing in Sonoma and Mendocino Counties on either side of the Russian River. Vineyards require additional irrigation water compared with grazing land and apple orchards, and the attractiveness of both the river and burgeoning wineries have created rapid population growth and increased recreational activities during the long, hot, dry summer season. Concurrent with these activities, several seagoing fish species migrate up the Russian River toward the headwater in Mendocino County during the dry season. This complex environment mandates that regional water resources be managed to minimize the impacts of our activities on the fishery habitat as the river passes through the Santa Rosa Plain.

[1] Sonoma County Water Agency, Santa Rosa, CA 95406

[2] Lawrence Berkeley National Laboratory, Berkeley, CA 94720

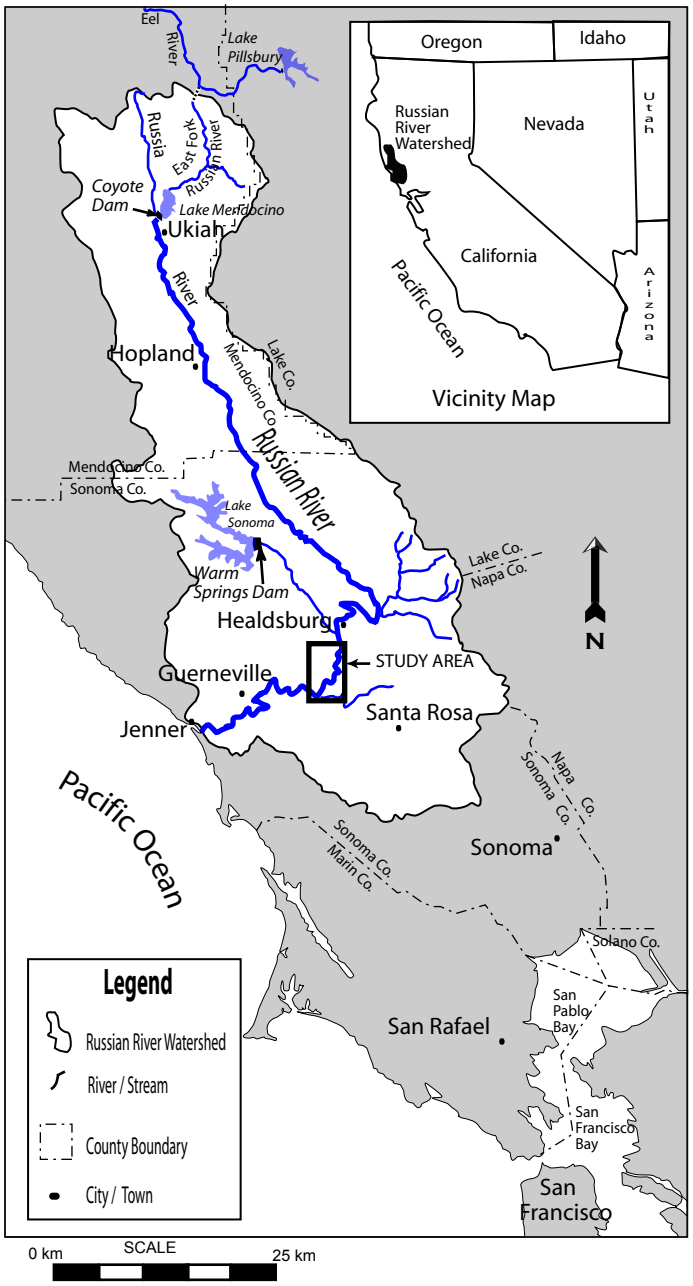

Figure 1. Regional view of the Russian River as it flows south from Mendocino County to Sonoma County, with a box demarcating the river reach where the present study is located. [Note the location of the San Andreas Fault demarked by the long, narrow bay in western Marin County. Along the plate boundary, the flow of coastal streams have been sharply redirected by the northern slip of the Pacific Plate as it passed the North American Plate.]

Figure 2. A recharge pond constructed between the Russian River and Westside Road. Power poles extending from supply wells through the ponds toward the road provide scale. Each recharge pond is operated through a cycle in which river water is diverted to the pond for a week or so, then the pond is allowed to go dry for as long as a month to retard the buildup of a clogging algal mat on the pond bottom.

Managing the river as a water resource

Water from the Russian River exchanges freely with the vast alluvial aquifer beneath the Santa Rosa Plain, due to coarse gravel deposits prevalent throughout the western portion of the basin. Since the middle of the last century, residents of Sonoma County have depended on water within these coarse sediments for municipal water supply, rather than diverting water directly from the river. This is because river water requires extensive treatment to remove dissolved materials and suspended sediments, while water extracted from the alluvial aquifer sediments is naturally filtered and requires no additional treatment beyond chlorination and possibly a pH adjustment prior to transmission to the distribution system. Traditionally, the water quality has been excellent though the water quantity is of periodic concern. The ability of the alluvial aquifer to produce water in necessary quantities is generally limited by the rate of recharge to the aquifer through the streambed. To augment this rate of recharge, infiltration ponds were developed along the river around 1960 to enhance recharge to the western edge of the Santa Rosa Plain (fig. 2). At a location in the river near the recharge ponds, an inflatable rubber dam was constructed to raise the river stage 3 m during the summer (fig. 3). The stage increase allows river water to be more readily diverted into the recharge ponds, and the resulting upstream backwater causes passive recharge of the alluvial sediments along the entire extent of the backwater. Thus, the water table is raised 3 m in several square kilometers of alluvial sediments on either side of the river. Typically, the dam is inflated in the spring as water demands increase and streamflows decline, then lowered in the late fall as water demands decrease and streamflows increase. Typically, water production from five supply wells located in the western portion of the Santa Rosa Plain is reduced by one-half when the dam and recharge ponds are taken out of operation in the late fall. Emerging water resources issues, including fish habitat concerns and optimization of water resources management, indicate that a quantitative model should be developed to accurately represent river exchanges with water in the alluvial aquifer in the region of the watershed encompassing the inflatable dam. Improved scheduling of dam and recharge pond operations, as well as supply well pumping patterns would be benefited by the development of a proven ground-water model for this region of the watershed.

Successful development of a ground-water model requires that key hydraulic parameters are determined for the streambed materials along the reach of the river flowing through the Santa Rosa Plain. Of prime importance is the careful characterization of the spatial and temporal value of the streambed conductance, which is determined by knowing both the streambed conductivity at a location along the river and the thickness of the streambed at this same location. Several tools are available to estimate these two hydraulic parameters, such as pumping tests and chemical tracers. Some pumping tests have been performed for specific locations; however, introduced chemical tracers are not an option for the Russian River, due to environmental and esthetic concerns along this scenic reach of the river (fig. 4). Fortunately, naturally occurring variations in water temperatures in the Russian River provide the necessary boundary conditions to use heat as a natural tracer of stream exchanges with water in the alluvial aquifer.

Figure 3. Inflatable dams are constructed of thick rubber for inflation with water for seasonal operation. This inflatable dam has fish ladders on either side to aid in fish migration that may occur during the seasonal operation of the dam. Portage for canoes and other small boats is initiated upstream of white float line.

Figure 4. Looking upstream along the Russian River from the Wohler Bridge in April. The inflatable dam, 500 m downstream of the bridge, is usually inflated in May, so that the stage of the river is low in April with bare stream banks exposed on either side of the river. Two supply wells adjacent to the river are visible on the bank. These wells pump water from the alluvium at a depth of about 20 m below the bottom of the streambed.

Measuring hydraulic conductivities in the streambed

Research is ongoing along the Russian River to determine the streambed hydraulic parameters, with an array of promising results now available. For analysis of heat as an environmental tracer of ground-water movement, a series of observation wells were instrumented for water levels and ground-water temperatures for comparison with river stage and surface-water temperatures. Observed temperatures are being used to optimize simulated temperatures from VS2DH (Appendix B), for predicting the hydraulic conductivity at specific locations along this reach of the river. As an example, figure 5 portrays the cross-section of the Russian River at well location TW-01, along with the location of the temperature measurement in the screen interval of the observation well near the river. Figure 6 compares the 'best-fitting' simulated ground-water temperatures with observed temperatures. Based on similar fits, a narrow range of predicted hydraulic conductivities was derived from the different observation wells. Hydraulic conductivity values and hydraulic gradients based on stage differences between the river and the observation well provide estimates of fluxes through the sediments near the river. Figure 7 gives examples of poor fits, graphically demonstrating the sensitivity of sediment temperatures to changes in water flux through the sediments. This sensitivity is a primary reason why the use of heat as a tracer of stream exchanges with the underlying streambed is emerging as a powerful hydrological tool for better understanding water and nutrient movement in the streambed. Once a good fit is determined using VS2DH for each observed well, a hydraulic conductance value may be assigned for that streambed section of the study reach. All together this hydraulic information gives a quantitative representation of the variation in streambed conductance along the entire reach of the river flowing through the western portion of the Santa Rosa Plain.

Using knowledge to move forward

The water resource challenges in the Santa Rosa Plain are becoming common throughout coastal areas, where conjunctive use of streams and ground-water may conflict with the

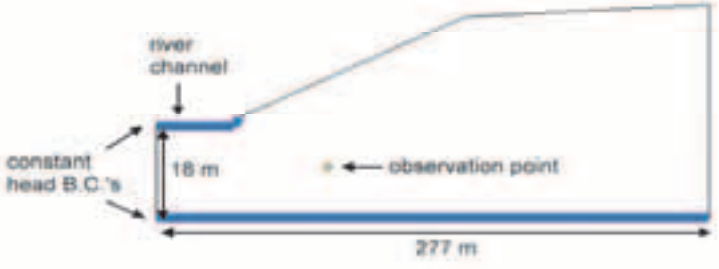

Figure 5. River cross-section used in the two-dimensional computer simulation model. The observation point where water-level and water temperature are monitored in the observation well is shown at the appropriate location in the river bank. (See Appendix A for a discussion of measurement methods.) Numerous observation wells are located along the river in the Santa Rosa Plain to measure differences in streambed hydraulic conductivity throughout the river reach.

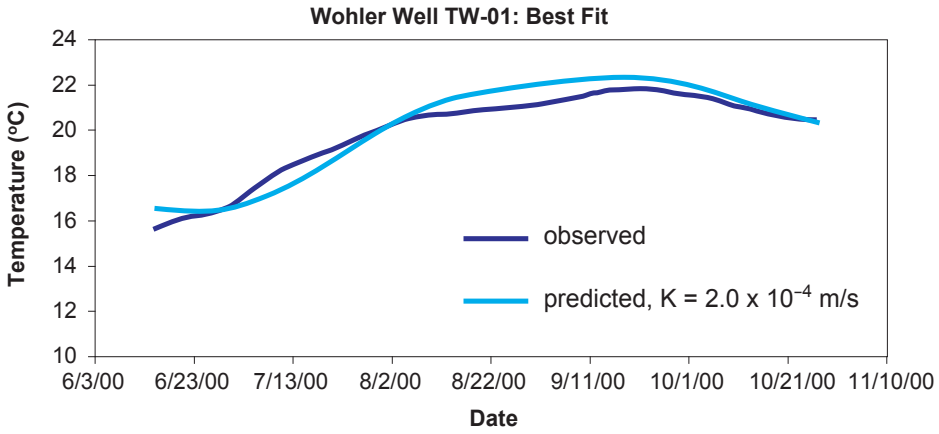

Figure 6. The observed sediment temperature over the season measured at the observation point in the well is compared with the 'best-fit' simulated sediment temperature, when a hydraulic conductivity value of 2.0 x 10-4 m/s (0.0002 m/s) was used in the simulation model. This hydraulic conductivity estimate can be multiplied by the known difference in water levels between the river and the well to determine the rate at which water moves through the alluvium from the river toward the observation well. (See Appendix B for a detailed discussion.)

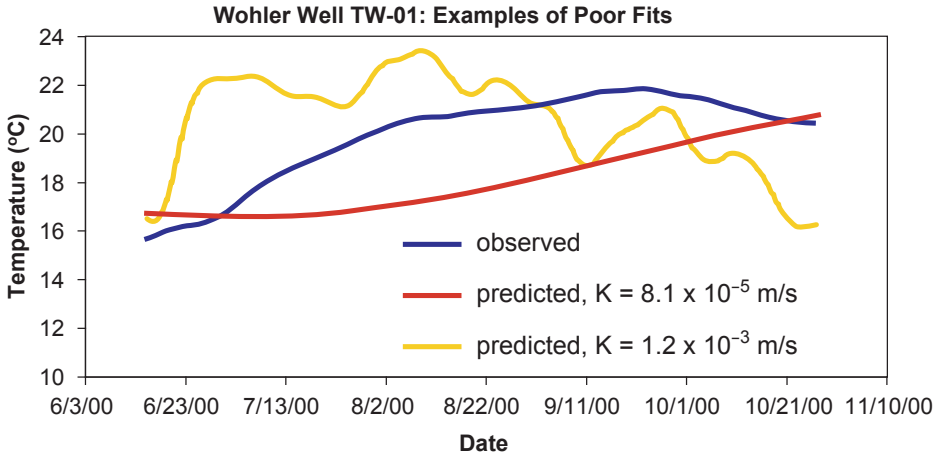

Figure 7. The observed sediment temperature over the season measured at the observation point in the well is compared with poor-fits of simulated sediment temperature. The predicted sediment temperature at the observation well is strongly affected by computer-simulated estimates for the hydraulic conductivity. The fact that the sediment temperature is so sensitive to hydraulic parameters makes the use of heat as tracer a very visual and potentially useful tool for determining the rate of exchange of water between the river and the alluvium underlying the western region of the Santa Rosa Plain.

fishery habitat requirements. Thus, successful use of heat as tracer to aid in understanding movement of water between the Russian River and the alluvium underlying the Santa Rosa Plain may have great transfer value to other coastal watersheds. Along the Russian River, continuous monitoring of stream and streambed temperatures provide the opportunity to develop a detailed pattern of temporal and spatial variations in streambed conductance for the reach encompassed by the series of observation wells. Detailed hydraulic information acquired along the river provides input for constructing a physically-based, ground-water flow model. As shown in figures 6 and 7, predicted hydraulic conductivities can be order of magnitude different than the best estimates using heat as a tracer. Good estimates of streambed hydraulic conductivities are essential input into a simulation model used for representing physical flow processes between the river's streambed. Computer simulation models with well characterized hydraulic parameters are useful in predicting the impacts of a range of possible scenarios, affording the opportunity to use these as a tool for improved management of water resources adjacent to the Russian River

Chapter 4

The Santa Clara River—the last natural river of Los Angeles

Jim Constantz, Marisa H. Cox, Lisa Sarma[1], and Greg Mendez

Introduction

The West has gone through a period of rapid growth since the middle of the last century, and nowhere is this expansion more apparent than Southern California. Today, the Santa Clara River in northwest Los Angeles County is the only remaining natural river carrying water to the Pacific Ocean (fig. 1). Other major streams reaching the Pacific are extensively channelized and lined with impermeable material, such as concrete, along much of their lowland reaches, so that the opportunity for stream water exchanges with ground water are severely curtailed. As a consequence, the Santa Clara River represents a unique remnant of the natural coastal hydrological cycle in this vast epicenter of Southern California. As shown in figure 2, the river emanates from headwaters on the western flank of the San Gabriel Mountains near an elevation of 1,200 meters, then flows in a westerly direction for nearly 50 km, before discharging into a coastal estuary in Ventura County. At the base of the San Gabriels, the river meanders through a gradually broadening valley at an elevation of 400 meters. In this reach (or section) of the river, the youthful city of Santa Clarita spreads along both banks, where the Valencia and Saugus water reclamation plants discharge wastewaters to the river. Like most streams in the Southwest, without effluent from water reclamation plants, the river would be ephemeral (that is, rarely contains streamflow) in this reach in a similar fashion to the dry reach to the west. In eastern Ventura County, the Santa Clara River is joined by Piru Creek from the north, which is perennial as a result of an upstream reservoir. Downstream of the confluence the Santa Clara River is perennial as it meanders through the bountiful agricultural valley of southern Ventura County.

The reach of the river between the treatment plants and the confluence winds through a broad valley with distinctive orange groves and other crops, which cover the flood plain of northwestern Los Angeles County and southern Ventura County. This reach gives one a glimpse back to more pastoral times in South California, as the Santa Clara River meanders over a sand-channel below cactus rimmed cliffs, giving way to green orchards, which radiate up toward arroyo scarred mountains. As growth continues, there has been increased environmental concerns that continued development may lead to increased discharge of effluent, which in turn may degrade the water quality not only of this pastoral reach, but of water flowing through Ventura County to the Pacific.

Figure 1. The Santa Clara River meanders over gravel beds and sand bars in its middle reaches. This view is looking upstream.

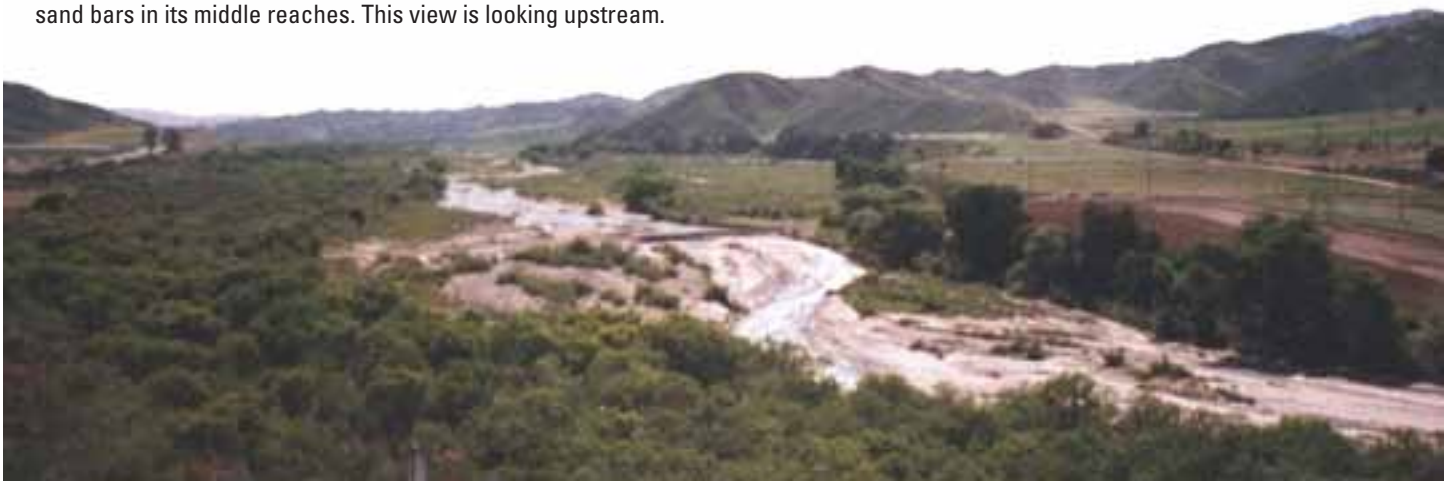

[1] Now with URS Corporation, San Francisco, CA

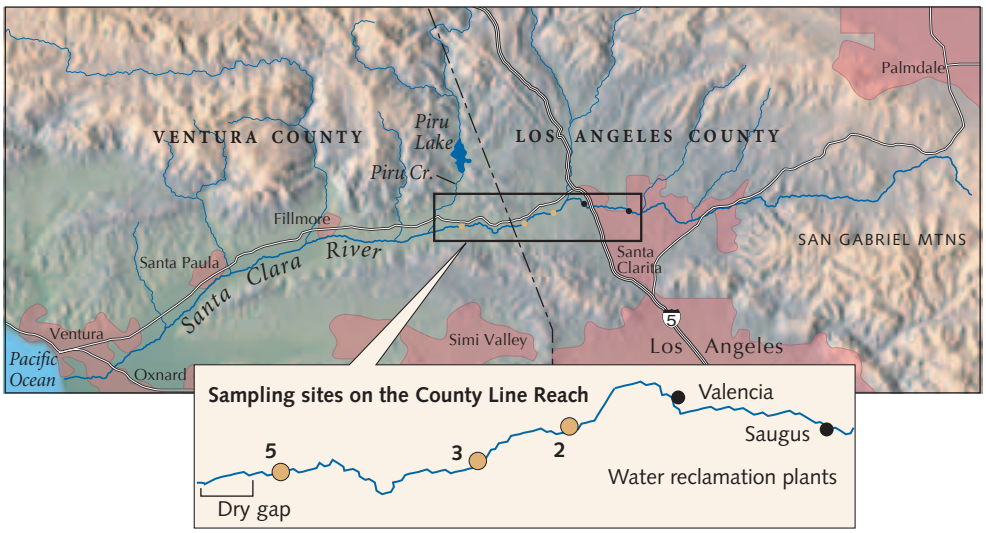

Figure 2. Relief map of the areas of Los Angeles and Ventura Counties containing the Santa Clara River watershed. The section of the river with the study reach is shown in the overlay map, including the locations of the Valencia and Saugus water treatment plants and the three locations in the river where sampling cross-sections were located.

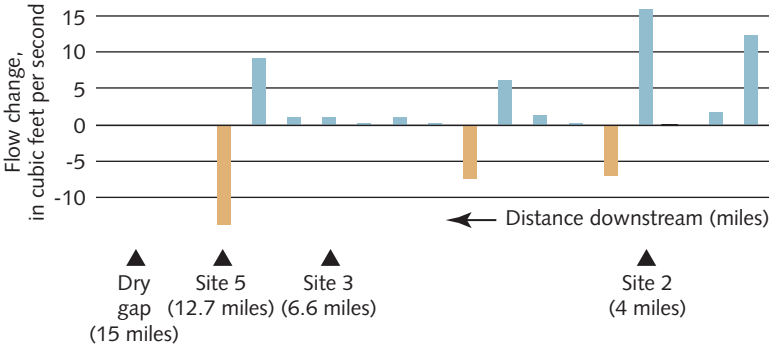

Figure 3. The plot of the change in streamflow compared to the immediate upstream location along the study reach. The blue bars indicate that the river gained streamflow compared with the upstream location, while a brown bar indicates that the river lost water compared with the upstream location.

The county-line reach may be key to water quality

As the Santa Clara meanders through the county-line reach, extensive opportunity exists for stream water to flow into the streambed sediments and adjacent sand bars, and either percolate down to the water table or emerge back into the river downstream. Figure 3 gives a bar graph of the relative gains and losses of water from or to the ground water as the river flows through the study reach. This significant exchange of stream and ground water results in changes in the downstream chemistry of both stream water and shallow ground water, which would not occur if the streambed were lined in a similar fashion to other rivers in Los Angeles County. West of the county-line reach, the present day river channel has a dry reach even with upstream effluent contributing to streamflow, and this dry gap flows only during heavy winter rains in the San Gabriels to the east. During most of the year, all stream water percolates into the streambed before the dry gap, and travels beneath the streambed as ground water. As mentioned before, the river becomes perennial again at the confluence with Piru Creek, and the ground water flowing beneath the dry gap is believed to discharge to the river downstream of the confluence. The revived river flows into the large agricultural valley in southern Ventura County, eventually discharging in the estuary near Oxnard. Thus, the amount of natural filtration of effluent-dominated stream water is affected by the volume of stream water exchanging with ground water upstream of the confluence.

Field Experiments along the county-line reach

Direct measurements of the hydraulics controlling this interaction represent the first step in defining where, when, and under what hydrological conditions these exchanges occur along the county-line reach. During the fall of 1999 and the spring of 2000, heat was used as a tracer to determine the characteristics of stream/ground-water exchanges along the reach. The use of heat as a tracer is not intended to determine the water quality of ground water near the river, but rather heat tracing can determine where and when stream water transports chemicals into the ground (or when and where ground water transports chemicals into the river). As input data for using heat tracing techniques, temperature monitoring equipment

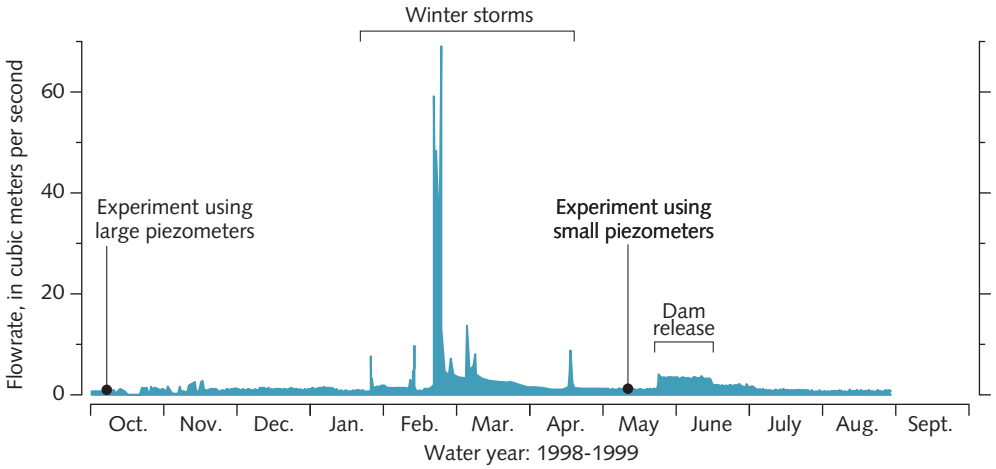

Figure 4. The streamflow hydrograph is shown for Water Year 1999 (Oct.98 through Sept. 99) at the USGS streamgage located downstream of Site 3 shown in figure 2.

was deployed in this reach of the Santa Clara River (SCR), through placement of equipment in the stream water, within underlying streambed sediments, and in nearby sandbars, at sites between the water reclamation plants and the terminus of streamflow at the upper end of the dry gap.

The Santa Clara stream hydrograph for the Water Year 2000 (October 1999 through September 2000) is shown in figure 4. The high streamflows of winter are bracketed by two extended low flow periods, typical for the Mediterranean climate of Central and Southern California. To use heat as a tracer of stream/ground-water exchanges, a series of piezometers, or observations wells (consisting of 0.10 meter internal diameter pipes) were installed beneath the stream and adjacent stream banks of this reach of the Santa Clara River. Figure 5 gives a typical cross-section containing a set of 6 small piezometers and a single large piezometer. Temperature was continuously monitored in the stream and all piezometers, to examine the interaction of stream and ground water as heat was transported across the streambed throughout the reach. Figure 6 shows two views of site 5.

As discussed in the first chapter, computer simulation codes are essential to fully quantify the degree of exchange of stream water with shallow ground water. These heat and water transport codes simulate the expected sediment temperature resulting from a series of shallow ground-water flow scenarios. The scenario that best describes the observed (measured) sediment temperature over time is deemed to be the best representation of the actual shallow ground-water flow characteris-

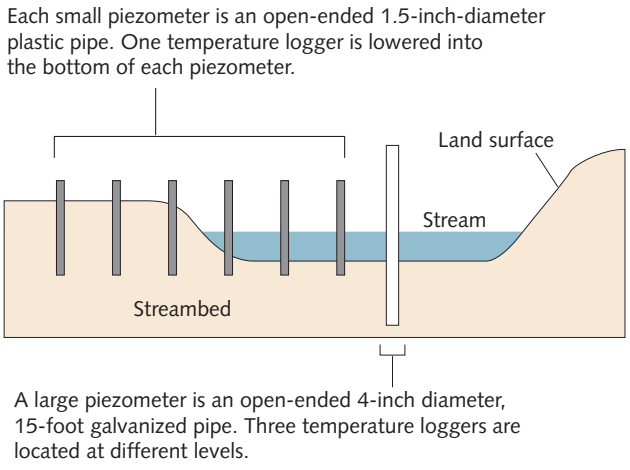

Figure 5. The positioning of a series of 6 small piezometers and a large piezometer at the cross-section sites within the study reach.

Figure 6. The left photograph shows Site 5 from the north. The right photograph shows a close up of Site 5 with the six small piezometers along side the large piezometer, and the step ladder used to aid in installation.

tics at that stream site. Figure 7 provides the type of sediment temperature patterns that would be predicted from simulation codes. In this case, the USGS heat and ground-water transport simulation code, VS2DH, was used to generate thermal patterns shown in the figure. In this hypothetical example, one can see that cool ground water dominates in the gaining simulation of streambed temperature patterns. For the losing simulation, the cooler and warmer stream water is transported deeply into the underlying sediments during the night and day, respectively. Often hypothetical simulations like these are used to aid in determining where and how deeply piezometers should be installed at a site. In this study, both shallow and deeper piezometers where installed to examine the shallow and deeper, vertical and horizontal ground-water flow within the stream sediments.

I. Deep streambed piezometers

Piezometers were installed into the streambed to a depth of 2 to 3 meters at Site 3 and Site 5, to examine the deeper streambed hydraulics. A temperature-logging device (i.e., electronic equipment that measures temperature at specified time intervals and stores this information in memory) was installed in the stream around the base of the piezometer and inside the piezometer at 0.5, 1.0, and 2.0 meters below the streambed surface (see Appendix A for details on the measurement of temperatures near streams). Figure 8 provides a visual display of the observed transport of heat into the streambed for Site 3 compared with Site 5. (Note the similarity with figure 7, except this figure displays the actual temperature pattern observed under the streambed during early October, 1999.) One can see that at the upstream site, Site 3, cool predawn water and warm afternoon water only slightly penetrated into the streambed, due to the low percolation rate of stream water. Downstream at Site 5, the rapid percolation of stream water carried both cool predawn stream water, and warm afternoon stream water below a depth of 2 meters. This thermal information not only helps hydrologists understand the patterns of stream exchanges with shallow ground water along the Santa Clara River, but is also useful to geochemists and microbiologists interested in the substream thermal environment along the river, for determining which microbes and chemical processes may be present in the near-stream ground water.

II. Shallow streambed piezometers

As depicted earlier in figure 5, a series of six shallow piezometers were installed at Sites 2, 3, and 5 to examine the stream interaction with the shallow streambed and adjacent streambank. Temperature was logged in a similar matter as described for the deeper piezometers, except only a single temperature logger was placed at the bottom of each small piezometer. Figure 9 shows thermographs (temperature patterns over time) for the piezometers at Sites 2, 3, and 5. Based on field observations, Site 2 was expected to have less exchange between the stream and underlying streambed compared with the downstream sites. As shown in the figures, a clear difference in the sediment temperature patterns is detected for the three stream sites. Stream temperature patterns are mimicked more closely and extend to greater depths as water flows downstream from Site 2 to 3 to 5, which indicates greater interaction with the streambed as water flows downstream along the county line reach. Furthermore, the temperature pattern beneath the adjacent sandbar also suggests that water in the streambed flows horizontally to a greater and greater degree downstream. As discussed in Appendix B,

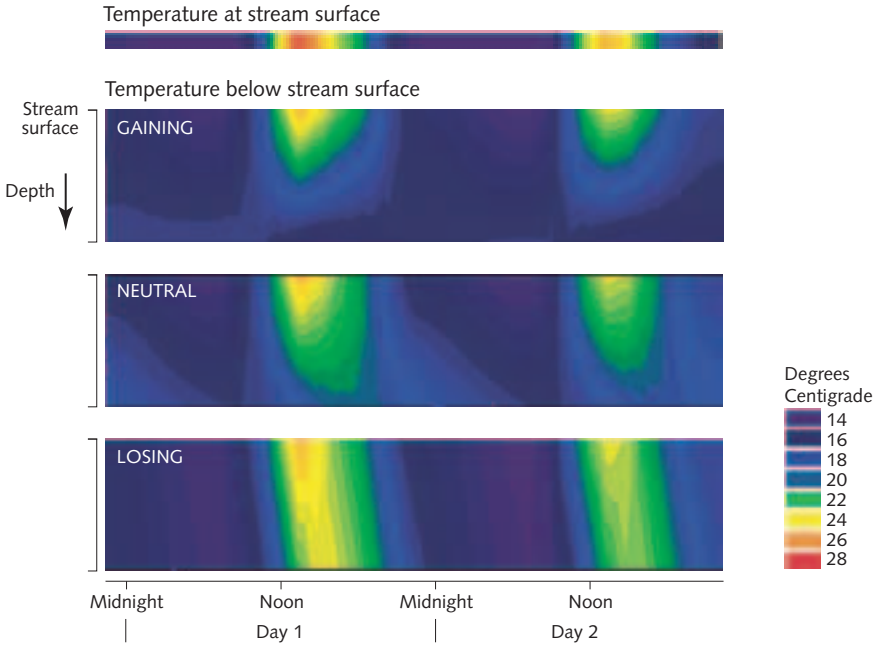

Figure 7. Computer simulation of the streambed temperature contours for cases in which a stream with the given water temperature (thin color ban at top) is gaining ground water, neutral, and losing ground water.

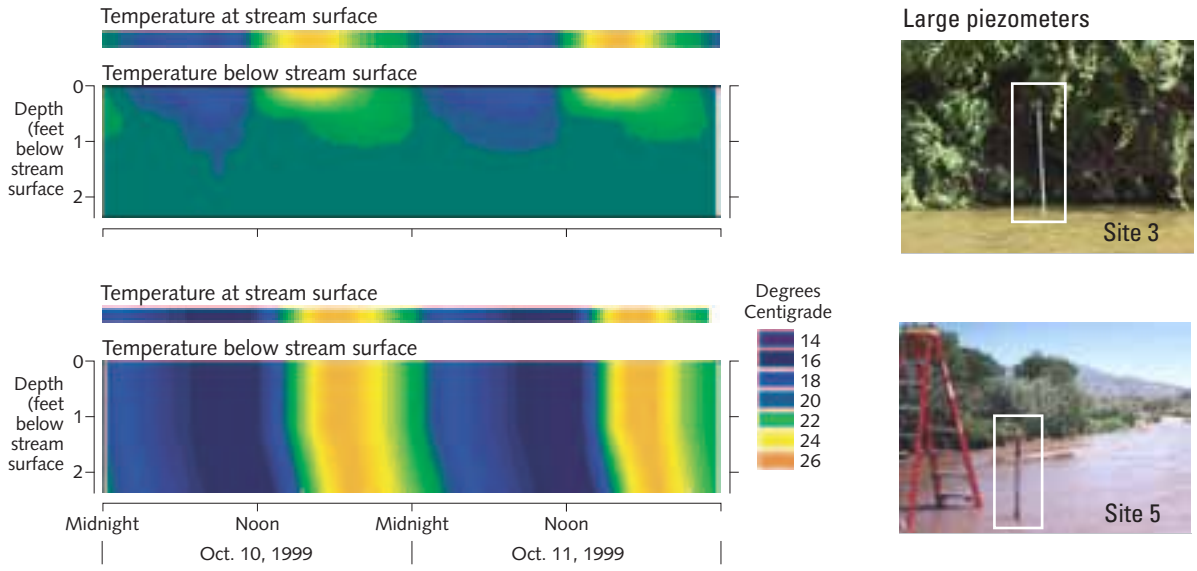

Figure 8. Observed streambed temperatures measured in large piezometers at Site 3 and Site 5, with the observed water temperature shown in the thin band at the top of each temperature contour.

streambed temperature data can be used as model input to predict both the vertical and horizontal movement of water in and out of the shallow streambed.

In conclusion, results from examining temperature patterns in stream sediments allows us to understand when and where stream water mixes with shallow ground water, and for how long this mixing takes place. This information then allows us to determine the amount of chemical exchange potentially occurring, which has a direct consequence on downstream water quality. Analysis of results aids hydrologists and civil engineers in predicting the impacts of future developments in the watershed on downstream water quality.

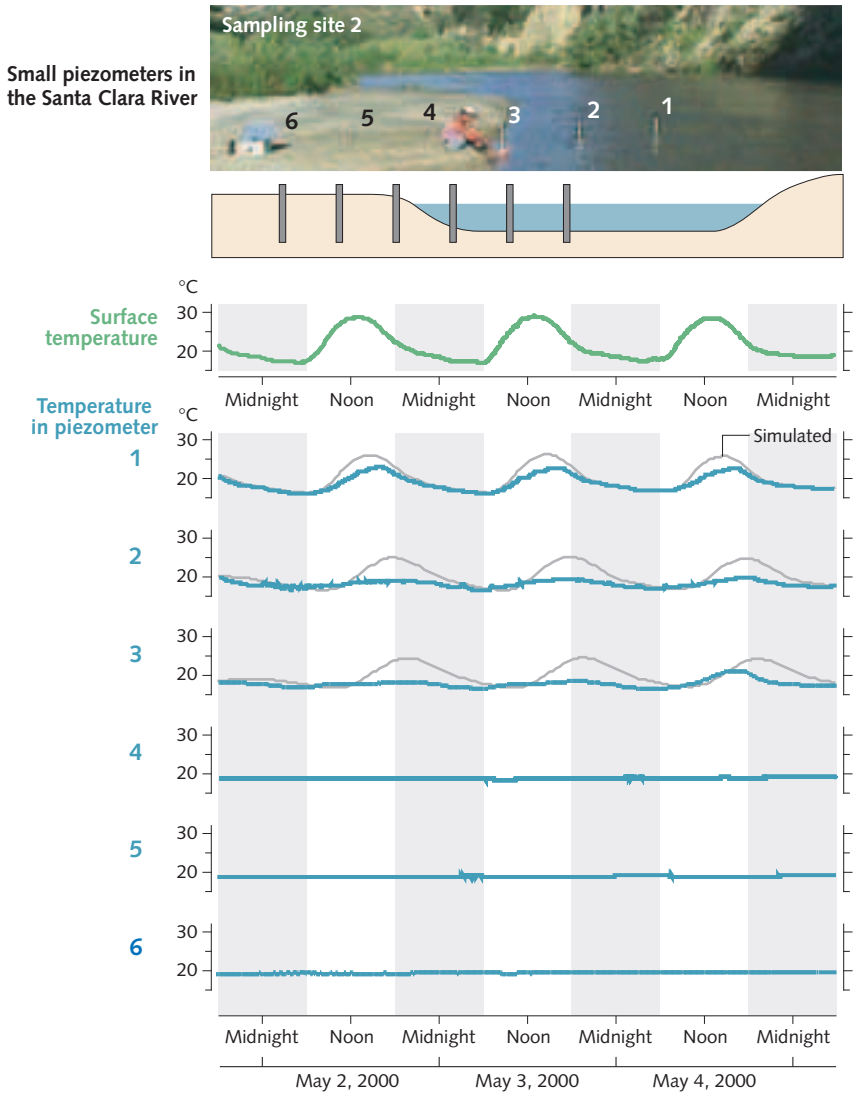

Figure 9. The observed stream temperature, the observed streambed temperature in all 6 small piezometers, and the simulated streambed temperatures for the 3 piezometers under the river for May 2-4, 2000 at Site 2, 3, and 5 along the study reach.

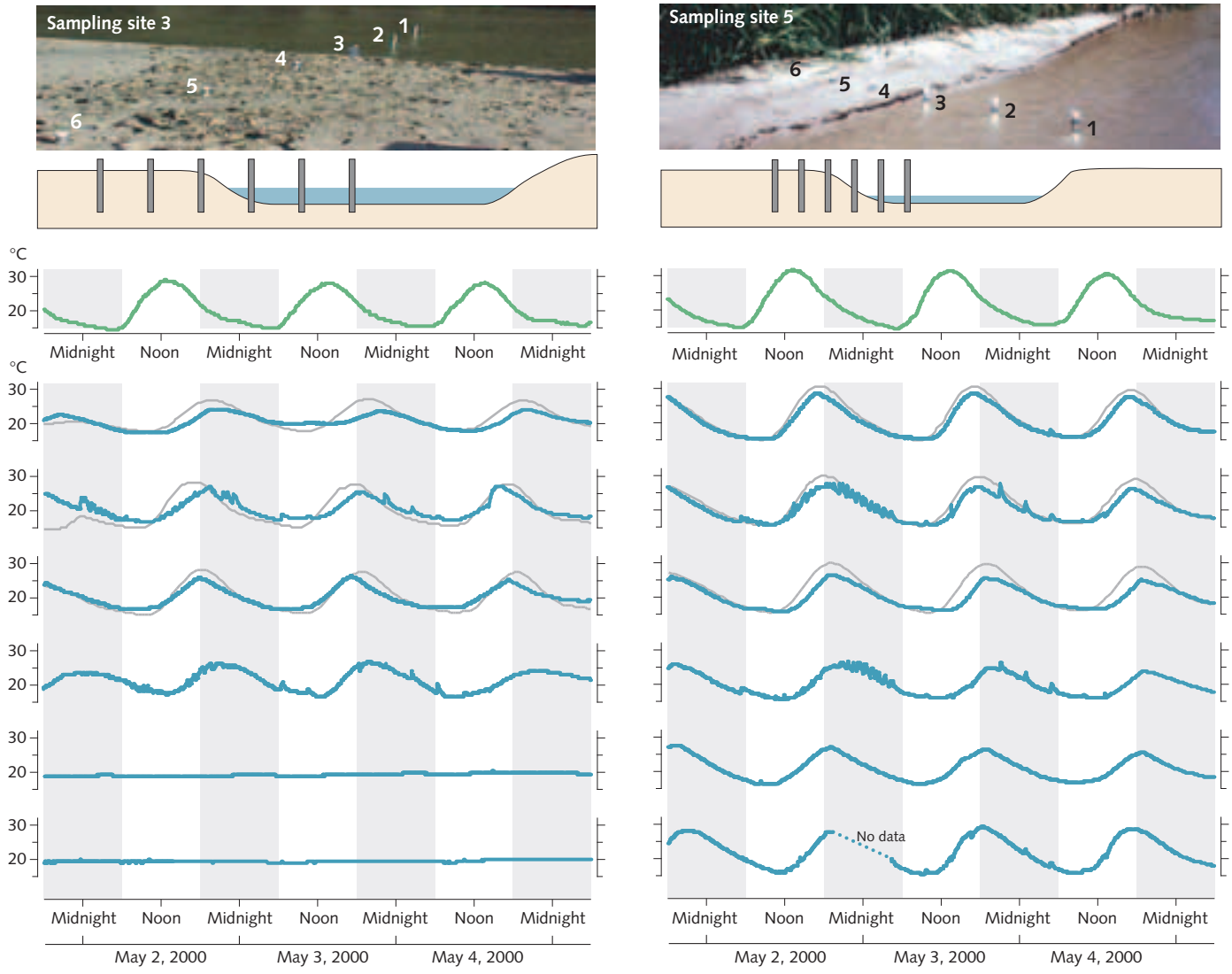
Sampling site 3
6
5
4
3
2
1
Sampling site 5
6
5
4
3
2
1
°C
30
20
Midnight
Noon
Midnight
Noon
Midnight
Noon
Midnight
May 2, 2000
May 3, 2000
May 4, 2000
No data

Chapter 5

Heat tracing in streams in the central Willamette Basin, Oregon

Terrence Conlon, Karl Lee, and John Risley

Introduction

The Willamette Basin is located in northwestern Oregon (fig. 1), extending south from Portland approximately 160 km. It is home to approximately 70 percent of the State's population and accounts for approximately 60 percent of gross crop sales in the State. The basin lowland is relatively flat, with fine-grained fertile soils. Annual rainfall is approximately 100 cm in the lowland; about 70 percent of the annual rain falls from October through March. The summer growing season is warm and dry, in contrast to the cool, moist winter months.

In the Willamette lowland, early settlers grew crops, such as wheat, that required little, if any, irrigation. As markets and technology changed, irrigation of a diverse group of crops has evolved. The demand for irrigation water has grown as the number of acres cultivated for crops requiring irrigation, such as nursery stock and row crops, has increased. In the dry, summer months, when irrigation demand is high, agricultural fields are irrigated with ground water withdrawn from wells and surface water withdrawn from streams. Irrigation from surface water is generally restricted to land adjacent to large perennial streams, where water is directly pumped from the stream to the fields, because there are few irrigation canals in the basin. Additional withdrawals from many streams in the Willamette lowland are restricted during the summer to protect the water rights of existing users, and to provide summer flows for fish habitat and pollution abatement. Increasing demand for irrigation water supply will likely be satisfied from ground water.

In the Willamette lowland, ground water naturally discharges to streams in many areas. Withdrawal of ground water from wells can capture ground water that naturally discharges to streams. In some cases, pumping ground water can lower water levels in aquifers near streams and reverse the flow of ground water so that stream water flows into the aquifer. These interactions between surface and ground waters are proportional to the head gradient between the stream and ground-water system, which may be related to the amount of water withdrawn from wells near the stream, and the hydraulic properties of the streambed.

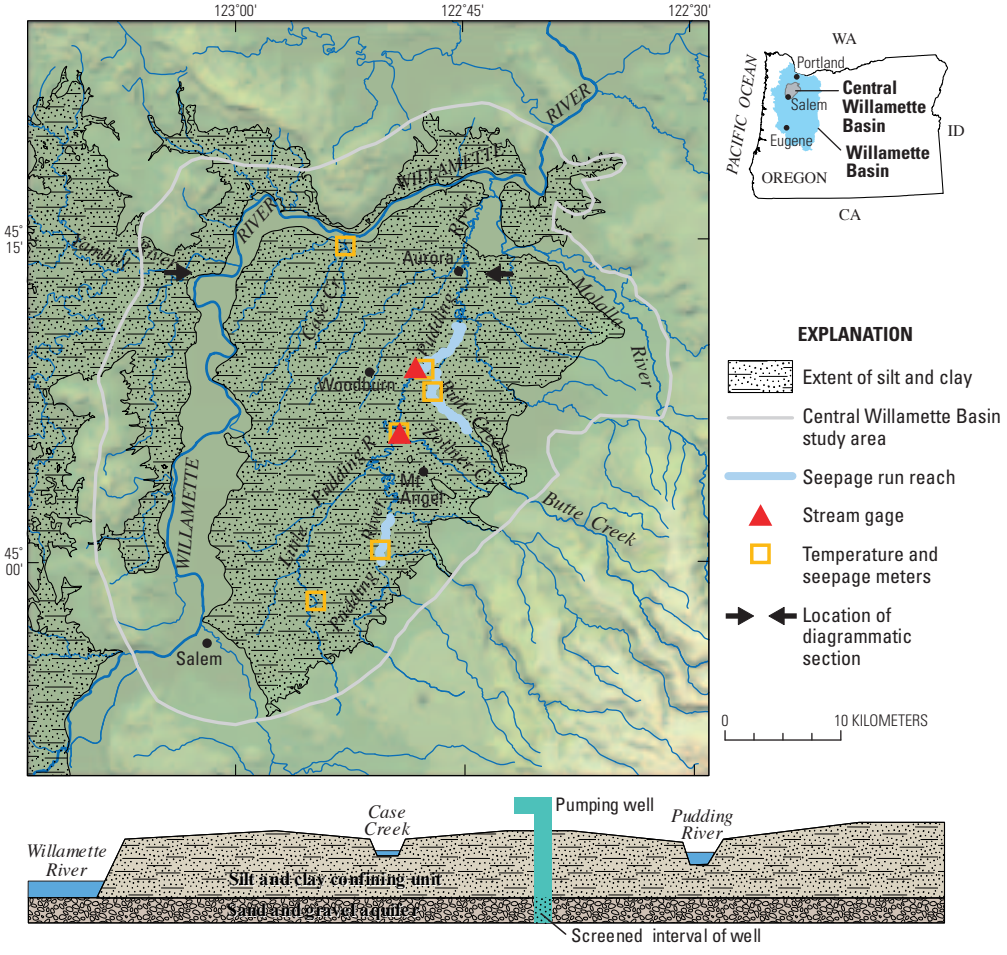

Figure 1. Location of seepage measurements and diagrammatic section, central Willamette Basin, Oregon

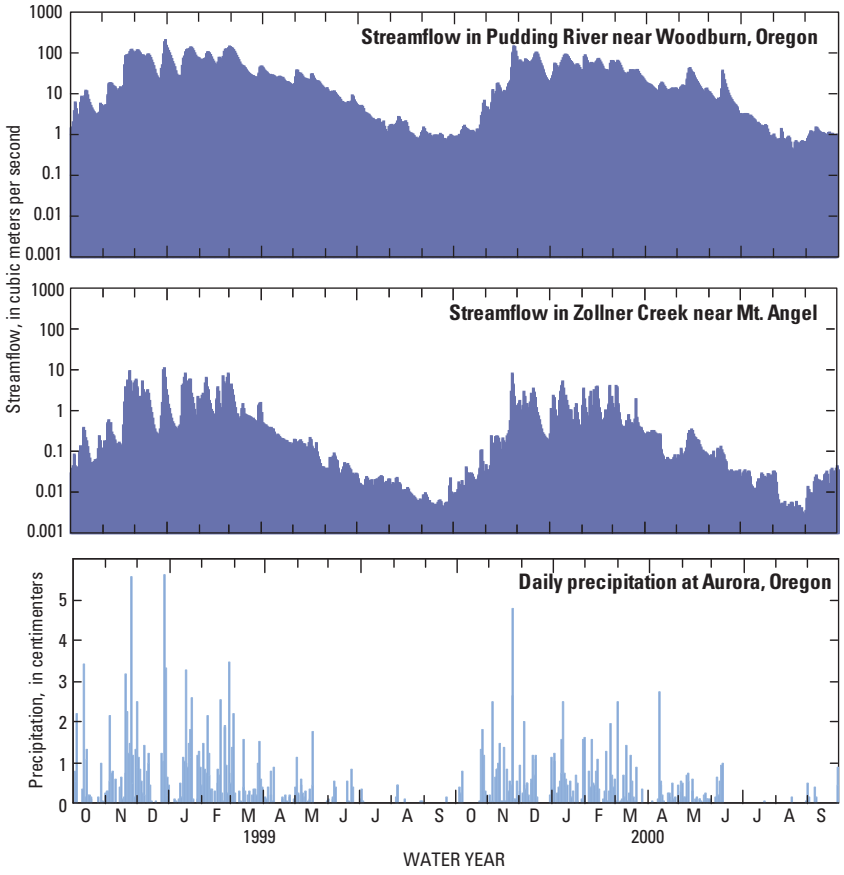

Figure 2. Streamflow and precipitation in the central Willamette Basin, Oregon

To better understand the interactions, it is necessary to quantify the amount of water that discharges, or seeps, from the aquifer to the stream, and the permeability of the streambed. This chapter discusses streambed seepage measurements made using heat as a tracer at six locations within the central part of the Willamette lowland and compares these measurements with measurements made using other techniques.

Streambed and streamflow characteristics

Most streams in the central Willamette Basin are perennial, or flow year round (fig. 2). Generally, the streambeds consist of fine-grained sediment, except in the Willamette River and the lower reaches of the Pudding and Molalla Rivers, which have gravel streambeds. The fine-grained sediment is mainly silt and clay (fig. 1) that was deposited as backwater deposits by repeated cataclysmic floods from breaching of ice-dammed lakes during the ice ages between 15,000 and 13,000 years ago. The silt and clay form a relatively flat terrace with elevations ranging from 30 m in the north to 100 m in the south. Thickness of the material ranges from 10 to 30 m. Beneath the fine-grained sediments are permeable sand and gravel deposits, from which wells withdraw ground water.

Streamflow in the smaller streams is greatest in the wet winter months and diminishes in the dry summer and fall months. Because the headwaters for these streams are either in the lowland or the foothills of the Cascades, snowmelt

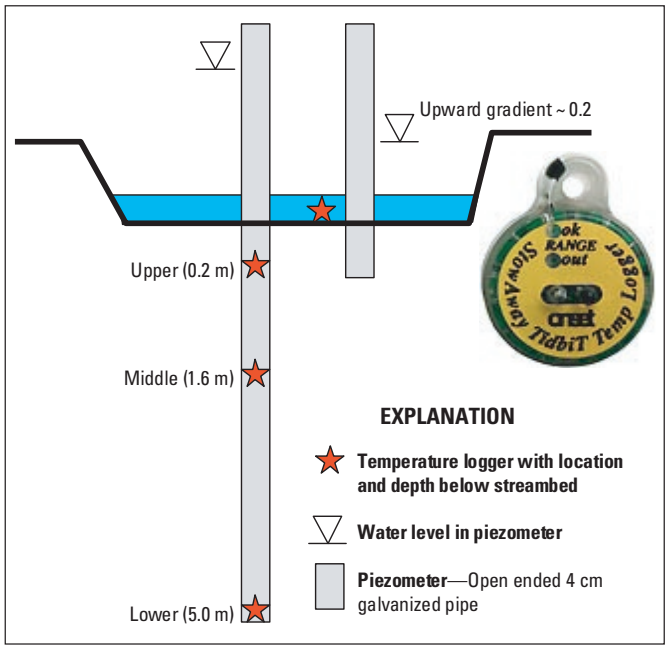

Figure 3. Diagram of installation to measure temperature and hydraulic gradient, Zollner Creek

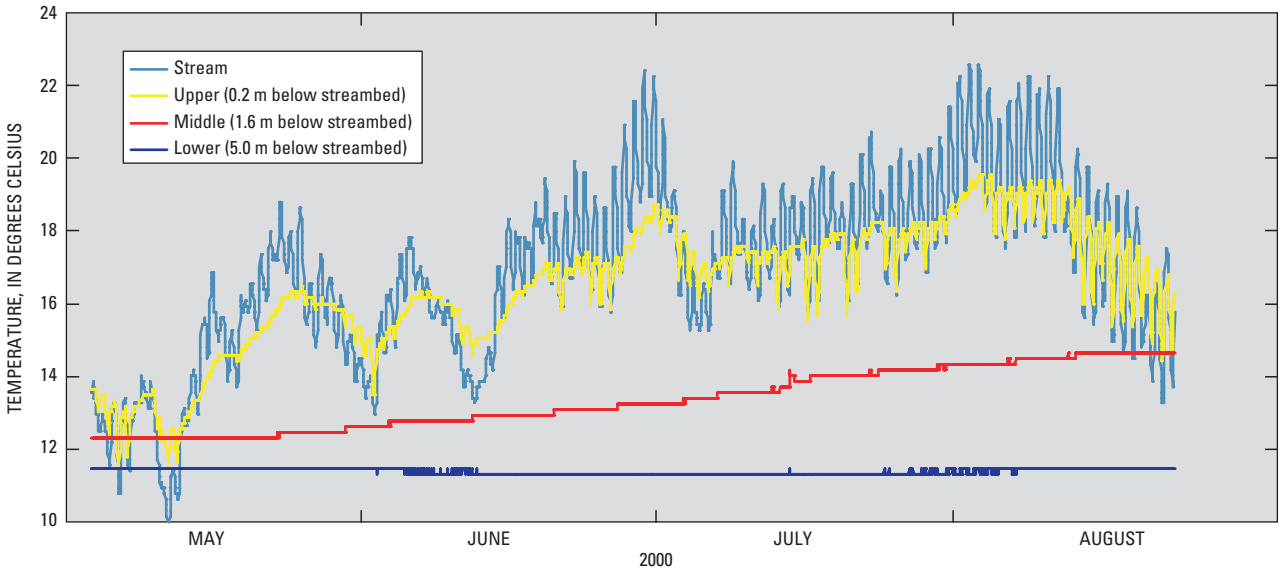

Figure 4. Observed temperatures, Zollner Creek

does not contribute water directly to these streams in summer. Beneath the streams, ground water generally flows upward, discharges to streams in the lowland, and helps to maintain stream flow in the dry summer months. Using heat as a tracer along with other methods, the amount of ground water discharging to streams was estimated at locations along several streams of interest.

Techniques to measure stream seepage

Three methods were used to measure the flow of water between aquifers and streams during the dry period of August 2000: heat as a tracer, seepage runs, and seepage meters. Six streams were instrumented with temperature sensors and seepage meters (fig. 1). The six streams can be classified by size and streambed material (table 1). Seepage runs were conducted on reaches of streams that included three of the six sites.

Using heat as a tracer requires measuring temperature in the stream and streambed over an extended period of time. Piezometers were hand-driven into the streambed at six locations (fig. 1) to measure temperature at different depths within the streambed, and to measure hydraulic gradients between the stream and ground water. A diagram of an installation is shown in figure 3. Water levels in the piezometer represent the water pressure at the bottom of the open-ended piezometer. Because the streambed is always saturated and the steel piezometer readily conducts heat, the temperature of the water in the piezometer is assumed to be in thermal equilibrium with the streambed temperature; that is, the temperature of the water in the piezometer reflects the adjacent streambed temperature (see Appendix A). Temperature loggers were sus-

Table 1. Characteristics of instrumented streams

Stream Name	Width (m)	Spring flow m^3/s	Fall flow m^3/s	Streambed Material	Temperature	Seepage Meter	Run
LARGE STREAMS							
Butte Creek	8	3	0.3	sandy silt	x	x	x
Lower Pudding River	15	10	1	sandy silt	x	x	x
Upper Pudding River	10	–	0.7	clayey silt	x	x	x
SMALL STREAMS							
Case Creek	3	0.1	0.05	clayey silt	x	x	
Little Pudding River	3	–	0.1	clayey silt	x	x	
Zollner Creek	3	0.06	0.02	clayey silt	x	x	

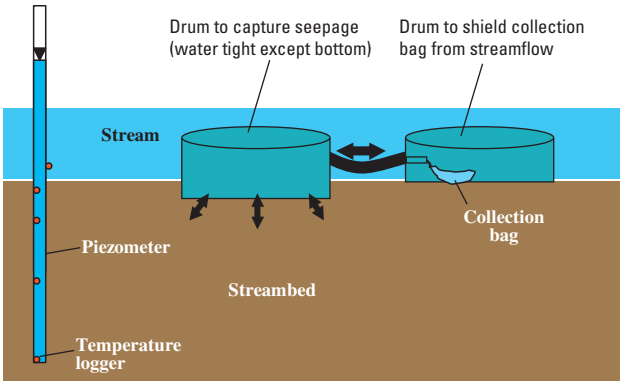

Figure 5. Diagram of seepage meter

pended within the piezometer to measure streambed temperatures at different depths below the stream. Streambed temperatures at shallow depths are similar to the stream temperature, while streambed temperatures at greater depths are generally colder and slowly increase with time during the summer (fig. 4). At the bottom of the well, streambed temperatures fluctuate less over time and represent the ground-water temperature with little effect from fluctuating surface temperatures (see Chapter 1).

The streambed temperature patterns beneath the streams at the six sites were modeled using the simulation code VS2DH to estimate seepage by matching simulated temperatures to observed temperatures (see Appendix B). Observed temperatures from the middle sensor were used to calibrate VS2DH models because at this depth temperatures exhibit seasonal variation and possible heat conduction down the steel piezometer is minimized.

During the summer of 2000, seepage was also estimated using seepage runs and seepage meters to compare with estimates from heat tracing. For seepage runs, streamflow is measured at two points along a stream reach, and after accounting for stream diversions and tributary inflow, the difference between the two measurements represents a seepage gain to or loss from the stream. If downstream flow is greater than upstream flow, the stream gains; if downstream flow is less than the upstream flow, the stream loses water to the aquifer (Riggs, 1972). Seepage run estimates where seepage is small relative to streamflow are often inconclusive or difficult to interpret because seepage is calculated from the difference of two streamflow measurements. The two streamflow measurements, in low seepage environments, are practically identical and the difference may be attributable to measurement error rather than seepage. Therefore, where seepage is relatively small, it is important to have other methods available, such as heat tracing and seepage meters, to estimate seepage.

Seepage meters measure the amount of water that enters or leaves an open-ended drum that is open to the streambed (Lee and Cherry, 1978). The seepage is measured by comparing the initial and final volumes of water in a bag connected to the seepage meter (fig. 5). Flow into the drum represents a gain to the river; flow out of the drum represents a loss from the river. To compare seepage run and meter results to heat tracing, the amount of water entering the reach or drum per unit time is divided by the area so that the rate of inflow can be directly compared to heat tracing estimates.

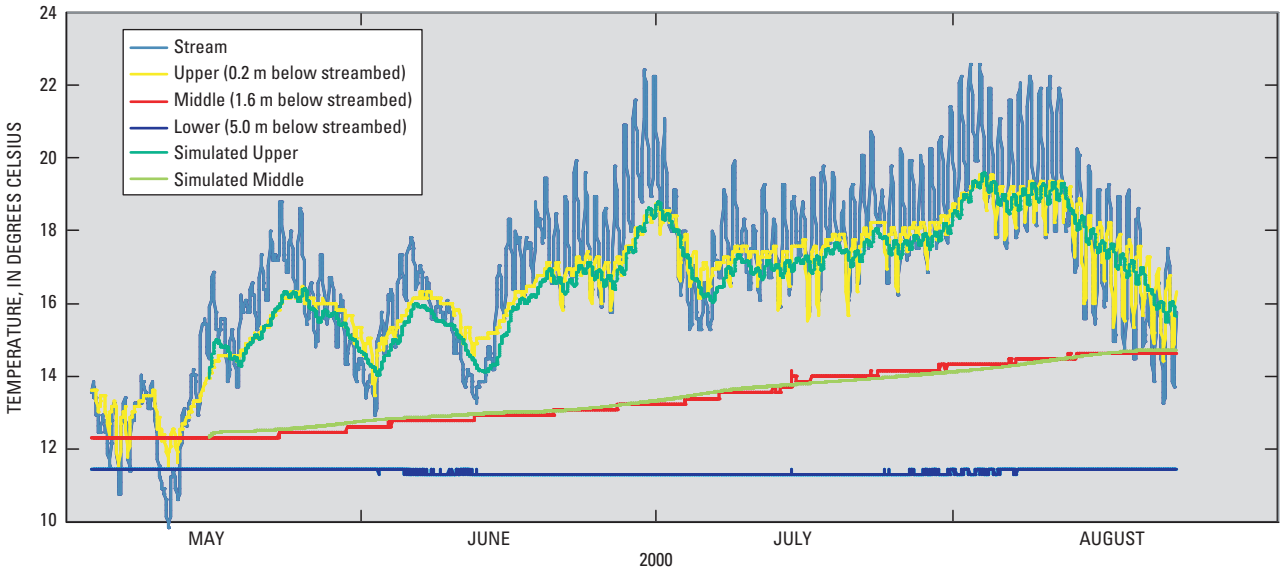

Figure 6. Simulated and observed temperatures, Zollner Creek

Seepage and streambed permeability from temperature measurements

The seepage values estimated using heat as a tracer in the central Willamette Basin are small compared to other seepage rates documented in this circular because of the relatively low permeability of the streambed material in the basin. The fit of simulated and observed values at most sites was similar to the close fit at Zollner Creek (fig. 6). Except for Case Creek, seepage was greatest in larger streams (lower Pudding River and Butte Creek) with some sandy material in the streambed (figure 7 and table 1). In smaller streams with fine-grained material in the streambed (Zollner Creek and Little Pudding River) and one large stream with a fine-grained streambed (upper Pudding River), seepage was less significant.

The variation in seepage was a result of different hydraulic gradients and hydraulic conductivities at each site. Because the hydraulic gradient at some sites was measured, the hydraulic conductivity can be estimated (Chapter 1). The variation in hydraulic conductivity ranged from 1 x 10^{-7} to 2 x 10^{-6} m/s (fig. 8), which is similar to published values for silt (Freeze and Cherry, 1979). Seepage in Zollner Creek was low (fig. 7) because the hydraulic conductivity is relatively low (fig. 8) and the hydraulic gradient is average. Seepage in the lower Pudding River is relatively high, despite an average hydraulic conductivity, because the hydraulic gradient is relatively high.

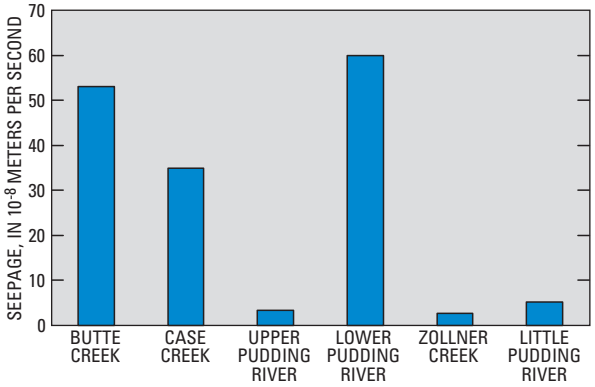

Figure 7. Seepage estimates using heat as a tracer

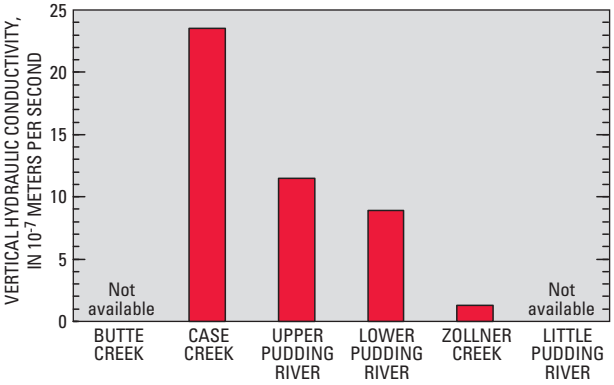

Figure 8. Vertical hydraulic conductivity estimates using heat as a tracer

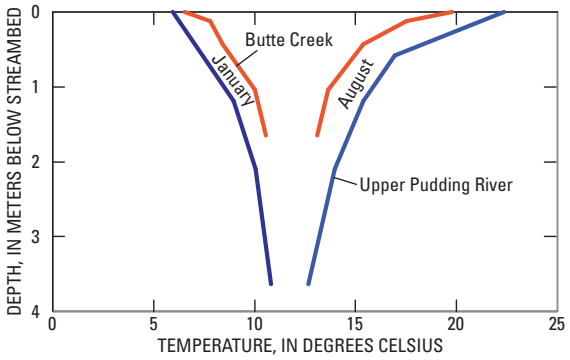

Figure 9. Temperature envelopes for two selected streams

Because seepage is the product of hydraulic conductivity and gradient, low seepage values may be the result of small values of hydraulic conductivity and/or gradient. As stated above, the streambed hydraulic conductivity is relatively low and reflects the fine-grained and compacted characteristics of the streambed at the six sites. The seepage values simulated using VS2DH for some locations are at the low end of sensitivity of the model; that is, simulating the streambed with a lower hydraulic conductivity will not change the simulated temperature significantly because the seepage was already very low. At low hydraulic conductivities (or hydraulic gradients), the model becomes increasingly sensitive to thermal properties, such as heat capacity and thermal conductivity. Thermal properties eventually become more important than hydraulic conductivity in simulating seepage.

Annual streambed temperature envelopes (Chapter 1) support the variability in estimated seepage. Because upward ground-water flow occurs at all six sites, a "collapsed" or shallow temperature envelope is expected at all sites. The greater the upward flow, the narrower and more collapsed the envelopes should be. This is evident for annual temperature envelopes for Butte Creek, a stream with relatively large upward flow, and the upper Pudding River, a stream with relatively low upward flow. Butte Creek's envelope is narrower, suggesting a greater rate of upward flow of ground water.

Comparison of seepage measurement methods

Seepage estimates using seepage runs and seepage meters were compared to heat tracing estimates. Generally, seepage estimates from the heat tracing method provided the highest estimate of seepage, except for Zollner Creek and Butte Creek, where seepage meter and seepage run measurements were greater (fig. 10). Generally, seepage estimates from the seepage meter method provided the lowest estimates. Estimates from seepage runs are difficult to compare with other methods because of measurement uncertainty and the assumptions used to convert volumetric seepage over a reach to a seepage

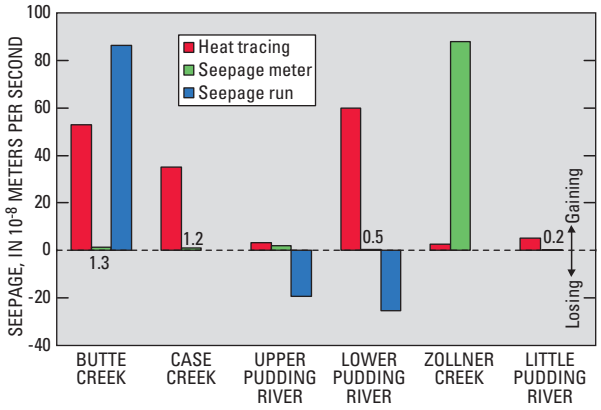

Figure 10. Comparison of seepage estimates using three methods

rate per area. Seepage estimated from seepage runs for Butte Creek compares well with the seepage estimated using heat as a tracer. Seepage was approximately 15 percent of streamflow in Butte Creek and was greater than the uncertainty in the measurements used in the seepage run.

A loss of stream water was indicated by seepage runs along the upper and lower Pudding River, which contradicts the gains measured by seepage meters and heat as a tracer. There are two possible explanations: (1) if the selected reach includes both losing and gaining subreaches, the sum of the seepage may be a loss from the stream to the ground-water system, but a seepage estimate using a point measurement method may indicate a gain from aquifer to the stream, and (2) the stream losses may, in fact, not be losses because the losses were within the uncertainty of the seepage run measurement. Although the seepage estimates at a particular site vary more than one order of magnitude, they provide a range that constrains the magnitude of the interaction between surface and ground water and can be used in other applications, such as analytical and numerical models.

Ground-water flow to streams in the central Willamette Basin

The results of this study show that heat tracing techniques are an excellent method to study the interaction of aquifers and streams in the Willamette Basin. The limited seepage from the aquifer to the stream and the low hydraulic conductivity estimated by the heat tracing technique indicate that the hydraulic connection between the stream and aquifer is limited by low hydraulic conductivities. Discharge of ground water to streams occurs, but at a rate that is small (sometimes less than 5 percent) relative to streamflow, resulting in seepage estimates that were less than the uncertainty in seepage run measurements. Ground-water withdrawals from the underlying sand and gravel aquifer may capture water that would normally discharge to these streams; however, the amount of water is small relative to streamflow.

Studies using heat as a tracer in streams in Oregon have provided estimates of streambed hydraulic conductivity and seepage between streams and the ground-water system. Quantifying seepage rates and hydraulic properties of the streambed helps hydrologists and water-resource managers to understand the interaction of surface and ground waters. With an improved understanding of these interactions, managers can make informed decisions about the effect of future ground-water withdrawals on streamflow.

Chapter 6

Trout Creek—evaluating ground-water and surface water exchange along an alpine stream, Lake Tahoe, California

Kip K. Allander

Introduction

Lake Tahoe is known as the "Jewel of the Sierra" mostly because of its deep, clear water and because it is surrounded by majestic snow capped peaks (fig. 1). Lake Tahoe straddles the Sierra Nevada about 300 km east of San Francisco, California (fig. 2), and is a favorite vacation spot to millions of tourists. Unfortunately, the beauty that attracts the tourists is being threatened because the lake has been losing its clarity at a rate of about 0.5 m/yr (Goldman and Byron, 1986, p. 7). Human activity in and around the lake has resulted in increased nutrients that support an increasing algae population, which reduces the clarity of the lake (Goldman, 1988).

Nutrients enter the lake from streams, ground water, atmospheric deposition, overland runoff directly to the lake, and by shoreline erosion (Reuter and others, 1998; Reuter and Miller, 2000). Streams that discharge into Lake Tahoe may be contributing the greatest percentage of nutrients due to the relative ease with which urbanization can increase both flow and nutrients (Byron and Goldman, 1989).

Environmental improvement projects were implemented in the mid-1970s, shortly after the Tahoe Regional Planning Agency (TRPA) was created by the California and Nevada legislatures in 1969. TRPA's mission is to lead the effort to preserve, restore, and enhance the unique natural and human environment of the Lake Tahoe region (Tahoe Regional Planning Agency, 2002). Since TRPA's inception, efforts have increased by Federal, State, and regional agencies to construct Best Management Practices (BMPs) as well as other environmental improvement projects in an attempt to reduce the negative effects of human activity on Lake Tahoe and its contributing areas. One of the earliest efforts was the development of regional treatment plants that collect sewage from homes and cabins around the lake and then pump the wastewater out of the basin into neighboring valleys. More recently, increased efforts have focused on reducing sediments and nutrients that enter the lake from its many tributaries.

Purpose and Scope

Water and nutrients in tributaries consist of a mixture of overland runoff, direct precipitation, and ground water. However, little information is available on the contribution of each source on flow and nutrients in each of the tributary streams that enter the lake. Knowing the contribution of each source is important to resource managers in developing an overall strategy in reducing nutrients in the streams. The purpose of the study along Trout Creek is to provide a better understanding of flow in Trout Creek in relation to ground water and the sources of nutrients in the stream. The study along Trout Creek is part of a larger effort by the U.S. Geological Survey and the TRPA to monitor and evaluate flow and nutrients in streams tributary to Lake Tahoe. Trout Creek was chosen for study because (1) it contributes the second greatest nutrient

Figure 1. Lake Tahoe, Nevada and California, looking south from the Mount Rose Highway (Hwy. 431). [P. A. Glancy, March 2000, U.S. Geological Survey]

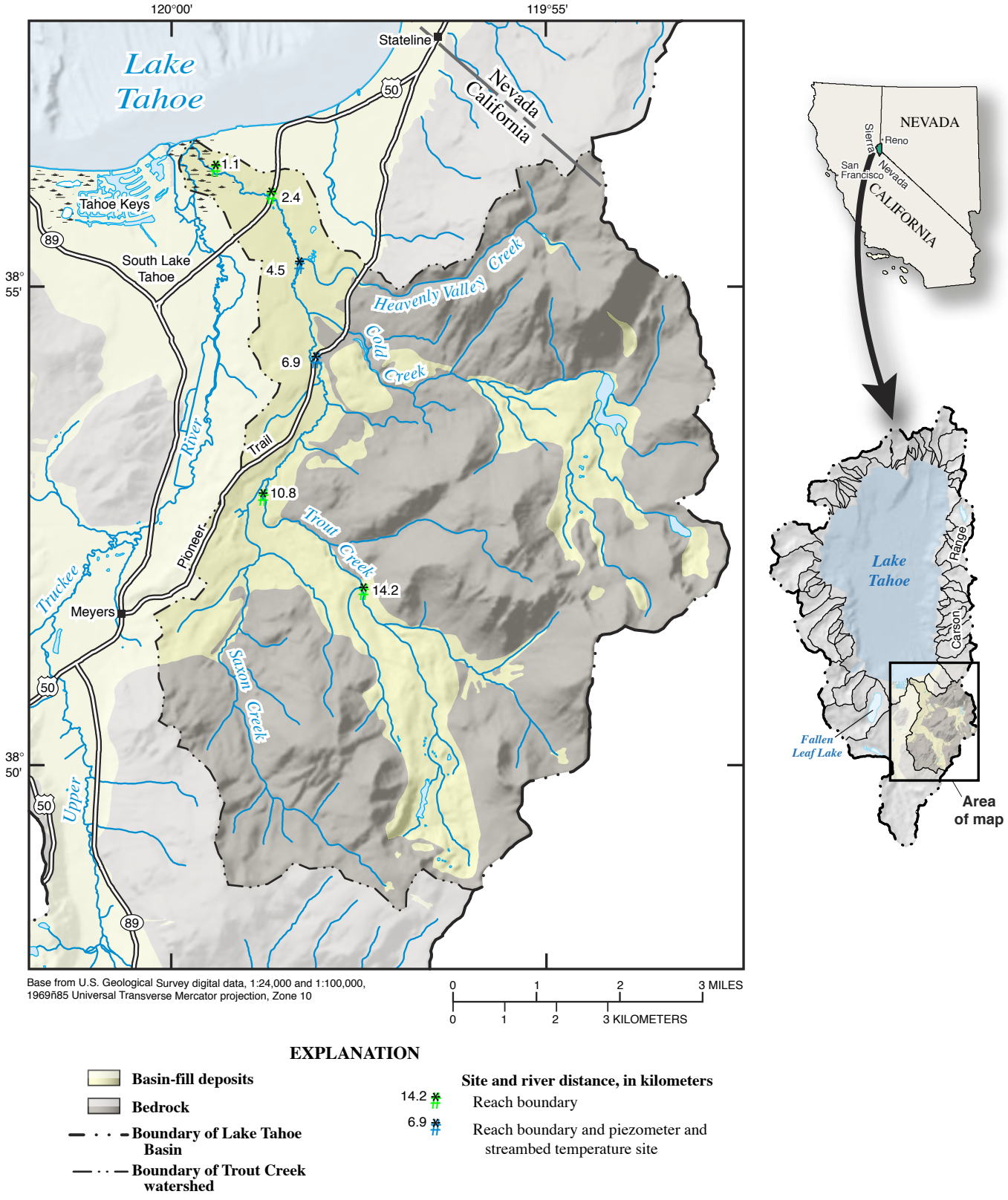

Figure 2. Location of study area

R. Whitney, January 1993, U.S. Geological Survey

Trout Creek at river distance 14.2 km above Lake Tahoe under typical mid-winter conditions; upper part of watershed is characterized by steep topography, steep stream-channel gradient, heavy forest and riparian vegetation, and deep snow pack in the winter. View is to the west looking mostly downstream.

T. G. Rowe, April 1993, U.S. Geological Survey

Trout Creek at river distance 6.9 km above Lake Tahoe under typical mid-spring conditions; middle part of watershed is characterized by gentle rolling topography, moderate to mild stream-channel gradient with meandering channel pattern, narrow flood plain with meadow being encroached by heavy forest and remnants of large winter snow pack. View is to the south looking upstream.

K. K. Allander, October 1999, U.S. Geological Survey

Trout Creek at river distance 4.5 km above Lake Tahoe under typical early fall conditions; lower-middle part of watershed is characterized by mostly flat with occasional low hill topography, mild stream-channel gradient with a mostly meandering stream-channel pattern, a moderately wide flood plain that is mostly meadow but with frequent riparian vegetation. View is to the south looking downstream from the Martin Avenue Bridge. Picture also shows in-channel instrumentation used to monitor stream stage, shallow ground-water levels, and streambed temperatures.

K. K. Allander, September 1996, U.S. Geological Survey

Trout Creek at river distance 1.1 km above Lake Tahoe under typical early fall conditions; lower part of watershed is characterized by nearly flat topography, very mild channel gradient with poorly defined channel geometry with frequent divergence of flow, large meadow that transitions into marsh before entering into Lake Tahoe. View is to the east looking upstream.

Figure 3. Photographs showing variability of Trout Creek watershed and stream characteristics.

and suspended-sediment load to Lake Tahoe (Rowe and others, 2002), (2) it has been urbanized along most of its lower reach, (3) it has extensive ongoing monitoring of surface and ground water, and (4) it is being restored by channel reconstruction throughout the developed urban area.

This chapter describes how streamflow, water-level, and temperature measurements were used to evaluate changes in ground-water contributions to Trout Creek. Recently, studies demonstrated that the combined analysis of streamflow and temperature aids in the delineation of losing versus gaining reaches along alpine streams (Constantz, 1998). For Trout Creek, the temperature measurements along with differences in water levels between the stream and the shallow ground water were designed to evaluate periods when ground water is contributing flow to the stream at two sites along the lower reach of the stream.

Description of Study Area

Although Trout Creek has the same name as the Trout Creek near Battle Mountain, Nevada, which is described in Chapter 8 of this report, the streams are distinctly different. This creek drains the west side of the Carson Range south of South Lake Tahoe (fig. 2) and has many small mountain tributaries. Trout Creek is perennial along much of its course and flows through large meadows and a marsh (fig. 3) before discharging to the south end of Lake Tahoe. Bedrock is composed mostly of Cretaceous age granodiorite of the Sierra

Nevada batholith (Tahoe Regional Planning Agency and U.S. Forest Service, 1971). The basin fill near the base of the mountains is mostly fluvial sand and gravel mixed with glacial deposits. The basin-fill sediments become finer near Lake Tahoe and grade mostly into sand with layers of silt and clay. Major tributaries to Trout Creek are Saxon Creek, Cold Creek and Heavenly Valley Creek (fig. 2). Annual precipitation in the Trout Creek watershed ranges from about 50 to 100 cm and occurs mostly as snow during the winter. However, significant precipitation may occur in the spring and fall as rainstorms or during the summer as thunderstorms. Hydrographs (fig. 4) for Trout Creek for water year 1996 reflect the seasonal climate patterns by exhibiting higher prolonged flows during spring snowmelt runoff as well as smaller duration peaks from rain events that can occur anytime of the year.

Methods Used to Evaluate Ground-Water Exchange Along Trout Creek

Streamflow measurements were made in the headwaters and along the main channel of Trout Creek, and at all the tributaries that were contributing flow to the main channel to estimate ground-water exchange along Trout Creek. Because streamflow measurements only provide an estimate of gains and losses during a specific time, two sites on Trout Creek were selected for continuous monitoring of seepage characteristics. Stream stage, ground-water levels, and subsurface temperatures were monitored at these two sites to evaluate if ground-water exchange varied during the year.

Streamflow Measurements

A series of streamflow measurements along Trout Creek and its tributaries were initially made on September 26, 1996, to identify reaches of Trout Creek that were gaining or losing flow from or to ground water. The measurements were made in the fall to minimize the influences of evapotranspiration and seasonal storms. Streamflow gains and losses from ground water along selected reaches of Trout Creek were estimated by subtracting all tributary flows along a reach and flow at the beginning of a reach from flow at the end of a reach. Cumulative gains from ground water were calculated by adding the

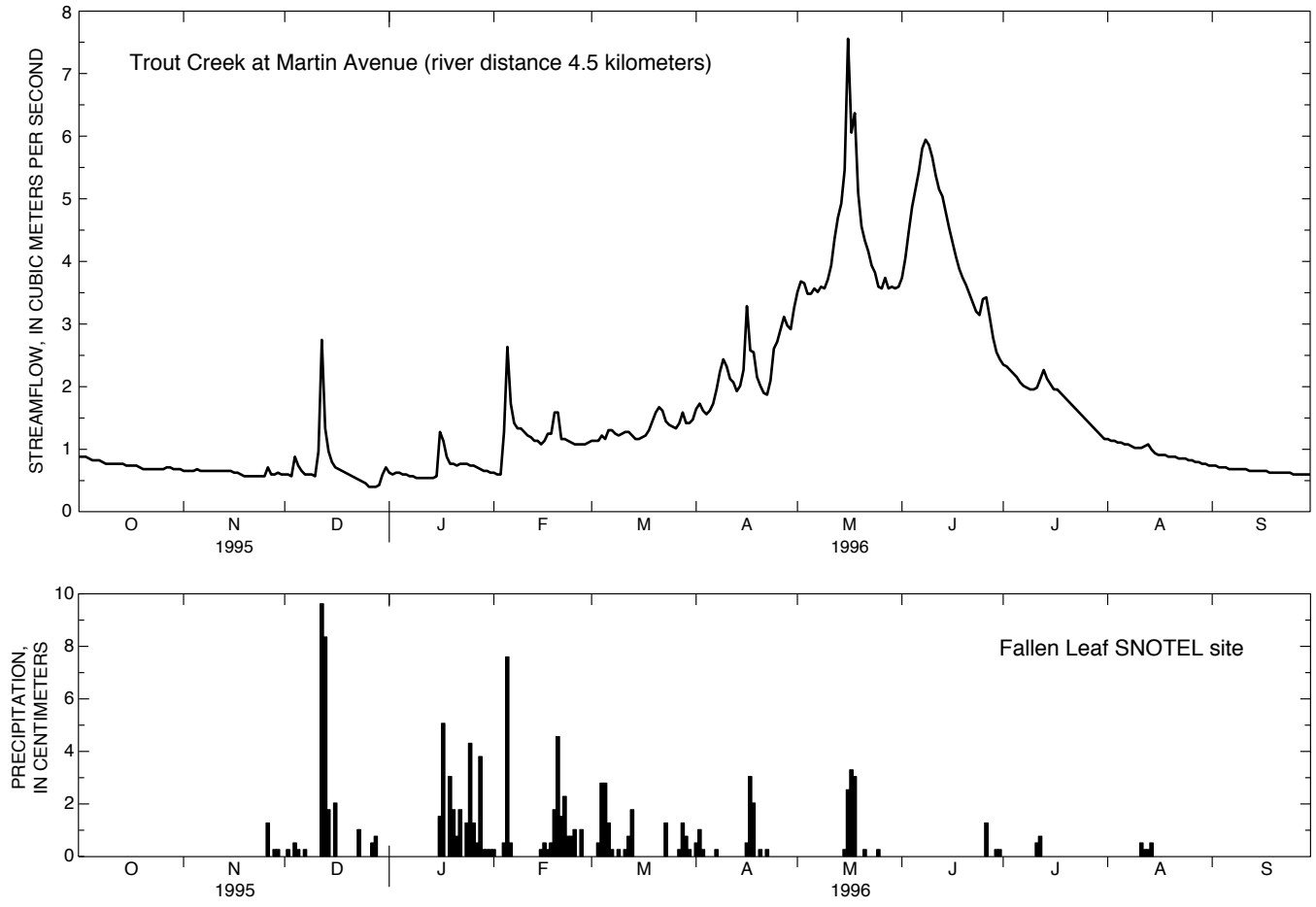

Figure 4. Hydrographs showing streamflow for Trout Creek near Tahoe Valley and daily precipitation below Fallen Leaf Lake, 1996 water year (precipitation data courtesy of USDA National Resource Conservation Service).

gains and losses from each reach in the downstream direction starting with zero gain at the most upstream measurement. Seepage rates per unit stream width were estimated for each reach by dividing the overall gain or loss between measurements by the length of the stream between measurement locations. The streamflow measurements were repeated each October from 1997 through 2001.

Water-Level Measurements

The two sites used are Trout Creek at Pioneer Trail near South Lake Tahoe and Trout Creek at Martin Avenue near Tahoe Valley (sites 4.5 and 6.9, respectively, fig. 2). During late-September 1999, two shallow monitoring wells were installed at each site about 7.5 m out from the edge of each stream bank (figs. 5A and 5B). Each well was placed between 2.1 and 3.0 m below land surface. A third monitoring well was installed near the thalweg of the main channel at each site and was 2.1 m below the streambed. Stream stage and the water level in the well beneath the streambed were monitored every 30 minutes using pressure transducers. Wells on the stream banks were monitored approximately once every 2 weeks using a standard engineers steel tape. Reference measurements were made for stream stage and in the well beneath the streambed to verify the pressure transducer measurements. Elevation of the tops of all wells were determined by running levels from known reference marks after initial installation then remeasured once each summer through the period of study.

Temperature Measurements

During September 1999, five thermocouple sensors were installed at the two sites at depths of 0.15, 0.6, 0.9, 1.5, and 2.1 m below the streambed and were located next to the streambed piezometer. The thermocouple sensors were logged at half-hour intervals. A description on thermocouple temperature sensors and their theory of operation is described in appendix A.

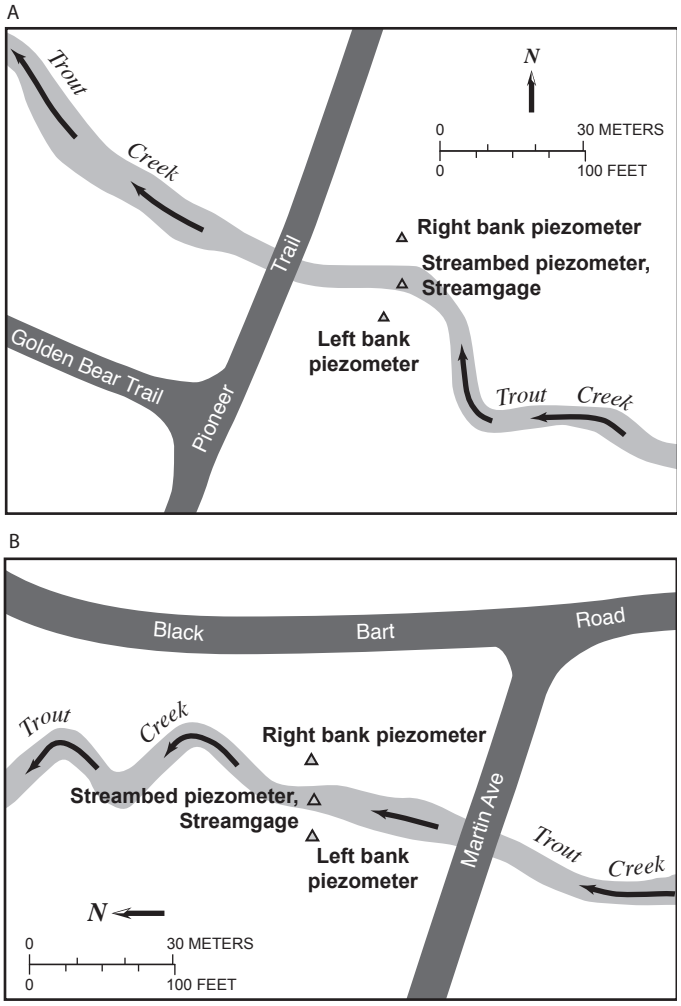

Figure 5. Site map sketch of Trout Creek at Pioneer Trail (A), and Trout Creek at Martin Avenue, near Tahoe Valley (B), California.

Ground-water exchange along Trout Creek

Streamflow measurements in Trout Creek were used to characterize flow, and to measure cumulative exchange between the ground water and stream during the fall periods. Water-level and streambed temperature measurements were used to monitor the directions of exchange between the shallow ground water and stream throughout the year.

Streamflow

Streamflow measurements in Trout Creek generally increased downstream (fig. 6A). Flow in Trout Creek each fall generally reflected the amount of precipitation that fell during the previous winter. Flows were greatest for measurements in September 1996 and October 1997-99. These flows correspond to previous winters in which precipitation was above normal. Flows during October 2000 and 2001 were much less than the above periods and reflect much lower precipitation during the previous winters. Following wet years, flow in Trout Creek between measurement sites at 4.5 and 1.1 km upstream of Lake Tahoe (fig. 2) would remain steady or increase slightly, however, following dry years, flow decreased (fig. 6A). Heavenly Valley Creek enters Trout Creek just below the site at 4.5 km upstream of the lake but its contribution generally is negligible during the fall. Similarly, Saxon Creek adds some flow to Trout Creek between measurement sites at 10.8 and 6.9 km upstream of the lake, but the majority of tributary inflow to Trout Creek is from Cold Creek between measurement sites at 6.9 and 4.5 km upstream of the lake. Inflow from Cold Creek about doubles the streamflow in Trout Creek. The elevation of Lake Tahoe ranged from 1902.8 m on October 19, 2000, to 1903.5 m above sea level on October 15, 1998, then dropped 3 m to an elevation of 1899.8 on October 17, 2001 (fig. 6A).

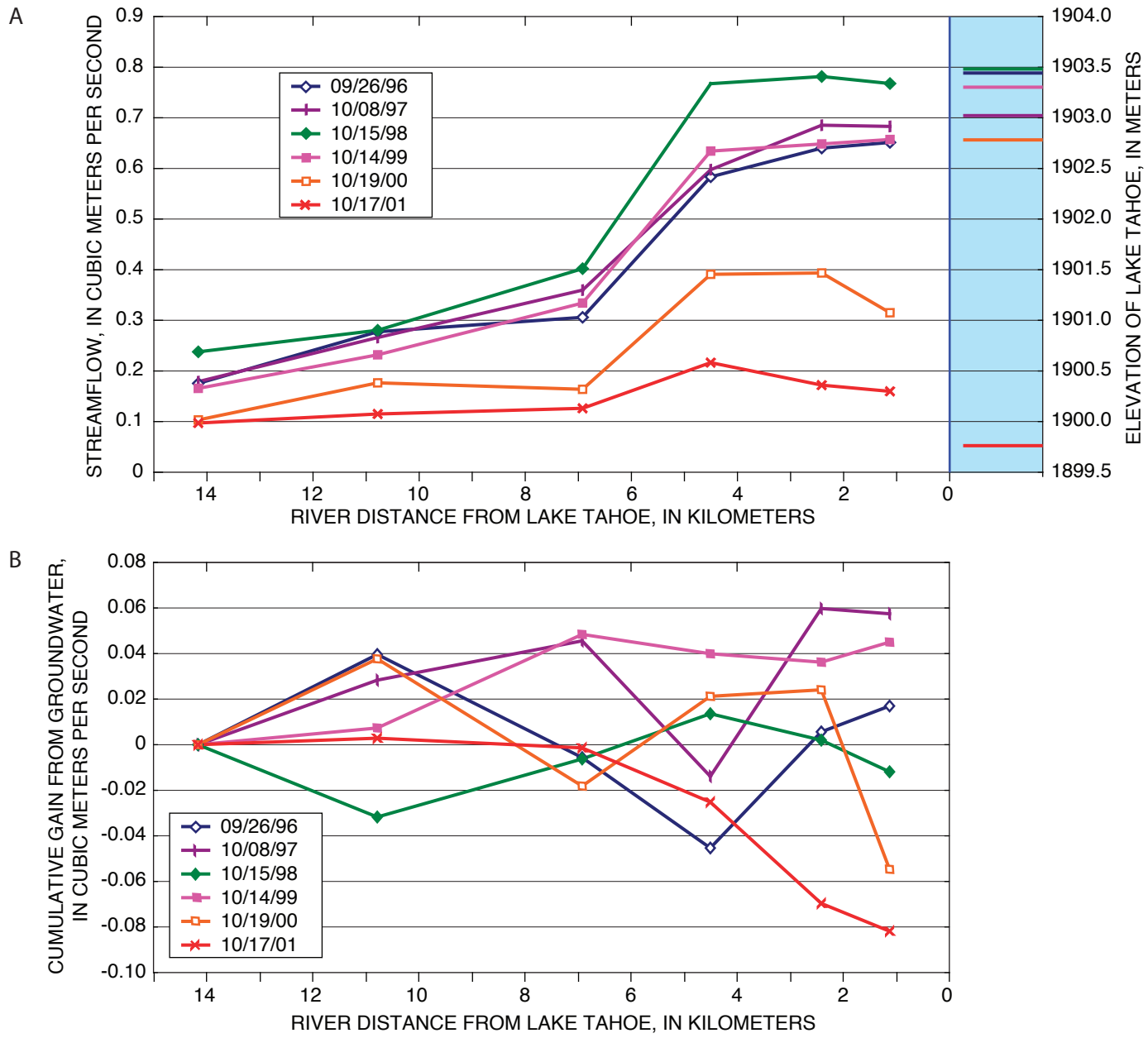

Figure 6. Instantaneous streamflow (A) and cumulative gains (B) along Trout Creek.

The cumulative gain from ground water along Trout Creek for each measurement beginning in September 1996 and continuing each October through 2001 showed a mixed pattern of gains and losses along the stream (fig. 6B), which indicates ground-water exchange along the stream is dynamic from year to year. Generally, however, Trout Creek gained flow between the uppermost and lowermost measurement sites following winters of above normal precipitation (September 1996 through October 1998) and lost flow following winters of below normal precipitation (October 2000 and 2001). On October 17, 2001, following two consecutive winters of below normal precipitation, Trout Creek was consistently losing between measurement sites 6.9 and 1.1 km above the lake and showed no gain upstream.

Water Levels

Measurements of ground-water levels adjacent to and beneath Trout Creek at Pioneer Trail and at Martin Avenue sites show patterns of ground-water exchange that vary through time (fig. 7). At the Pioneer Trail site, ground-water levels generally were above the stream from October 1999 through April 2000, from late-January 2001 through mid-May 2001, and again from mid-December 2001 through mid-Janu-

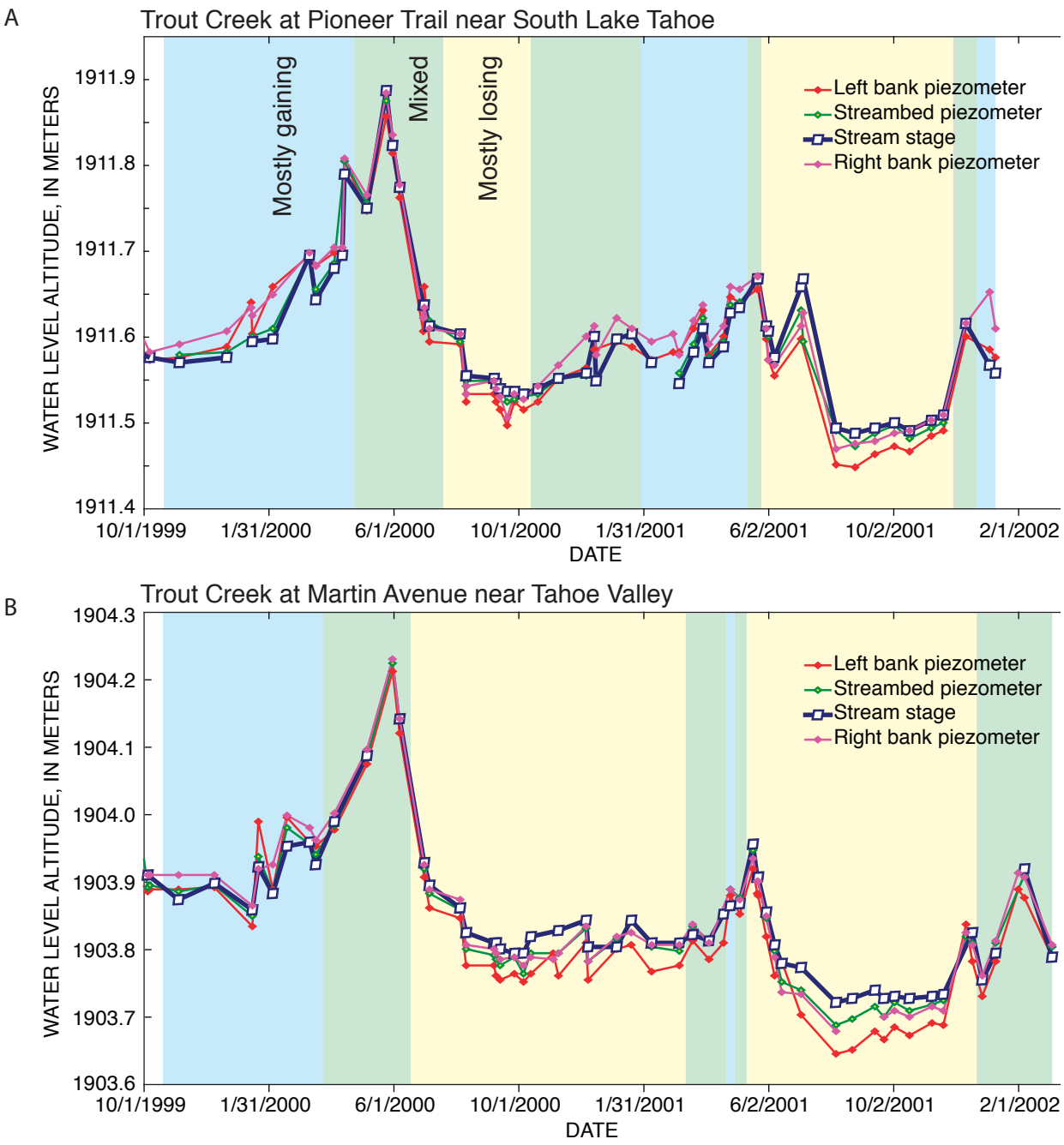

Figure 7. Water-level hydrographs of Trout Creek piezometers and stream stage.

ary 2002, which indicates ground-water flow was to Trout Creek. Ground-water levels were below the stream from mid-July 2000 to mid-October 2000 and again from late-May 2001 to December 2001, which indicates the stream was losing flow to ground water. Exchange during the remaining intervals is mixed because water levels were above the water level of the stream on one side of the stream and below on the other side.

At the Martin Avenue site, ground-water levels generally were above the water level of the stream from mid-October 1999 through March 2000, for a brief period during April 2001, and again from mid-February 2002 through early March 2002, which indicates ground-water flow was to Trout Creek. Ground-water levels generally were below the level of the stream from mid-June 2000 through mid-March 2001 and again from mid-May 2001 through December 2001 indicating the stream was losing flow to ground water. Exchange during the remaining intervals is mixed because water levels were above the stream on one side of the stream and below on the other side. Trout Creek at Martin Avenue generally had shorter periods when the stream was gaining flow from ground water

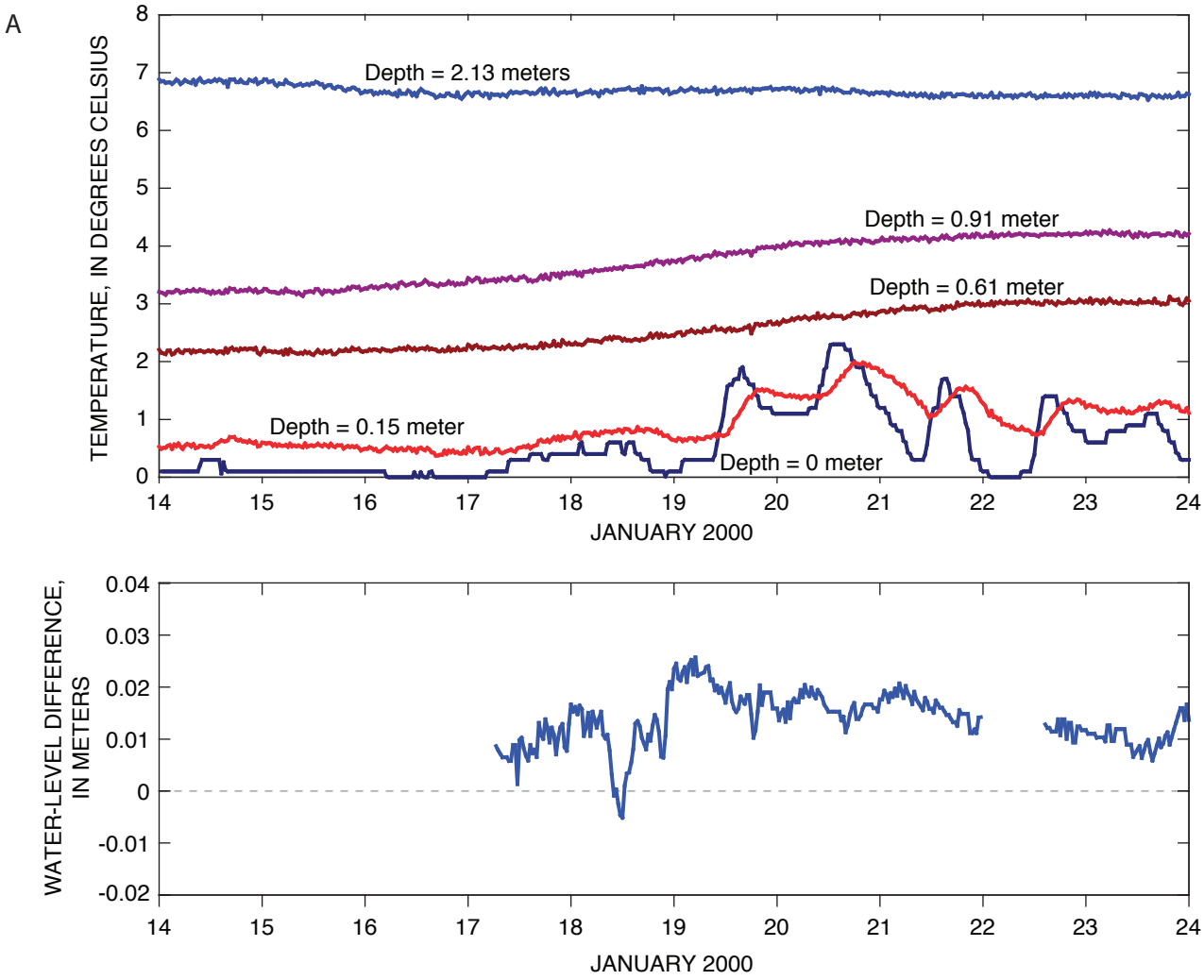

Figure 8. (A) Streambed temperature profile and difference in water level between stream and shallow groundwater (positive difference in water level indicates upward gradient) for Trout Creek at Pioneer Trail during a gaining period.

and longer periods when it was losing flow to ground water than at the Pioneer Trail site (fig. 7).

The Trout Creek at Pioneer Trail and at Martin Avenue sites exhibited a similar seasonal pattern of directions of ground-water exchange with the stream during the 2000 water year (fig. 7). Both sites were mostly gaining flow from ground water in winter and early spring periods during increasing snowmelt conditions. Both sites became a mix of ground-water exchange conditions during peak snowmelt conditions and were mostly losing flow during the end of snowmelt conditions. In water year 2001, the sites had similar patterns but with some differences in timing and duration. Trout Creek at Pioneer Trail followed a pattern similar to the previous water year, but Trout Creek at Martin Avenue had a much smaller mixed flow period and almost a non-existent period of mostly gaining conditions.

Temperature

Streambed-temperature profiles in conjunction with differences between stream and ground-water levels also can illustrate the dynamic nature of ground water exchanged at the Pioneer Trail and Martin Avenue sites (figs. 8 and 9, respectively) during the study period. An increase in the hydraulic gradient between the ground water beneath Trout Creek and the stream at Pioneer Trail on January 18, 2000 (fig. 8A, bottom graph), is reflected initially by an increase in temperature at a depth of 0.91 m with a subsequent increase in temperature at a depth of 0.61 m and then by an increase in the stream temperature (fig. 8A, top graph). Below a depth of 0.61 m, the higher temperatures and the lack of a diurnal temperature signal contrast with the diurnal temperature of the stream indicating that movement of heat is upward from below. The

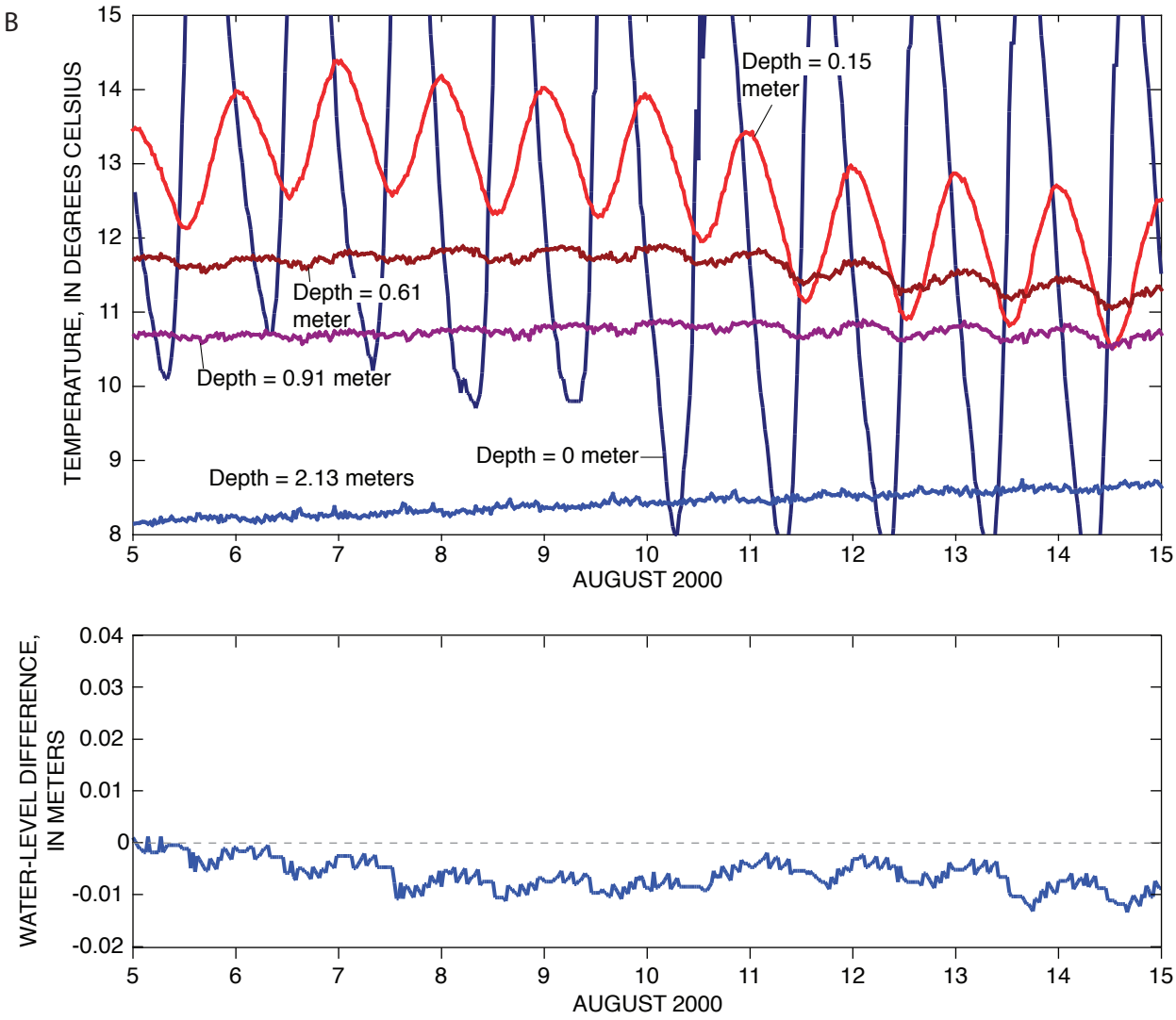

Figure 8. (B) Streambed temperature profile and difference in water level between stream and shallow groundwater (positive difference in water level indicates upward gradient) for Trout Creek at Pioneer Trail during a losing period.

increase in stream temperature prior to the increase in temperature at depth 0.15 m indicates that ground water is entering the stream above the sensors. The presence of a diurnal signal at a depth of 0.15 m indicates considerable mixing of stream water. In contrast, during August 2000, the difference between ground-water and stream levels becomes more negative, which indicates that the stream is losing flow to ground water (fig. 8B) and is reflected by the diurnal stream temperature signal being propagated to a depth of 0.91 m below the streambed.

A similar pattern in temperature was recorded at the Martin Avenue site for periods when the ground-water level was above the stage in the stream (fig. 9A) in February 2000. A rapid increase in the gradient between the ground water and the stream on February 14 resulted in a rapid increase in temperature at depths of 0.61 and 0.15 m below the streambed as well as in the stream. During the rapid increase in temperature, there were no diurnal fluctuations in stream or ground-water temperature. The diurnal signal returned in the stream once the gradient declined, however, the higher temperatures at the 0.15 m depth indicates ground water is maintaining a higher temperature immediately beneath the stream, which in turn indicates that ground water is discharging to the stream. These temperature data are consistent with the gaining period observed through the water levels of the wells adjacent to and beneath the stream during mid-October through March 2000 (fig. 7B). With the exception of December 24-25, 2001, the water-level gradient between the ground water and the stream was slightly greater than zero during the last week in December 2001 and stream temperature was near freezing (fig. 9B). Temperatures at depths of 0.61 and 0.15 m were slightly greater than the stream temperature indicating that heat was being transferred to the stream, which is consistent

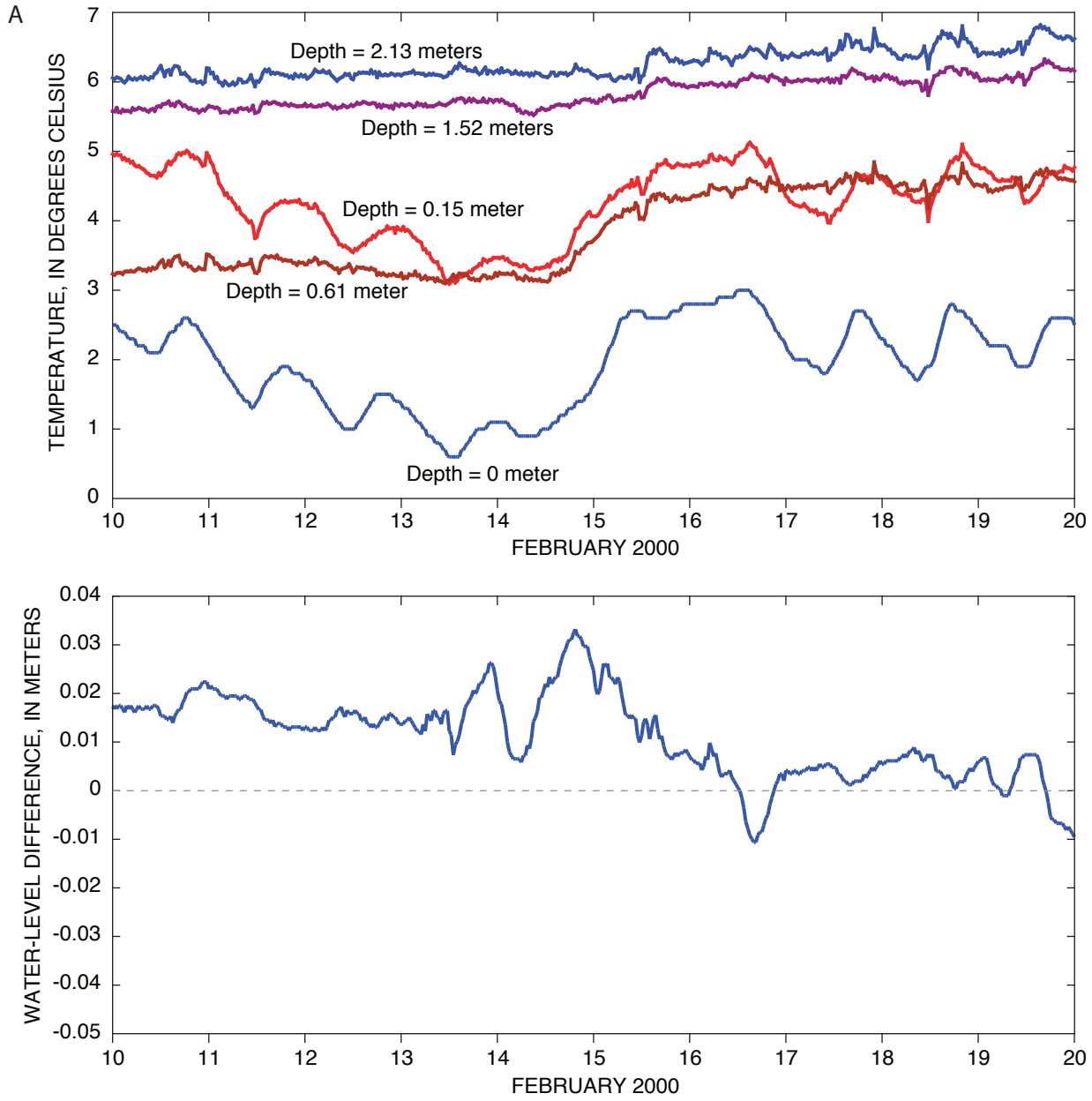

Figure 9. (A) Streambed temperature profile and difference in water level between stream and shallow groundwater (positive difference in water level indicates upward gradient) for Trout Creek at Martin Avenue near Tahoe Valley during a gaining period.

with the slight upward gradient observed between the ground water and the stream. Beginning December 23, the gradient changed such that the stream stage was higher than the water level in the well beneath the streambed before returning to a slightly upward gradient during the evening of December 25. During this brief period, the temperature at a depth of 0.15 m dropped briefly to that of the stream and the temperature at a depth of 0.61 m dropped 0.8°C before slowly increasing to the temperature prior to December 23. However, the most noticeable change is the drop in streambed temperature of more than 2°C at a depth of 1.52 m, which indicates water influenced by stream temperature was briefly flowing downward into the underlying ground water. As the hydraulic gradient returned to near zero, the temperature at this depth began to rise slowly (fig. 9B).

Summary

In summary, measurements of flow along Trout Creek during the fall and detailed measurements of stream stage, ground-water levels, and temperature at two sites on Trout

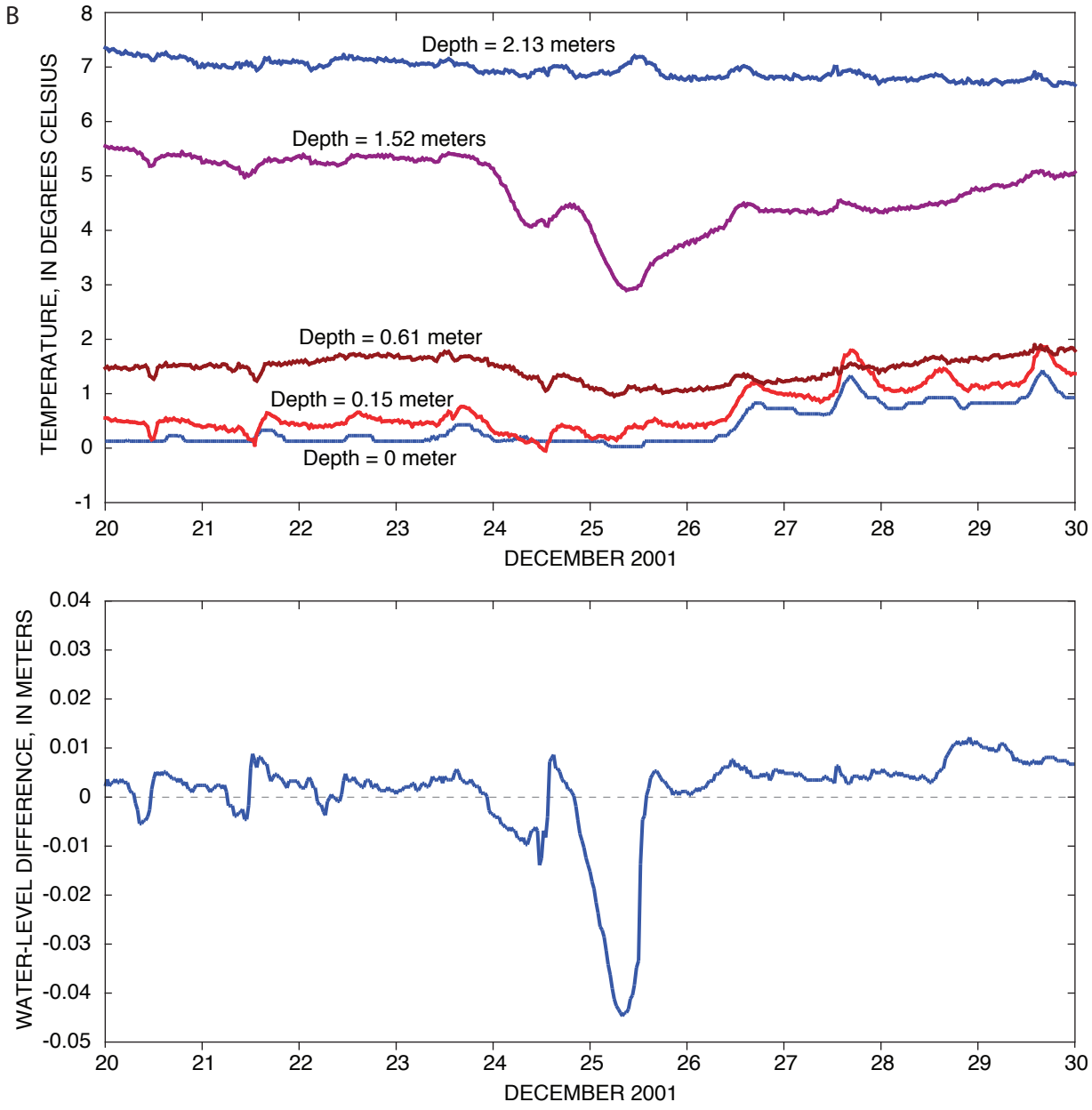

Figure 9. (B) Streambed temperature profile and difference in water level between stream and shallow groundwater (positive difference in water level indicates upward gradient) for Trout Creek at Martin Avenue near Tahoe Valley during a losing period.

Creek show a dynamic ground-water exchange that varies seasonally and spatially. Detailed measurements at the two sites indicate that ground water is contributing flow to Trout Creek during the winter and early spring and losing flow during the summer and fall. Analyses of the data are ongoing. Purpose of the analyses is to determine the extent and duration of ground water contribution to Trout Creek. Knowing this contribution and the nutrient concentrations in ground water are important in designing environmental improvement projects that are effective in reducing nutrients to Trout Creek and to Lake Tahoe.

Chapter 7

Combined use of heat and soil-water content to determine stream/ground-water exchanges, Rillito Creek, Tucson, Arizona

John P. Hoffmann, Kyle W. Blasch, and Ty P. Ferre´[1]

Introduction

The city of Tucson and surrounding communities obtain virtually all their municipal, agricultural, and industrial water from ground water that is withdrawn from thick alluvial aquifers underlying the desert basins. A large fraction of this ground water entered the aquifers as recharge after percolating through channel deposits along ephemeral streams (Matlock and Davis, 1972; Davidson, 1973; Hanson and Benedict, 1994). Most of the ground water in the underlying aquifers is thousands of years old (Kalin, 1994), and the amount of water that recharges the aquifers is insufficient to meet current and future demands. The resultant ground-water deficit, which will grow as the population increases, is manifested in water-level declines of more than 60 meters since the middle of the 20th century. To help mitigate the deficit, an in-stream recharge facility has been proposed in the Rillito Creek channel on the north side of Tucson. The source of water for the recharge facility is likely to be Colorado River water, transported from Lake Havasu and delivered to the Tucson area through the Central Arizona Project aqueduct.

Infiltration of streamflow is known to occur in ephemeral streams in the Southwestern United States; however, a better understanding of the infiltration processes can improve the effectiveness of in-stream recharge facilities. This chapter describes one component of an investigation designed to improve our understanding of infiltration processes in ephemeral-stream alluvium. In particular, we discuss the variability of infiltration rates during a streamflow event and show how temperature methods in conjunction with soil-water content measurements can be used to evaluate potential sites for recharge facilities.

In this chapter, we show examples of how numerical simulations using temperature methods are used to estimate rates of infiltration in the shallow Rillito Creek stream-channel deposits during an ephemeral streamflow event. Water-content changes measured at several depths are used to estimate the rapid infiltration rate at the onset of streamflow. The variation in infiltration rates during a streamflow event is examined. Drainage rates at the cessation of streamflow, determined on the basis of soil-water content measurements, are compared to estimated infiltration rates near the end of streamflow for each profile. These estimated infiltration rates and drainage rates are compared with previous estimates of these rates obtained by other techniques.

Rillito Creek

Rillito Creek has a drainage area of 2,256 square kilometers at the streamflow-gaging station Rillito Creek at Dodge Boulevard (09485700) and has two major tributaries: Tanque Verde Creek and Pantano Wash (fig. 1). The creek is typical of ephemeral streams in the arid and semiarid Southwestern United States. During most of the year, the creek is dry; however, after prolonged or intense periods of rainfall and (or) snowmelt, it has flowed for several hours to several days along its 20-kilometer length. Precipitation runoff and snowmelt from the Santa Catalina Mountains to the north and the Rincon Mountains to the east, as well as urban runoff from the northeastern suburbs of Tucson, contribute most of the flow to Rillito Creek. Rillito Creek is a losing stream along its westward course toward its confluence with the Santa Cruz River.

Rillito Creek is underlain by recent stream-channel deposits and Pleistocene or older basin-fill deposits (Anderson, 1987). The channel deposits, which were derived from the surrounding mountain ranges, comprise fine- to coarse-grained alluvium and are about 10 meters thick. They predominantly are sand and gravel and contain less than 10 percent clay and silt, indicating that streambed infiltration is rapid. The underlying basin-fill deposits generally are finer grained and extend to depths of several hundreds of meters. Both deposits generally are loosely compacted but the basin fill is moderately compacted in places. Depth to ground water beneath Rillito Creek typically ranges from less than 3 meters in the upper reach near the confluence of Tanque Verde Creek and Pantano Wash to about 45 meters near the confluence with the Santa Cruz River to the west.

[1] Department of Hydrology and Water Resources, University of Arizona, Tucson, AZ 85721

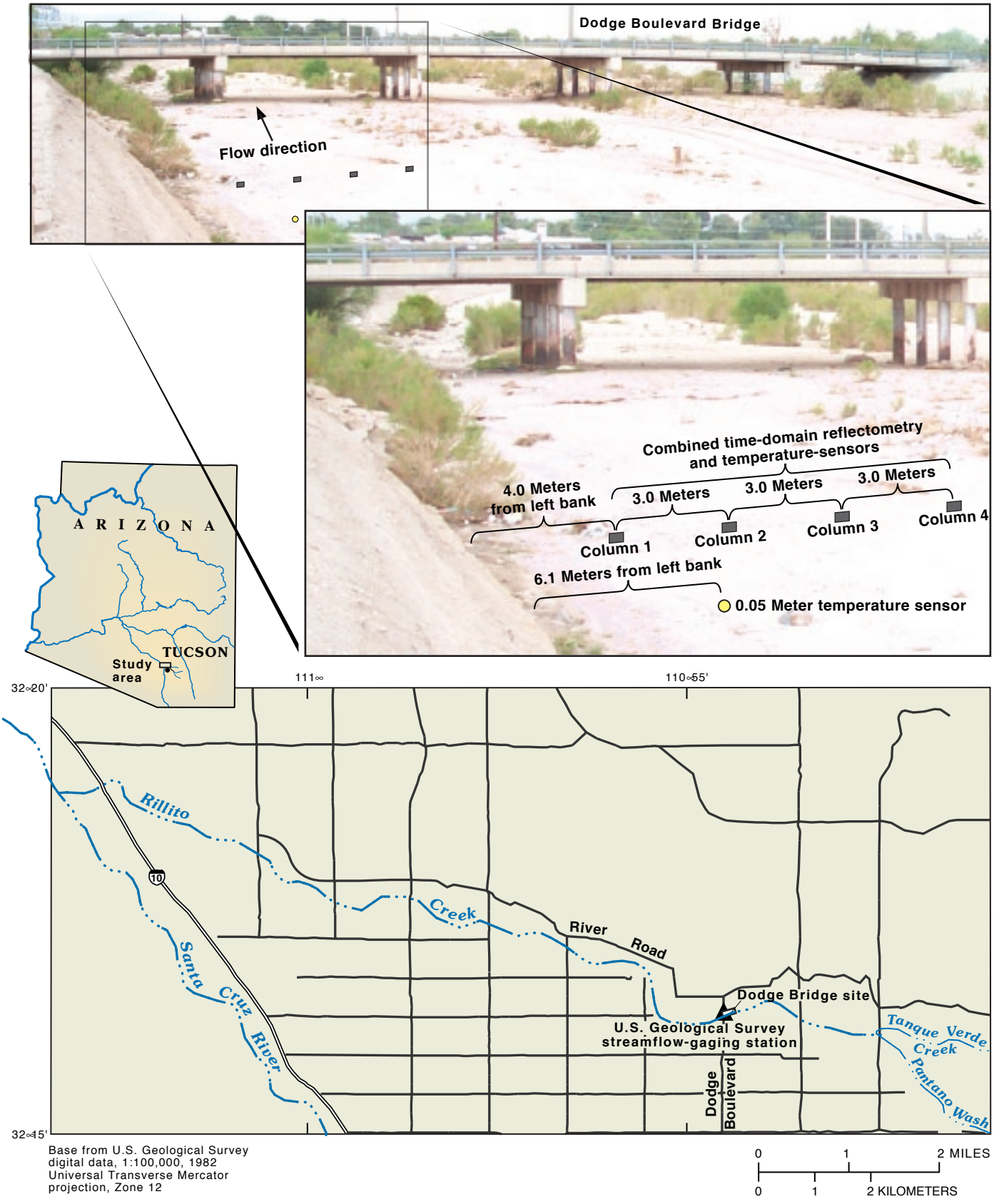

Figure 1. Location of study area showing position of instrumentation relative to left streambank.

Field instrumentation

The streambed was instrumented with a two-dimensional vertical array of 28 paired thermocouple temperature probes and time-domain reflectometry (TDR) moisture probes placed perpendicular to flow (fig. 2). The thermocouples used measure temperature with a precision of about 0.1 degree Celsius; TDR probes measure volumetric water content with a precision of about 3 percent (see Appendix A for discussion of thermocouple accuracy). The paired probes were arranged in four columns (profiles C1, C2, C3, and C4 in figure 2) spaced 3 meters apart. There are seven rows (depths) within the array at depths of about 0.50, 0.75, 1.0, 1.25, 1.50, 2.0, and 2.5 meters below the stream-channel surface. Depths of the probes varied by as much as 0.25 meters owing to deposition and erosion during flow events. A near-surface temperature sensor also was placed adjacent to the paired two-dimensional array at a depth of 0.05 meter. Depth to the regional water table is about 42 meters at the site. The U.S. Geological Survey (USGS) streamflow-gaging station Rillito Creek at Dodge Boulevard is 45 meters downstream from the site.

Temperature data

As discussed in chapter one, heat can be transferred through sediments by advection and conduction. Although both advective- and conductive-heat transport occur during infiltration, advective-heat transport is more prevalent in high water flux settings, whereas conductive-heat transport is more prevalent in static or very low water flux conditions. For most hydrologic applications related to infiltration through alluvial sediments, advection is the primary mechanism for the transport of heat by flowing water and conductive heat transport is regarded as a negligible component of heat transfer.

Subsurface temperatures change rapidly at the onset of streamflow (fig. 3) because heat transport is coupled directly with water flow through advection. The temperature changes are reduced in amplitude and show an increasing lag time with depth. Temperature changes occur in both the horizontal and vertical dimensions (fig. 4).

Soil-water content data

The highly transient conditions that exist at the onset of streamflow are difficult to simulate numerically; therefore, a direct analysis of water-content measurements probably is the most accurate method of estimating initial infiltration rates. Infiltration rates at the onset of streamflow can be estimated using wetting-front arrival times at successive TDR probes. Once streamflow ends, the water that has infiltrated into the subsurface continues to redistribute vertically and horizontally. The rate of drainage depends on the distribution of water

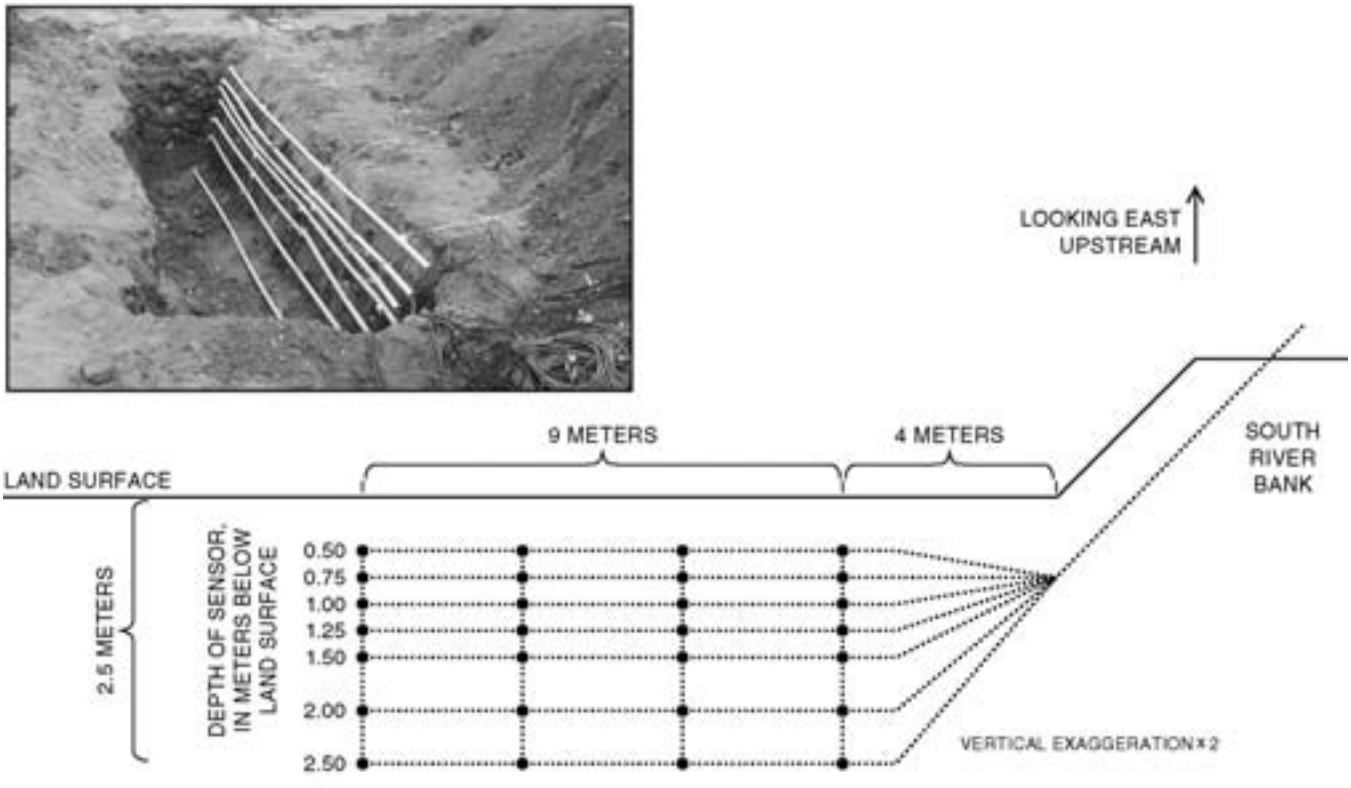

Figure 2. Photograph and schematic of the two-dimensional array of sensors within the stream-channel deposits. Each black circle represents a temperature and time-domain reflectometry sensor. Refer to figure 6-1 for location of array within Rillito Creek.

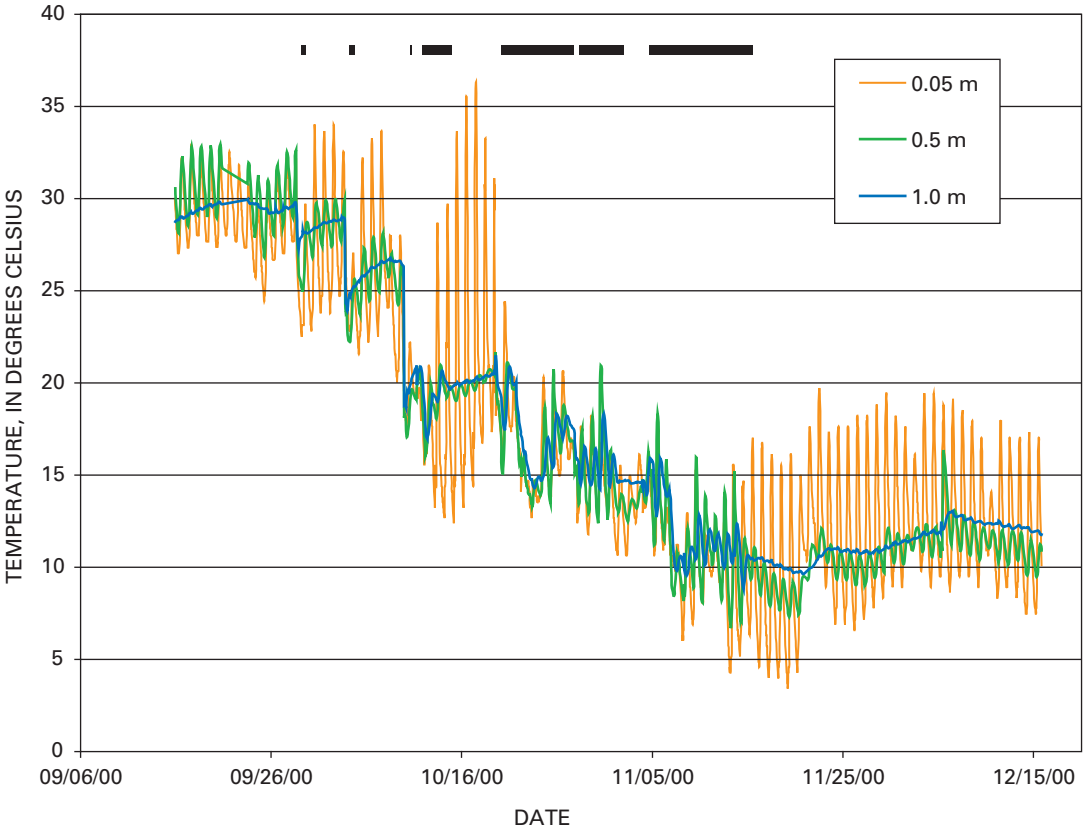

Figure 3. Thermograph of Rillito Creek sediments at depths of 0.05, 0.5, and 1.0 meter. Solid bars above thermographs show periods of streamflow.

throughout the subsurface at the end of streamflow. Drainage rates, similar to infiltration rates, are determined from the elapsed time between sharp decreases in water content at each depth (fig. 5). Drainage rates through the Rillito Creek stream-channel deposits typically are between 0.5 and 1.0 meters per day (Blasch and others, 2000).

Water-content data show rapid changes at the onset of streamflow (fig. 5). Volumetric water content increases from about 20 percent to 40 percent within minutes of the onset of streamflow. These initial infiltration rates were as high as 3.5 millimeters per second, which if sustained would be equivalent to 300 meters per day. The high rates are likely to include vertical and lateral flow components. Similar to the temperature data, the water-content data indicate that infiltration occurs in both the horizontal and vertical directions at the onset of streamflow (fig. 6). Drainage rates determined from water-content measurements after the cessation of flow for the same event for which modeled simulations are presented in this chapter were about 0.46 meter per day.

One-dimensional simulation results

As discussed in chapter one, temperature and water-content measurements are interpreted using numerical models that describe water flow and heat transport. Multidimensional flow simulations are required to accurately represent infiltration into a heterogeneous medium, such as layered stream-channel deposits, and near the margins of the wetted perimeter of the advancing wetting front where capillary flow dominates. However, infiltration is predominantly vertical near the center of streamflow in a homogeneous medium after a period of sustained flow. Infiltration was assumed to be predominantly vertical within the relatively homogeneous stream-channel deposits of Rillito Creek; therefore, simplified one-dimensional model simulations were used. The time from the onset of flow required for predominantly vertical infiltration to occur varies depending on streamflow conditions and the texture of the streambed material. For instance, small braided ribbon flows over fine-grained material may never result in predominantly vertical infiltration, whereas large bank-to-bank flows of coarse-grained material may produce predominantly vertical infiltration beneath the streambed within minutes.

Thermographs predicted by numerical simulations are fitted to measured thermographs from the field by adjusting model parameters within appropriate ranges until the best match is found between simulated and measured thermographs (see Appendix B for details). A typical set of measured Rillito Creek thermographs and the best-fit numerically simulated thermographs are shown in figure 7. Numerical simulations

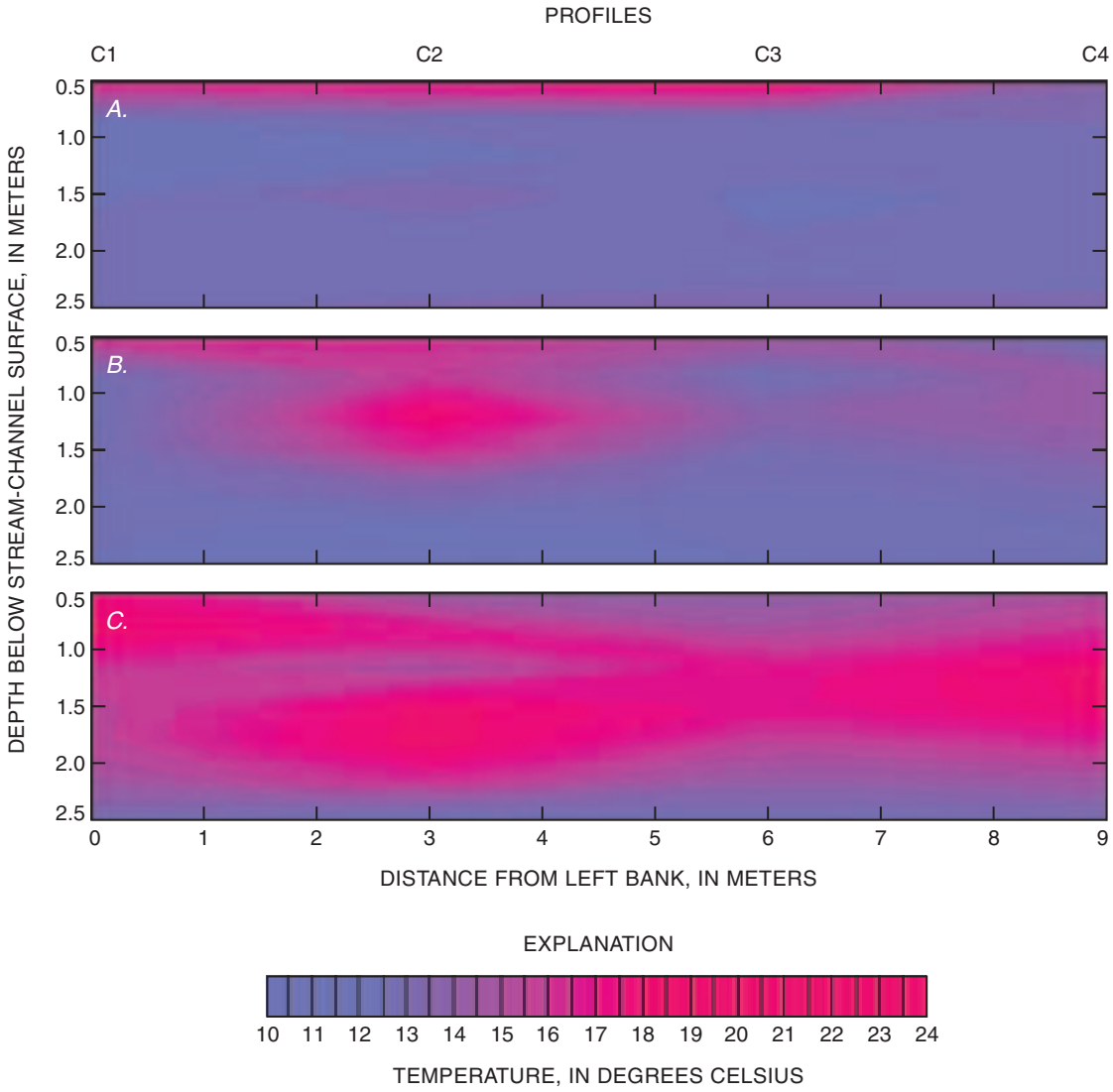

Figure 4. Two-dimensional temperature distribution within shallow stream-channel deposits. (**A**) Thermal transport through conduction before the onset of a streamflow event. (**B**) Thermal transport through a combination of advection and conduction at the onset of a streamflow event. Multidimensional percolation through the sediments. (**C**) Combined advection and conduction thermal transport to the deeper sediments several hours into a flow event.

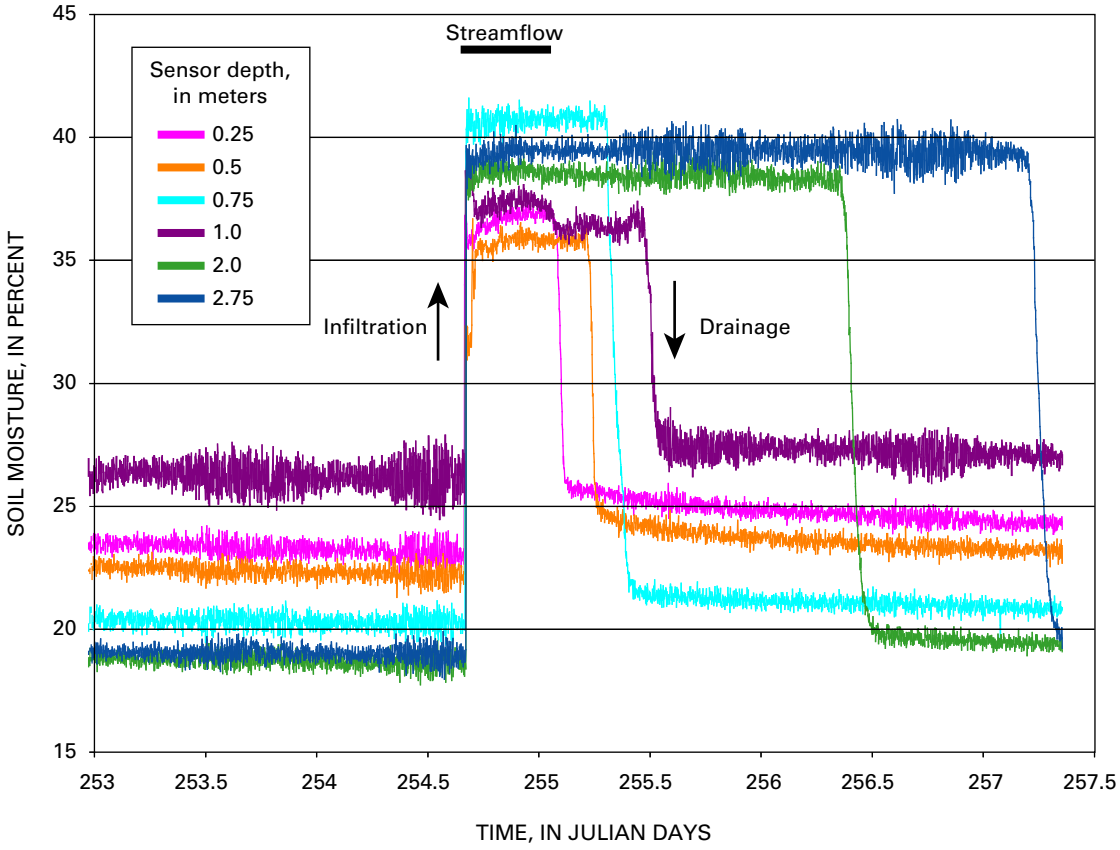

Figure 5. Water-content data showing rapid increases at the onset of streamflow; a stabilization of water content during the streamflow event; and subsequent drainage after the streamflow is over.

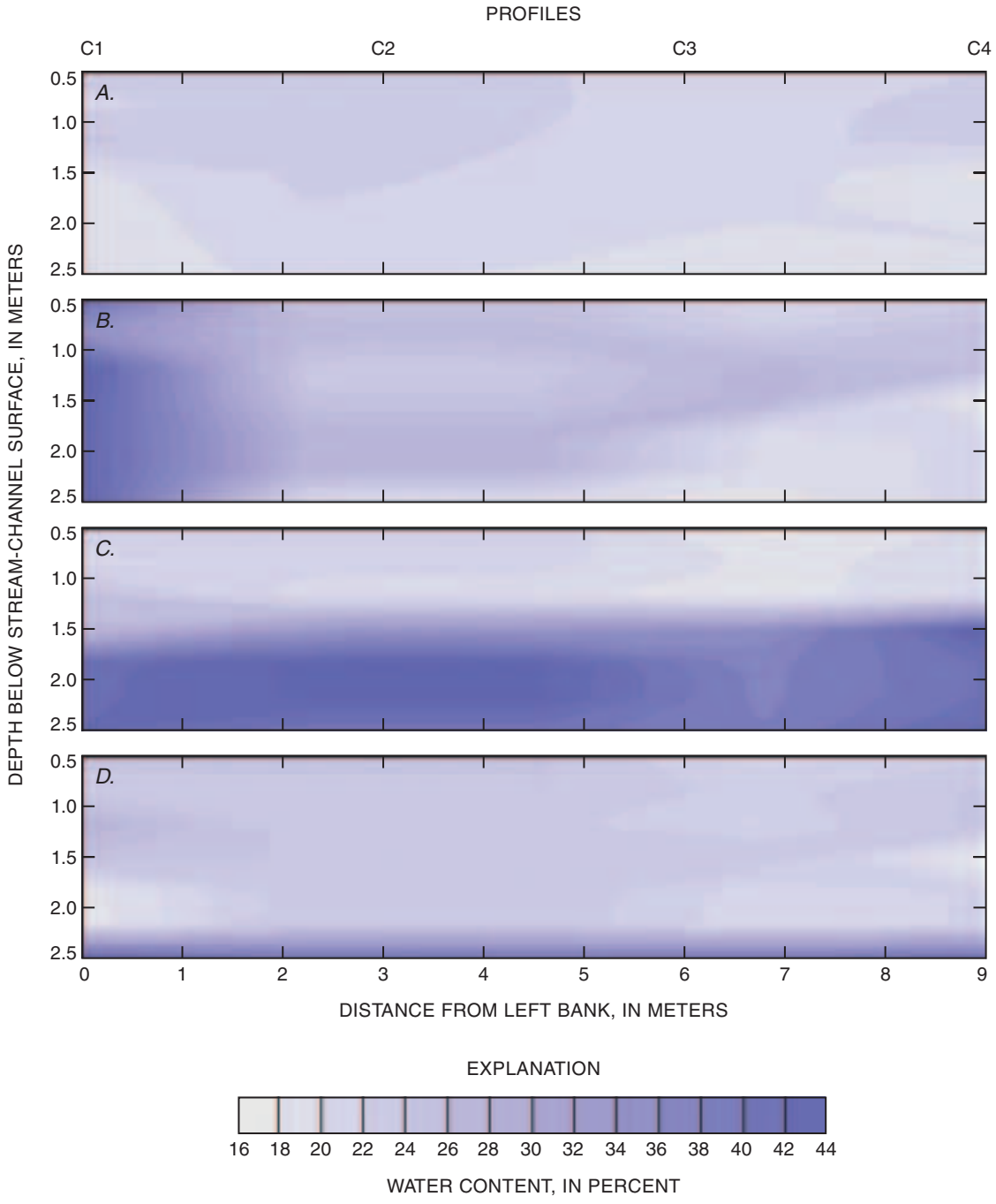

Figure 6. Two-dimensional water-content distribution in sediments beneath Rillito Creek. (**A**) Soil-water content before the onset of streamflow. (**B**) Soil-water content 5 minutes after the onset of streamflow. (**C**) One-dimensional dewatering immediately after the cessation of flow. (**D**) One-dimensional dewatering approximately 2 days after the cessation of flow.

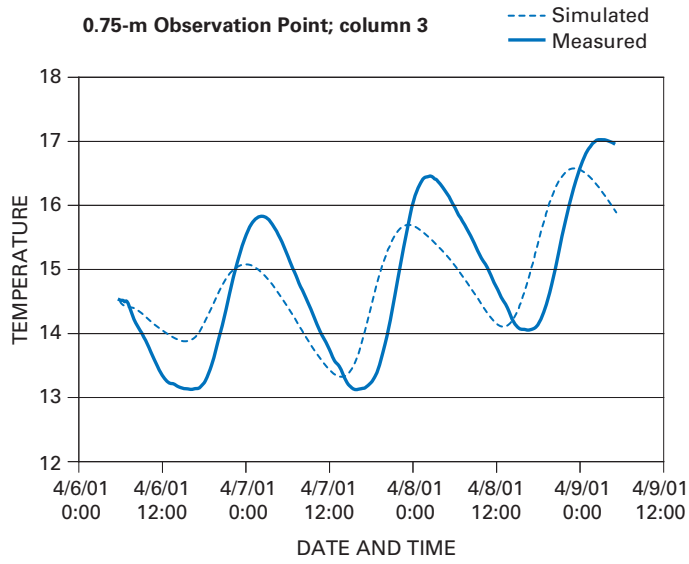

Figure 7. Measured and simulated thermographs at a depth of 0.75 meter, column 3.

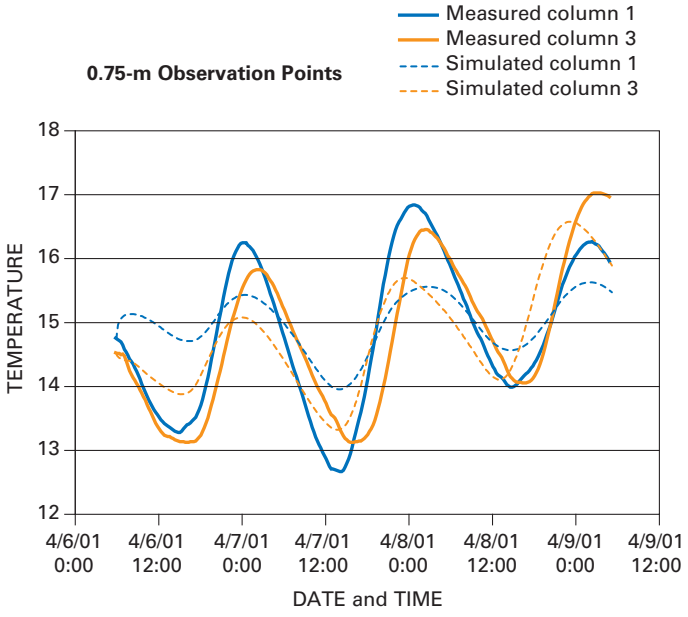

Figure 8. Set of measured and simulated thermographs for two adjacent columns.

shown in this chapter are for a bank-to-bank flow event in April 2001. Vertical flow is assumed since temperature changes were measured predominantly in the vertical direction. Although the simulated and measured thermographs are in general agreement, significant departures exist. Simulated temperatures can differ from measured temperatures for several reasons, such as incorrectly defined boundary conditions, incorrect hydraulic and thermal property assignments, or an inability for a one-dimensional model to represent multidimensional infiltration. In the case of the latter, multidimensional simulations might yield thermographs that are in closer agreement to field data than those shown in figure 7.

An example of simulated thermographs that best match the measured thermographs at 0.75 meter depth in two profiles is shown in figure 8. There is general agreement between simulated and measured thermographs. The predicted infiltration rates vary from less than about 0.35 to about 0.39 meter per day throughout the 2-day flow period (fig. 9). This represents a variation in predicted infiltration rates of less than 10 percent among the four columns, indicating that infiltration was uniform and predominantly vertical. The infiltration rate generally declines as the streamflow events proceed.

Discussion

Ground-water recharge is a critical component of the hydrologic cycle. Currently, many areas in the Southwestern United States pump more ground water than is naturally recharged. Current and future artificial recharge sites will

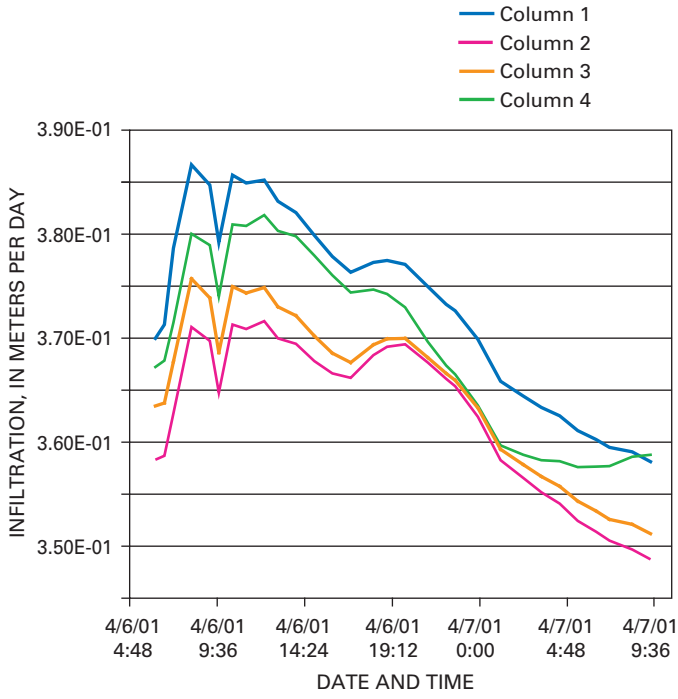

Figure 9. Simulated infiltration rates at columns 1, 2, 3, and 4 during a streamflow event.

become increasingly important in achieving sustainable water supplies. The potential exists to use water-content measurements and temperature measurements to evaluate the potential suitability of in-stream recharge facilities and to provide guidance on citing such facilities.

Infiltration rates can be estimated from temperature measurements; these estimates may be complimented by initial infiltration and drainage-rate estimates from water-content measurements. The water-content measurements enable better estimates of rapid infiltration rates associated with the onset of streamflow. In Rillito Creek, initial instantaneous rates were estimated to be as high as 3.5 millimeters per second, which included both vertical and lateral flow components that occurred only during the onset of streamflow.

Within several minutes after streamflow has been established, the stream-channel deposits become fully saturated and remain so during subsequent flow. For this reason, temperature measurements are more useful for estimating infiltration rates during streamflow than are water-content measurements. One-dimensional analyses of temperature measurements collected during a streamflow period in April 2001 show that infiltration rates through the Rillito Creek stream deposits were sustained at about 0.37 meter per day; however, there was a general decline in infiltration rates over time during a flow. A decline in infiltration during streamflow events in the Rillito has been recognized using temperature methods by other investigators (Bailey and others, 2000a, b). They attributed this decline to the accumulation of a fine-grained surface layer that effectively clogged the streambed. One of their simulations required a change in the hydraulic conductivity of the shallow streambed sediments during streamflow to reproduce the observed subsurface thermographs. Another set of simulations showed that the hydraulic conductivity of this shallow streambed material changed four orders of magnitude between two sequential streamflow events.

An estimated sustained infiltration rate of about 0.37 meter per day during streamflow agrees well with the estimated post-streamflow drainage rate of 0.46 meter per day. These rates show general agreement with estimates ranging from 0.41 to 0.50 meter per day made by other investigators along Rillito Creek (Burkham, 1970; Lane, 1983; Katz, 1987). The good agreement among these independent measures provides confidence that the temperature method enables accurate estimates of infiltration. As such, vertical arrays of temperature probes can be located along stream reaches to estimate the potential for in-stream recharge and to provide guidance on citing recharge facilities. However, high infiltration rates at shallow depths are not sufficient to ensure that water can be recharged at a high rate. Generally, the primary constraints on recharge rates are the total amount of water that infiltrates into the subsurface over time and the rate at which that water can move down through the entire subsurface into an aquifer. To estimate potential recharge rates, long-term vertical infiltration rates need to be estimated. Infiltration rates determined from shallow measurements should be considered an upper limit of the potential recharge rate for a particular site.

Chapter 8

Trout Creek—estimating flow duration and seepage losses along an intermittent stream tributary to the Humboldt River, Lander and Humboldt Counties, Nevada

David E. Prudic, Richard G. Niswonger, James L. Wood, and Katherine K. Henkelman

Introduction

Water in the Great Basin of Nevada is used by a variety of competing interests, including irrigation, mining, and municipal. A rapidly increasing population and expansion of large gold-mining operations are placing additional demands on the region's limited water resources. Several deep open-pit mines in the Humboldt River basin of north-central Nevada require dewatering (fig. 1), which has nearly doubled ground-water withdrawals in the Humboldt River basin. Ground water pumped from the mines is being used to irrigate crops, to generate power, to recharge ground water, and to augment flow in the Humboldt River. Although mine dewatering has increased flow in the Humboldt River, which is used for irrigation, the long-term effects of this dewatering on the ground-water resources and flows in the Humboldt River are not completely understood. Studies in cooperation with the Nevada Department of Conservation and Natural Resources are designed to gain a better understanding on how ground-water withdrawals in the basin affect flow in the Humboldt River, an important agricultural water supply in northern Nevada.

Ground water pumped for agriculture in the Humboldt River basin is from alluvial aquifers beneath the valleys, whereas most of the open pits being dewatered are in consolidated-rock aquifers at the base of or in the adjacent mountains. Average annual precipitation is less than 250 mm/yr on the valley floors and ranges from about 300 mm/yr on the lower parts of mountains to more than 1,000 mm/yr on some of the highest peaks. Water entering the basin-fill aquifers is mostly from (1) infiltration along intermittent channels on alluvial fans where streams exit the mountains; (2) infiltration along through-flowing streams such as the Humboldt River; and (3) subsurface flow from consolidated rocks in the adjacent mountains. Infiltration of precipitation on alluvial fans and valley floors is usually insufficient to supply large quantities of recharge to the basin-fill aquifers. Infiltration beneath the intermittent channels on the alluvial fans and streams that cross the valley floors is limited generally to snowmelt runoff, which occurs from late winter to early summer.

Purpose for study on Trout Creek

The purpose of the study on Trout Creek is to determine the frequency, duration and quantity of water that exits the mountains and enters the basin fill as seepage losses on the alluvial fan from snowmelt runoff and as subsurface flow from the consolidated rocks in the mountains to the basin-fill aquifer along the Humboldt River. Trout Creek, a tributary to the Humboldt River (fig. 2), was chosen as one of seven sites in the desert Southwest to study the distribution and frequency of recharge beneath intermittent streams that flow across alluvial fans as part of the Southwest Ground-Water Resources Project of the USGS. Trout Creek was chosen because it is within the area of a larger regional study and because it is typical of small intermittent mountain streams in the northern Great Basin where flow in the channel is dependent primarily on snowmelt runoff and on an occasional intense thunderstorm of short duration. Initial work on Trout Creek began in spring of 1999 and will be completed in 2003.

Description of Trout Creek drainage

Trout Creek drains the northwest flank of Battle Mountain near the town of Valmy, and is about 25 km west of the town of Battle Mountain in north-central Nevada (figs. 1 and 2). Trout Creek is perennial only for short reaches upstream of a northeast-southwest trending normal fault where flow is supported by small springs discharging from quartzite, chert, siliceous shale and greenstone of Ordovician Age (Willden, 1964). Near the fault, the stream is confined to a narrow steep channel (figure 3*A*). Downstream of the fault, the channel has cut into older alluvium that covers greenstone, chert, and argillite of Pennsylvanian Age and rhyolitic flows and pyroclastics of Tertiary Age (Willden, 1964). Near the base of the volcanic rocks, seasonal springs and seeps discharge water into the stream during snowmelt (fig. 3*B*). At Marigold mine, the channel was moved westward to accommodate expansion of the mine (fig. 2). The stream reenters its original channel about 2 km below Marigold mine (fig. 2). After leaving the

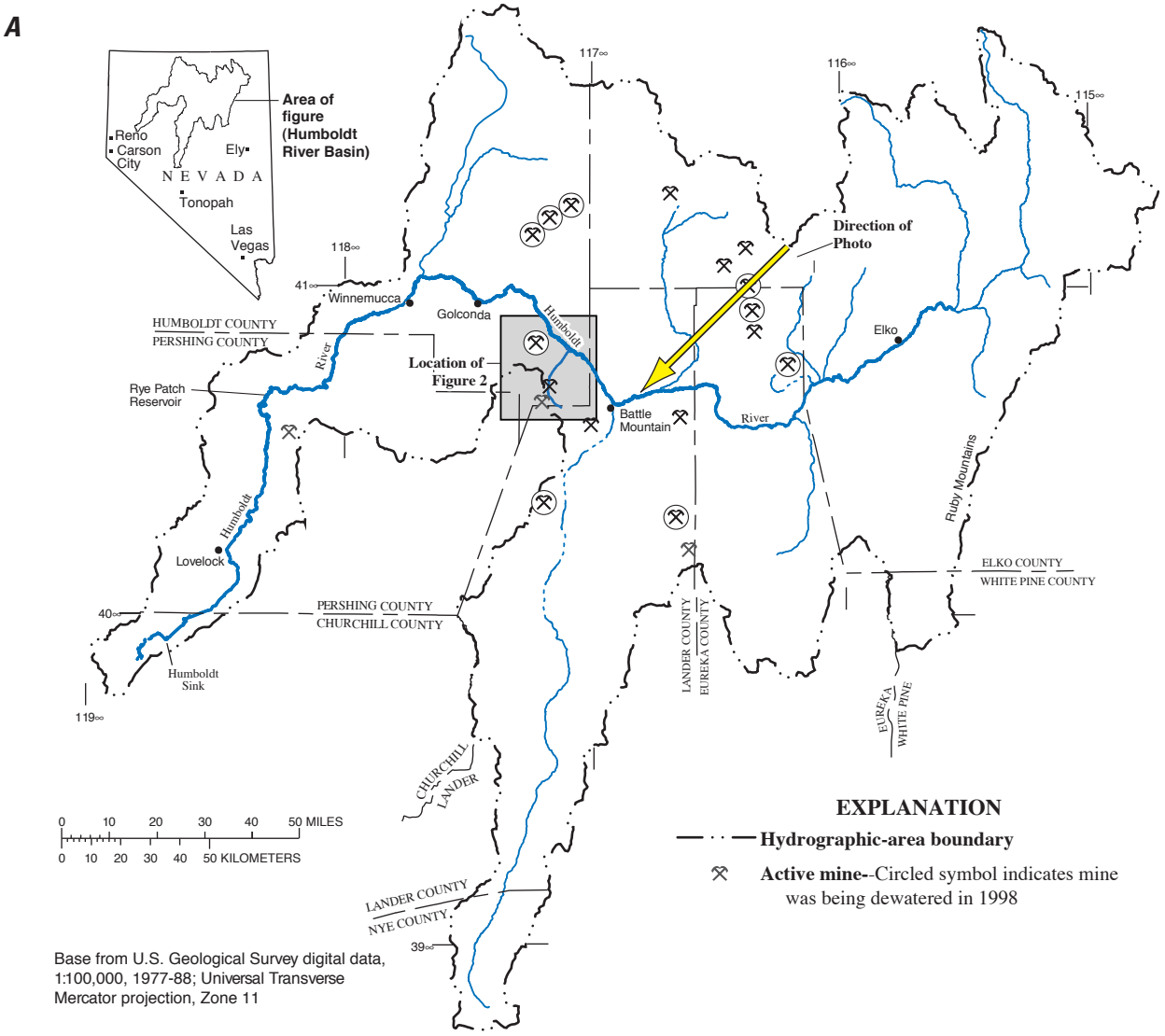

B

FRANCIS DEBOIS, FALLON, NEVADA, 1994

Figure 1. (***A***) Map showing gold mines in the Humboldt River basin of Nevada that were being dewatered in 1996; and (***B***) oblique aerial photograph of one of the active mines being dewatered.

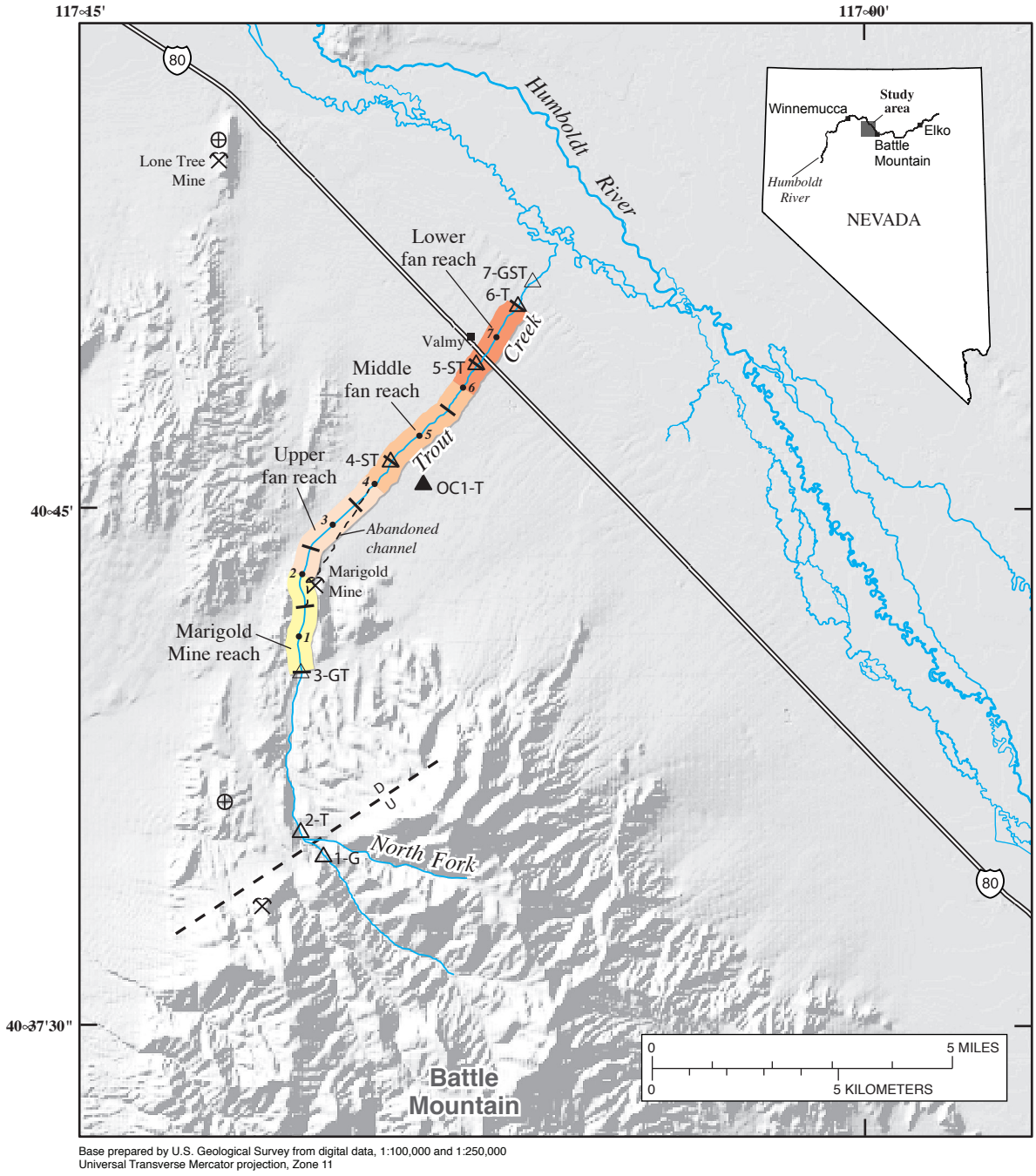

EXPLANATION

- **Modeled reach**
- **Weather station**
- 7-GST △ **Channel measurement site and identification**—G is stream gage, T is surface temperature recorder, and S is subsurface temperature recorder
- OC1-T ▲ **Off-channel measurement site and identification**—T is surface temperature recorder
- •1 **Model node**
- **Stream cross section used in model**
- **Mine**
- D/U **Fault**—D is downthrown side, U is upthrown side

Figure 2. Location of Trout Creek in the Humboldt River basin, north central Nevada showing types of data collected along channel and extent of surface-flow routing model. Location of figure 2 is shown on figure 1.

Trout Creek where it crosses normal fault and emerges from canyon; North Fork Trout Creek enters from left; view is to south.

Trout Creek downstream of North Fork; springs discharge along creek near intersection of roads; temperature logger at site 2 is downstream of road; view is to north.

Trout Creek on alluvial fan below Marigold mine; subsurface temperature datalogger at site 4 is in orange box, view is to north.

Trout Creek at base of fan near Humboldt River floodplain; weir and gage at site 7 is in foreground; view is to south.

Figure 3. Photographs of Trout Creek (A) where it emerges across normal fault; (B) downstream of North Fork tributary; (C) on alluvial fan below Marigold mine; and (D) at base of alluvial fan near Humboldt River floodplain. Location of sites on Trout Creek is shown on figure 2.

mountains, the stream flows north in a channel incised into a broad alluvial fan (figs. 3*C* and 3*D*) to the flood plain of the Humboldt River where the channel is no longer identifiable. Sediments of the alluvial fan are composed of sand and gravel mixed with clay and silt. Since 1999, flow reached the Humboldt River flood plain only for a few weeks during the spring of 1999 following a winter of above normal snowpack in the mountains.

Above Marigold mine, the regional water table is within the pre Cenozoic-Age rocks (fig. 4) and is more than 150 m below the stream. The seasonal springs just downstream of the fault likely form as a result of perched water in the volcanic rocks during spring snowmelt. Depth to ground water gradually decreases to less than 10 meters next to the Humboldt River. Dewatering of the Lone Tree mine northwest of Trout Creek (fig. 2) began in 1992 and has caused the water table beneath Trout Creek to decline about 20 meters at Marigold Mine.

Duration of flow estimated from temperature and stream stage

Streams flowing onto alluvial fans likely are an important source of recharge to the alluvial aquifer in the Great Basin region. Yet the extent and duration of flow, and seepage loss rates along small mountain streams are often unknown. A series of recording temperature sensors were placed in Trout Creek (sites 2, 3, 4, 5, 6, and 7; fig. 2) and off channel (OC1; fig. 2) in April 1999 in an attempt to monitor the duration of runoff at different locations along the channel as described in Appendix A. Initially, the temperature sensors were placed on the streambed but this resulted in excessive heating of the sensors during the summer. Subsequently, the sensors were buried about 7 cm below the streambed in the channel and beneath land surface off channel. Additional temperature sensors were installed on the bank adjacent to sites 3, and 4 in March 2000

because initial evaluation of temperature data indicated that changing weather conditions complicated the interpretation of flow and no flow with stream temperature.

Subsurface temperature measurements were made at three locations along the channel (sites 4, 5, and 7; fig. 2). Temperature measurements were made by attaching thermocouples placed at depths of 10, 20, 50, 100 and about 150 centimeters beneath the channel to dataloggers (small computers) that routinely collected temperature at 30-minute intervals. The subsurface temperature measurements were designed to estimate seepage loss rates using the approach described in Appendix B, and also were useful in identifying the duration of flow.

In addition to temperature measurements along and beneath the channel, three automated stream stage (water-level) recorders (pressure transducers) were installed along the channel to monitor flow. Newmont Mining Corporation installed the first stage recorder upstream of the fault

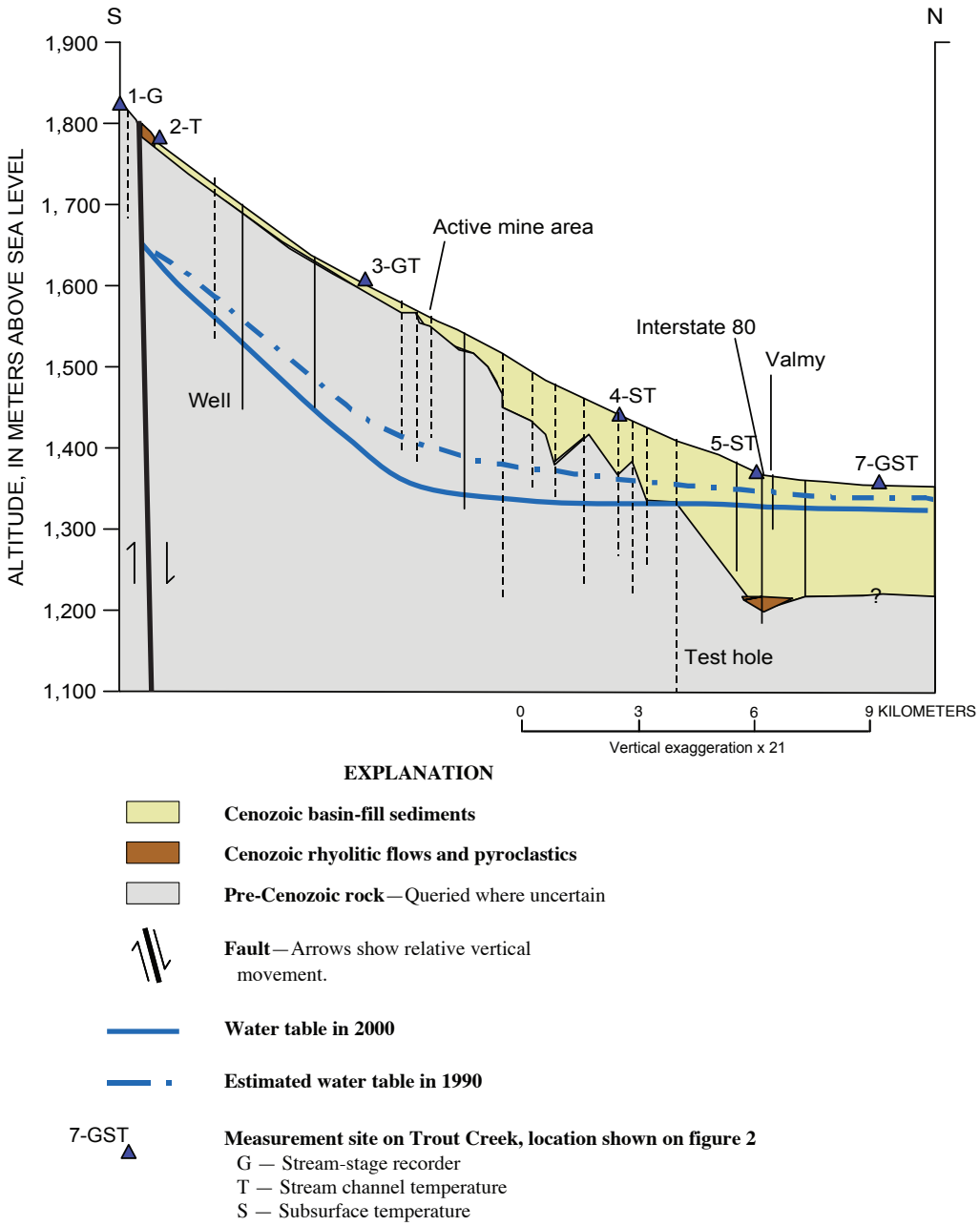

Figure 4. Profile along Trout Creek from upper stream gage to Humboldt River floodplain showing thickness of Cenozoic sediments and volcanic rocks beneath the stream channel. Geologic information is from test holes and wells drilled near Trout Creek (Glamis Gold Mining Company, Valmy, Nev., written commun., 2002 and Nevada State Engineers Office, Carson City, Nev., written commun., 2002). Water-level data from Glamis Gold Mining Company, Nevada State Engineers Office, Newmont Mining Corporation (Winnemucca, Nev., written commun., 1999), and U.S. Geological Survey. Location of sites is shown on figure 2.

(site1; fig. 2) in October 1999. Two additional recorders were installed by the USGS in March 2000 just upstream from Marigold mine (site 3; fig. 2) and at the base of the alluvial fan (site 7; fig. 2). Stage in the stream is recorded every 15 minutes at site 1 and every 30 minutes at sites 3 and 7. Relationships between stage and discharge at sites 1 and 3 were determined from repeated flow measurements made with a pygmy meter over the range of observed flow. A rectangular-notch weir was installed during November 1999 at site 7; however, no flow has been recorded at this site since the weir was installed.

Flow in Trout Creek upstream of the fault (site 1 on fig. 2) was observed from October 1999 through early July 2000 before becoming intermittent during July through September 2000 (fig. 5). Spring snowmelt began near the end of February at site 1 and peaked in April. The daily mean discharges at sites 1 and 3 from the end of March to early June 2000 show good correlation, with less flow and a slight delay in peak discharge at site 3 (fig. 5). The gage at site 3 (6.2 km downstream from site 1) was not installed until March 29, 2000 and flow extended about 1 km downstream of this site on that date. Flow at site 3 ceased in June 2000 and the channel remained dry through September 2000. No flow was measured at site 7, at the base of the fan, from mid-March to September 2000 and there was no evidence of flow from November 1999 when a weir was installed to mid-March 2000.

The duration of flow at selected locations on Trout Creek was estimated from streambed temperatures. Considerable interpretation, which may vary depending on the character of runoff in an intermittent channel, was needed to estimate the duration of flow from streambed temperatures. Flow at site 3, above Marigold mine, commenced on March 22, 2000, a week before the automated water recorder was installed at the site (fig. 6). Prior to March 22, the minimum streambed temperature each day was routinely below freezing. In contrast, the minimum temperatures at site 2, where flow was continuous, remained above freezing. Once flow commenced at site 3, the minimum temperatures corresponded more closely to the

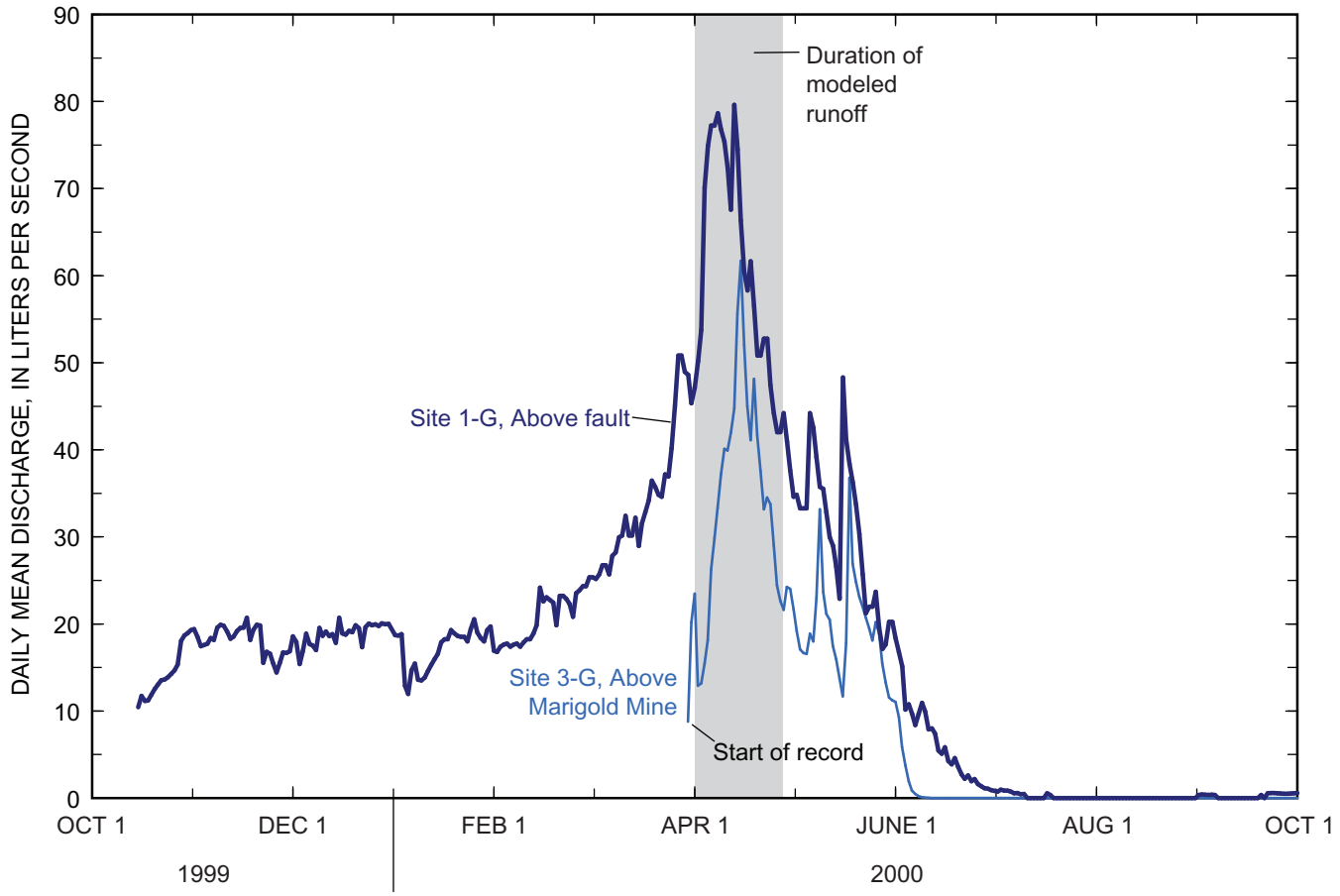

Figure 5. Daily mean discharge at two sites along Trout Creek during water year 2000. Daily mean discharge estimated from water levels (stream stage) recorded every 15 minutes at site 1 and every 30 minutes at site 3. No flow was recorded at site 7 since water-level recorder installed in March 2000. Data at site 1 is from Newmont Mining Corporation (Winnemucca, Nev., written commun., 2002). Location of sites is shown on figure 1.

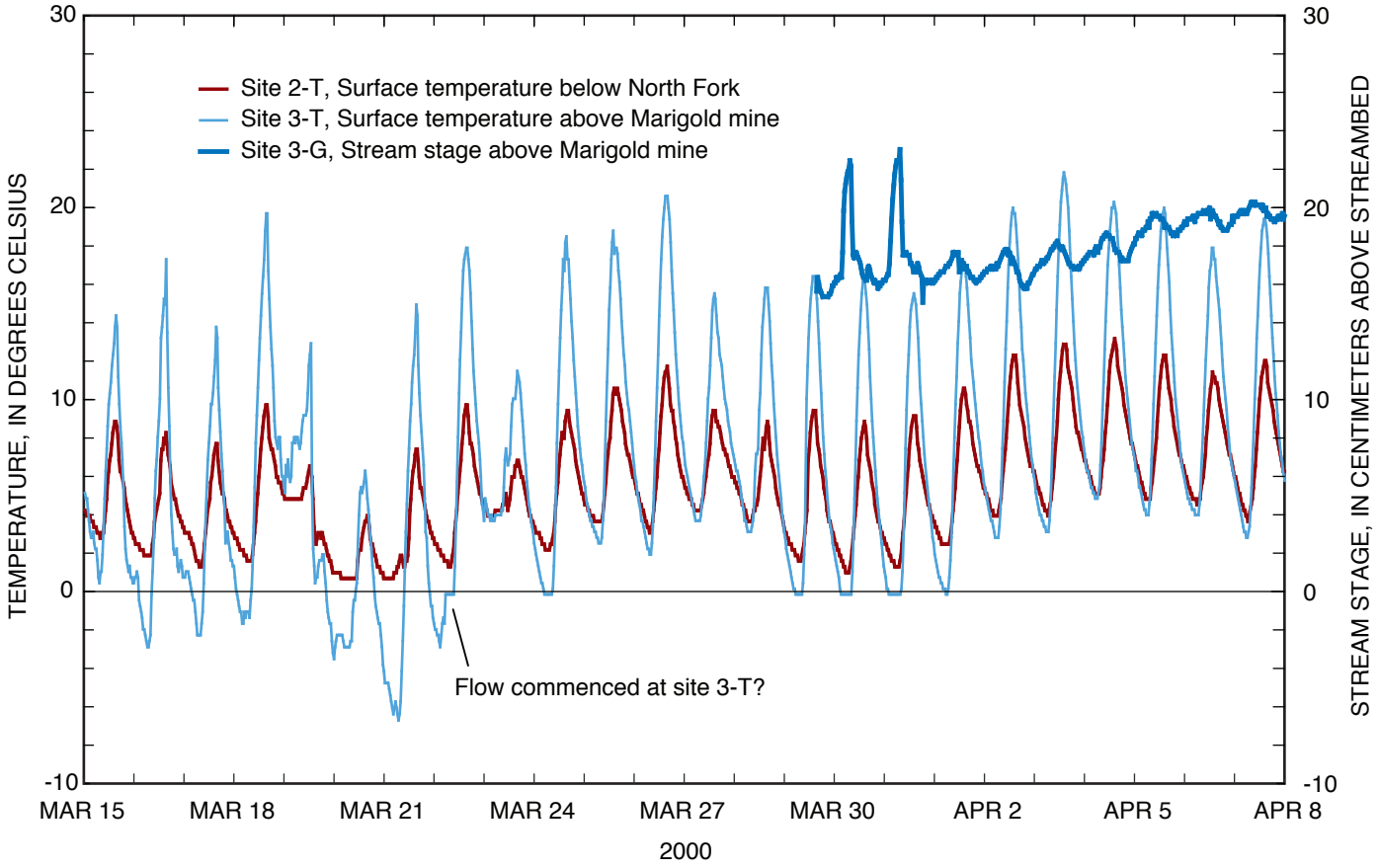

Figure 6. Estimate of when flow began in March 2000 at site 3 from streambed temperatures. Location of site 3 is shown on figure 2.

minimum temperatures at site 2, except during some nights when water at the temperature sensor froze (temperatures slightly less than 0° C). Flow at site 3 was continuous until June 5, when flow ceased in the late afternoon and became intermittent until mid June (fig. 7*A*). The stage recorder was in operation during the first three days of the period of intermittent flow at site 3. Temperature of the streambed shows a deflection when flow ceased each afternoon and when it began in the morning. Apparently, sufficient moisture was left in the channel during each night that the minimum temperature remained similar to that at site 2, even though there was no flow in the channel. Although there is no record of stage from June 7 to June 28, 2000, temperatures at site 3 from June 7 to June 17 (fig. 7B) suggest that flow continued to be intermittent until June 14; afterwards the streambed dried sufficiently and the minimum temperature was higher than at site 2.

Flow at site 4 (below Marigold mine) did not commence until April 9, 2000. On that date, the daily minimum temperature at site 4 began to correspond to that at site 3 (fig. 8). Prior to flow at site 4, the daily minimum and maximum temperatures were warmer than those at site 3 because site 4 is at a lower altitude (fig. 2) and because air temperatures had begun to warm rapidly. Once flow began at site 4, the minimum temperatures were similar to that at sites 2 and 3. However, the maximum temperature in the channel increased downstream (from site 2 to site 4) in response to heating of water during daylight hours and the maximum temperature at site 4 was similar to that at the off channel site OC1-T (fig. 2). Flow at site 4 may not have been continuous throughout the period of flow because temperature deflections similar to those during intermittent flow at site 3 were observed as noted on figure 8.

Higher minimum temperatures after flow ceased in the channel at sites 3 and 4 suggest that the total period of flow (neglecting brief periods of intermittent flow) along the channel could be simply evaluated by comparing the streambed temperatures along the channel to a temperature recorder buried at a similar depth away from the channel. Such a method may not be usable everywhere, particularly if the minimum temperature at the off-channel site is similar to the minimum temperature of water in the channel.

The duration of flow down Trout Creek during snowmelt runoff in 2000 was estimated by subtracting the daily minimum temperatures at an off-channel site (OC1-T, fig. 2) from the daily minimum temperatures at sites 2, 3, 4, and 5 in Trout Creek (fig. 9) starting March 29, 2000 when the temperature sensors were all placed 7 cm below either the land surface or the streambed. The difference in the daily minimum temperature between site 4 and OC1 was near 0° C except during flow in the channel. The generally close agreement in minimum temperature between site 4 and OC1 during periods of no flow

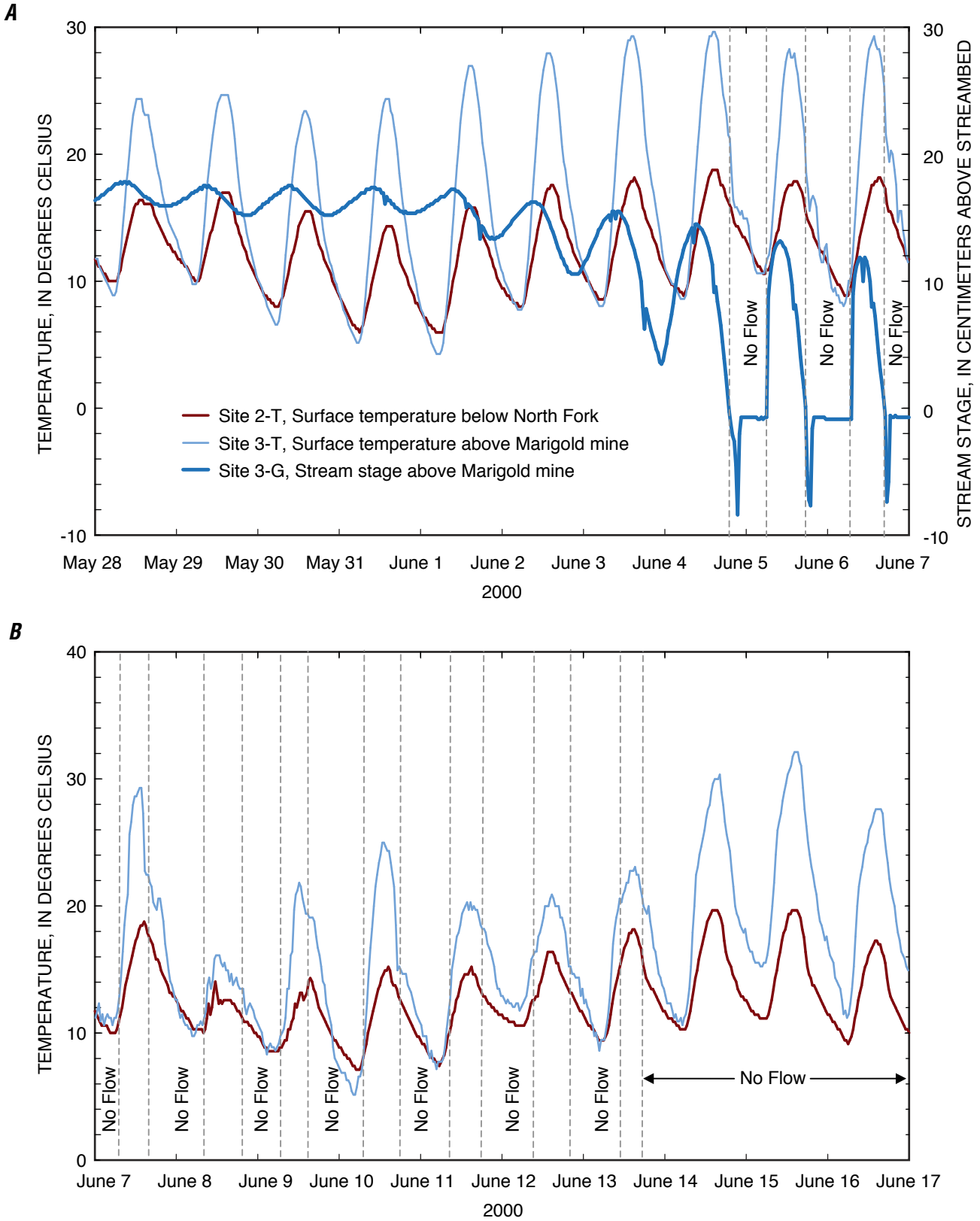

Figure 7. (***A***) Changes in streambed temperature compared with water level in stream (stream stage) during first week of June 2000. (***B***) Estimates of no flow determined from streambed temperature only during second week of June 2000. Location of site 3 is shown on figure 2.

is because site 4 is close to OC1 and because it is in a wide and shallow section of channel used to divert Trout Creek around Marigold mine. Minimum temperatures at the other sites (sites 2, 3, and 5) were generally less than the minimum temperature at OC1 even during periods of no flow because the channel is more incised at these locations and the steeper banks provide shade. Differences in daily minimum temperature during flow at sites 2, 3, and 4 (April 9–May 15) were similar except at site 4, where flow may have been discontinuous starting April 21 and continuing into May. Periods of no flow at site 4 were marked by a rapid increase in the minimum temperature relative to OC1 (difference is less negative) followed by rapid decrease in daily minimum temperature when flow recommenced. From field observations, snowmelt runoff during 2000 did not reach site 5 and the difference in daily minimum temperatures between site 5 and OC1 were consistently less than differences at sites 2, 3, and 4 during periods of flow (fig. 9).

The end of snowmelt runoff at site 4 likely occurred on or near May 15 when the difference in daily minimum temperature at site 4 became less than at sites 2 and 3 (fig. 9). The end of snowmelt runoff at site 3 likely occurred near June 14 when the difference in daily minimum temperature became less than at site 2. Lastly, the generally increasing difference in daily minimum temperature between site 2 and OC1 (differences generally became more negative between the two sites from May to July) ceased on July 19 and the difference in daily minimum temperatures became less (fig. 9). This change suggests that flow ceased on or before that date at site 2, although there may have been periods of intermittent flow beginning at the end of June. The decrease in the temperature difference between site 2 and OC1 on July 19 also corresponds to the beginning of no flow at site 1 less than 1 km upstream (fig. 5).

Subsurface temperatures beneath the streambed at sites 4, 5, and 7 (fig. 2) were also used to estimate the duration of flow. During flow, heat in the stream is transmitted down as water infiltrates through the streambed. A marked changed in subsurface temperatures at depths greater than 50 cm beneath the streambed were observed beginning on April 9 (fig. 10A). The marked change in subsurface temperatures corresponds to a sudden change in temperature of the streambed (fig. 8) and provides additional evidence that flow began on April 9 at site 4. Estimating brief periods of discontinuous flow or when

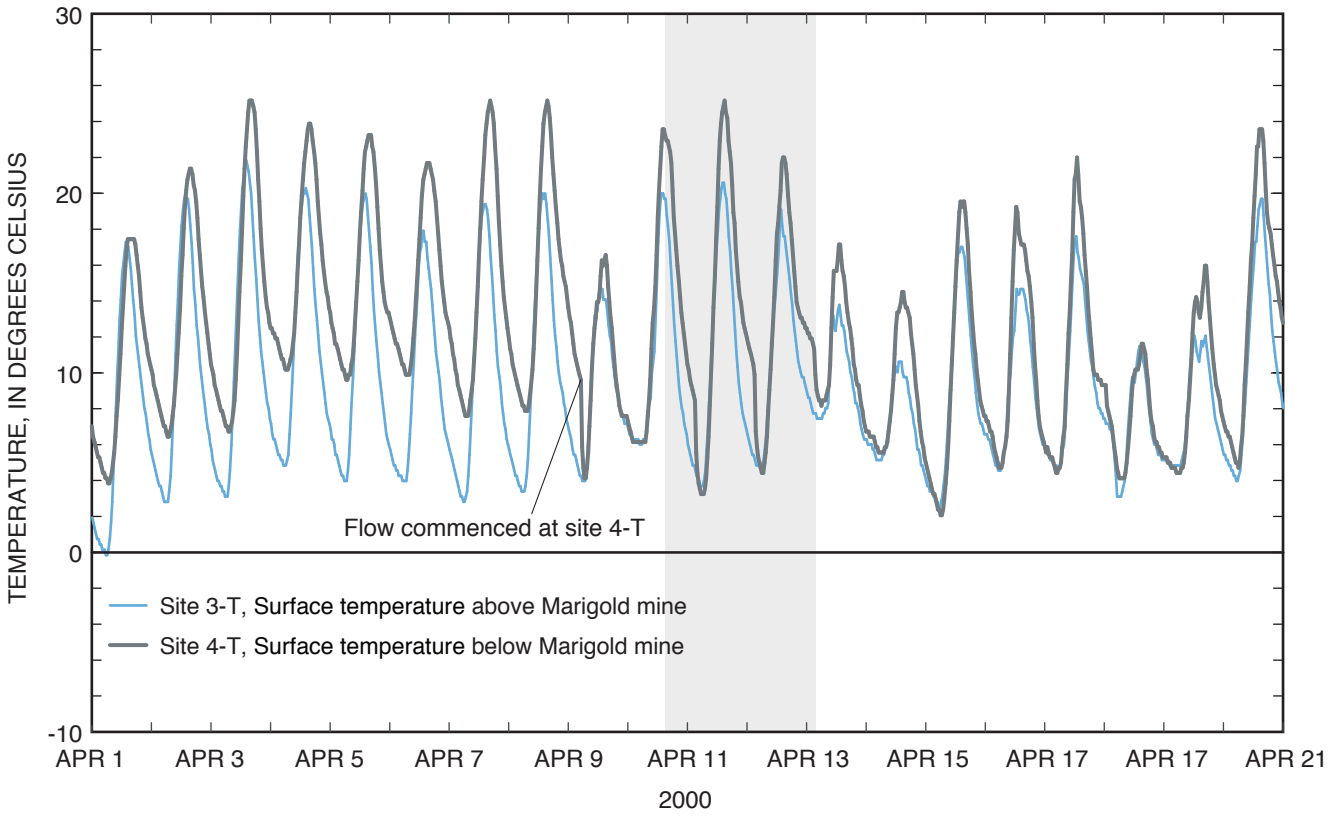

Figure 8. Estimate of when flow began and period of intermittent flow (gray shaded area) in April 2000 at site 4 from streambed temperatures. Location of site 4 is shown on figure 2.

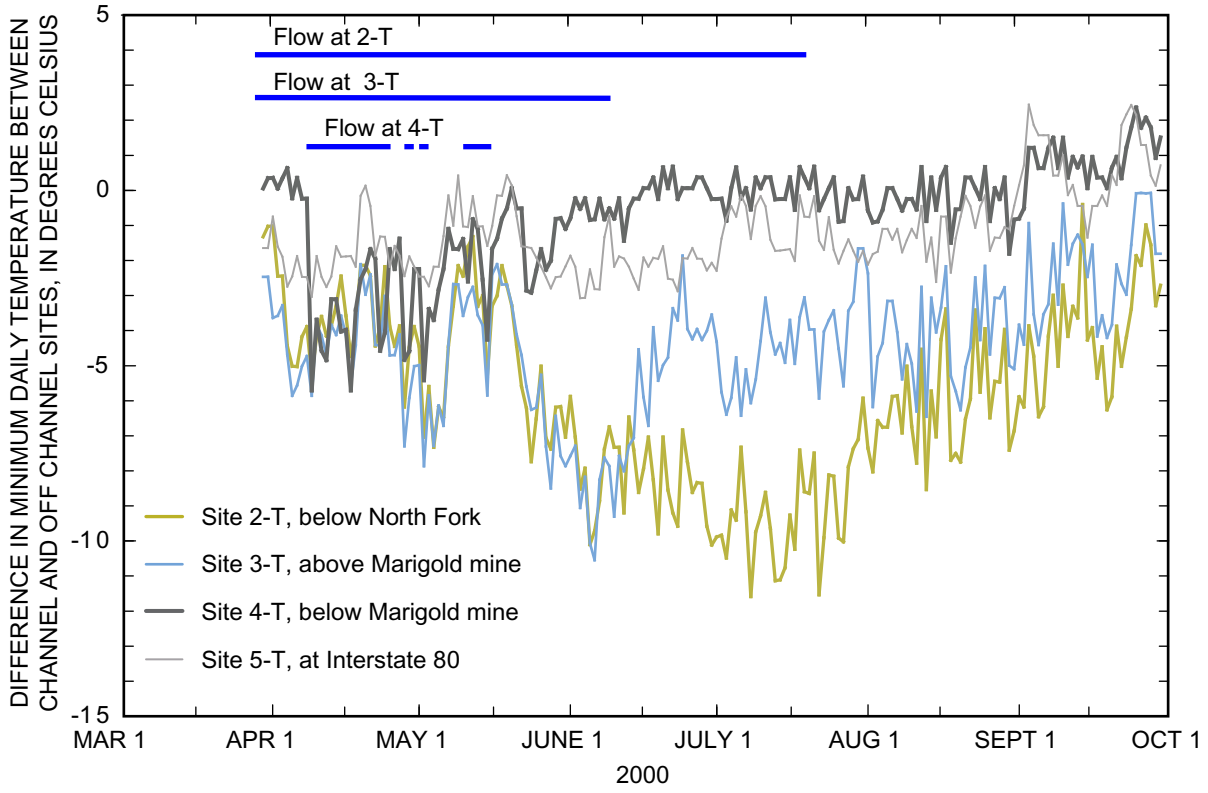

Figure 9. Flow in stream determined from difference in daily minimum temperature at channel sites 2, 3, 4, and 5, and off-channel site OC1. Recording temperature sensors in Trout Creek were buried 7 centimeters beneath the streambed and off channel sensor was buried at a similar depth in soil. Location of sites is shown on figure 2.

flow in the channel ceases entirely is difficult to evaluate using the subsurface temperature profile because drainage through the sediments beneath the streambed continues for some time after flow in the channel has ceased. However, fluctuations at depths of 100 and 138 cm decreased after April 27, suggesting flow in the channel may have ceased on or before that date. Fluctuations in temperature also were observed at depths of 100 and 138 cm on May 1 and could have been caused by brief flow in the channel. The subsurface temperature profile at site 5 does not indicate flow because there were no temperature perturbations below a depth of 50 centimeters similar to those observed at site 4 (fig. 10), which is consistent with field observations.

Streambed hydraulic conductivity and seepage loss rate estimated from subsurface temperature profile at site 4

During infiltration into the sediments beneath a stream, heat in the stream can be used as a tracer to estimate the ability of the sediments to transmit water (the property known as the hydraulic conductivity), which is important for estimating the rate of water flow (or seepage) through the sediments (Chapter 1 explains why heat can be used to estimate the seepage loss rate through a streambed). Consequently, temperature changes in sediments beneath the stream were used to estimate the hydraulic conductivity and seepage losses along a stream as described in Appendix B. During the spring of 2000, flow only reached site 4, the uppermost site, where thermocouples had been placed beneath the streambed. Thus, site 4 was the only place where an estimate of streambed hydraulic conductivity and seepage loss rates could be determined from a subsurface temperature profile. The inverse-simulation method described in Appendix B was used in the analysis. The period of flow from April 13 through April 19, 2000 was used for the analysis. Stream-water temperatures were used for the upper boundary and subsurface temperatures at 20, 50, and 100 cm below the streambed were used as observations for model calibration. The model extended laterally on each side of the stream 15 m so that lateral flow would not be inhibited by no-flow boundaries on the sides. The best-fit simulation to the measured temperatures at depths of 20 and 50 (fig. 11) resulted in an estimate of the saturated streambed hydraulic conductivity of 0.56 m/d and a downward seepage loss rate of 0.46 m/d (Appendix B; and Niswonger, 2001).

Uncertainty in the inversely predicted streambed seepage loss rate at Trout Creek was analyzed using Monte Carlo techniques (Niswonger and Rupp, 2000). The standard devia-

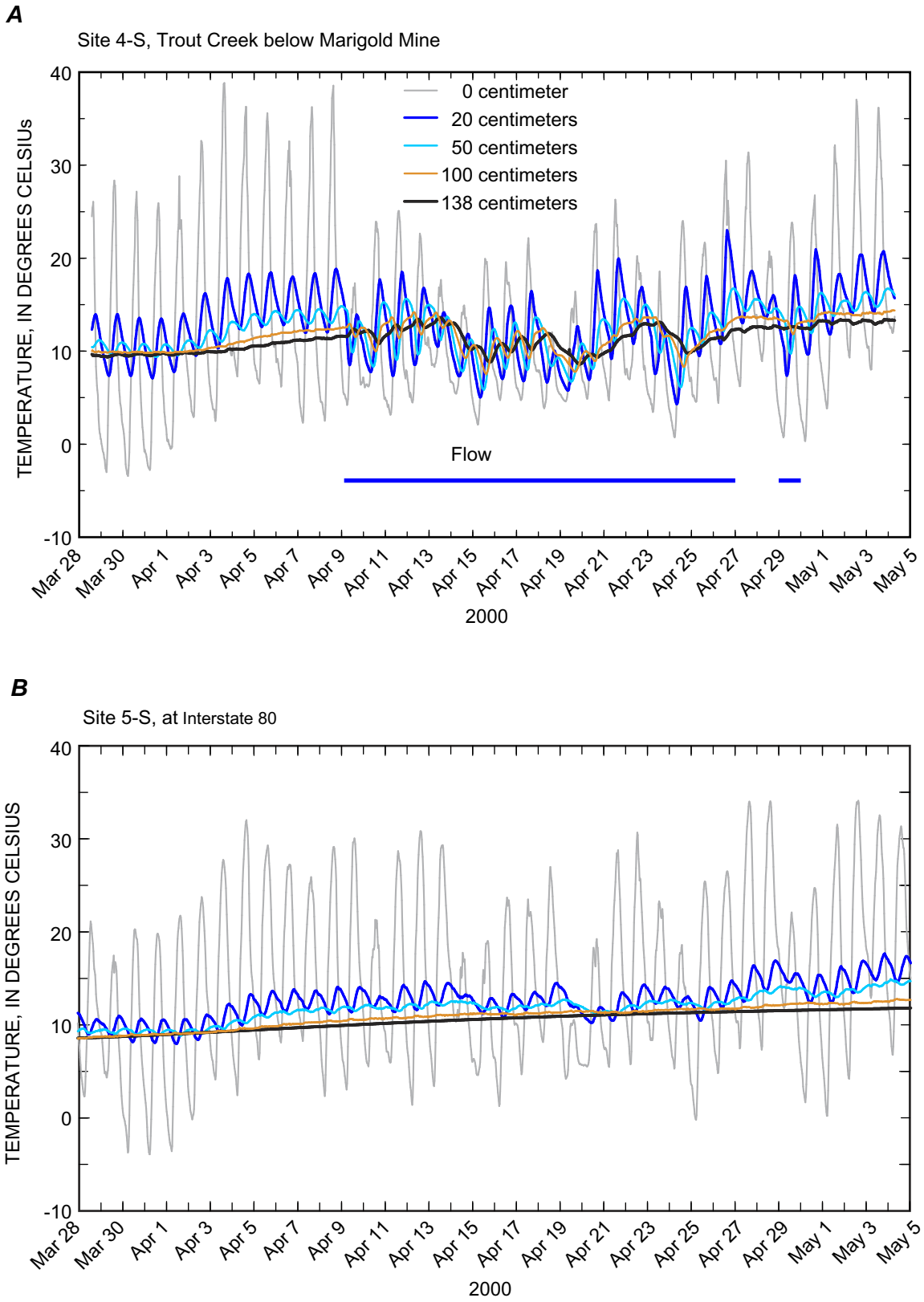

Figure 10. Temperature in sediments beneath Trout Creek from March 28, 2000 to May 5, 2000 at (***A***) site 4 on alluvial fan below Marigold Mine and (***B***) site 5 at Interstate 80. Location of sites 4 and 5 is shown on figure 2.

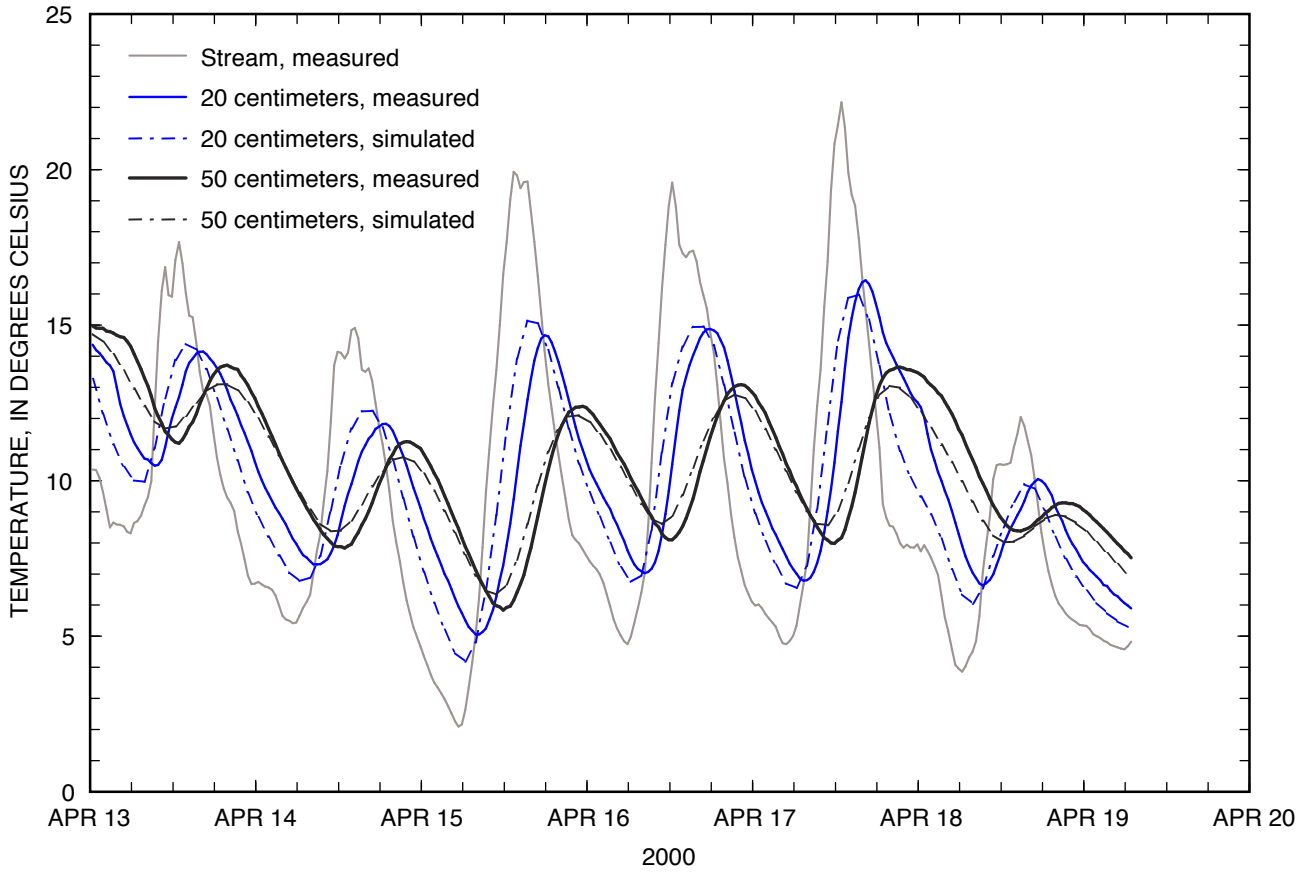

Figure 11. Comparison of simulated to measured temperatures for depths 20 and 50 centimeters beneath Trout Creek at site 4 from April 13 to April 20, 2000. Estimated seepage rate into the streambed is 52 centimeters per day. Location of site 4 is shown on figure 2.

tion in the predicted seepage loss rate converged to a value of 0.11 m/d for an average seepage loss rate of 0.52 m/d after 450 realizations. This uncertainty suggests the ninety-five percent confidence interval in the predicted seepage loss rate was ±0.22 m/d and was due to errors in representing stream sediment thermal parameters in the model. A similar uncertainty analysis was performed testing the effects of temperature measurement error on the predicted seepage loss rate (Niswonger and Rupp, 2000). The mean and standard deviations for the temperature measurement error were estimated based on manufacturer recommendations and other sources of error due to instrument installation. Ninety-five percent confidence in the predicted seepage loss rate due to temperature measurement error was much smaller than for thermal parameter uncertainty and was about ±0.05 m/d.

Estimates of flow and seepage losses incorporated into a model of Trout Creek

Seepage loss rates as a function of stream stage were estimated for eight channel cross sections along Trout Creek in a manner similar to estimating the hydraulic conductivity and seepage loss rate from the subsurface temperature profile at site 4, except the hydraulic properties determined at site 4 were held constant and stream stage was allowed to vary over the vertical range of each channel cross section. The estimates of seepage loss rates as a function of stage were then incorporated into a one-dimensional surface flow model (Niswonger, 2001). The model was formulated specifically for the case when there is an unsaturated zone separating the stream from the underlying aquifer, which is typical for intermittent streams that flow across alluvial fans in the Humboldt River Basin. The surface water model was used to evaluate the duration and quantity of seepage loss along the channel during differing flows from snowmelt runoff. Because there is little vegetation in or adjacent to the channel, much of the seepage loss along Trout Creek eventually recharges the underlying basin-fill aquifers.

Due to the intermittent nature of Trout Creek, an important aspect of the simulation model was the ability to simulate reaches of no flow. The modeled reach was divided into sections delineated by measured cross sections (fig. 2). The modeled reach began at site 3 where detailed stage and flow estimates were available.

Discharge was measured at sites 2, 3, 4, 5, and 7 on May 12, 1999 and at sites 2, 3 and 4 on April 13, 2000 (fig. 12). No flow was observed at sites 5 and 7 on April 13, 2000. The

average seepage loss between sites 3 and 4 was about 6 L/s per km over the 7.3 km reach of the stream on both dates. The seepage loss downstream of Interstate 80 (sites 5 and 7) on May 12, 1999 was about 20 L/s per km; or more than 3 times as much as that estimated between sites 3 and 4. Although, the channel becomes wider downstream of Interstate 80, the slight increase in area determined from measured channel cross sections was insufficient to produce the observed loss indicating that the streambed is more permeable downstream of Interstate 80.

The model was initially calibrated to the discharge measurements on May 12, 1999 using the measured flow and stream stage at site 3 as the upper boundary. The streambed hydraulic conductivity determined from the subsurface temperature profile was used over the modeled reach between sites 3 and 5 and resulted in a reasonable match of the measured seepage loss rate on both dates (as determined by the slope of the measured and simulated flows). The change in the modeled seepage loss rate does not correspond entirely to that measured between sites 5 and 7 because the model computed flows at the midpoint between cross sections, thus an increased seepage loss rate was simulated slightly upstream of where flow measurements indicate a change. More importantly, the dramatic increase in the seepage loss rate between sites 5 and 7 on May 12, 1999 could only be simulated when the hydraulic conductivity of the streambed was increased to 1.2 m/d.

Slight variations in the simulated channel seepage losses between sites 3 and 5 on both dates result from variations in the channel's wetted perimeter at a particular stage from one channel cross section to the next. Slight changes in the slope of the measured discharge along the channel profile are consistent with variations in the simulated flow. The model was able to mimic variations in seepage losses according to differences in channel dimensions along the stream profile. This suggests that variations in seepage loss rates between sites 3 and 5 are due to variations in channel dimensions and not as much to variations in the hydraulic conductivity of the streambed sediments.

After establishing that the model was calibrated with respect to seepage loss rates and discharge, the model was used to simulate snowmelt runoff from March 29, 2000 to April 27, 2000. During the modeled period, flow at site 3 (fig. 5) was used as the upper-modeled boundary (fig. 13).

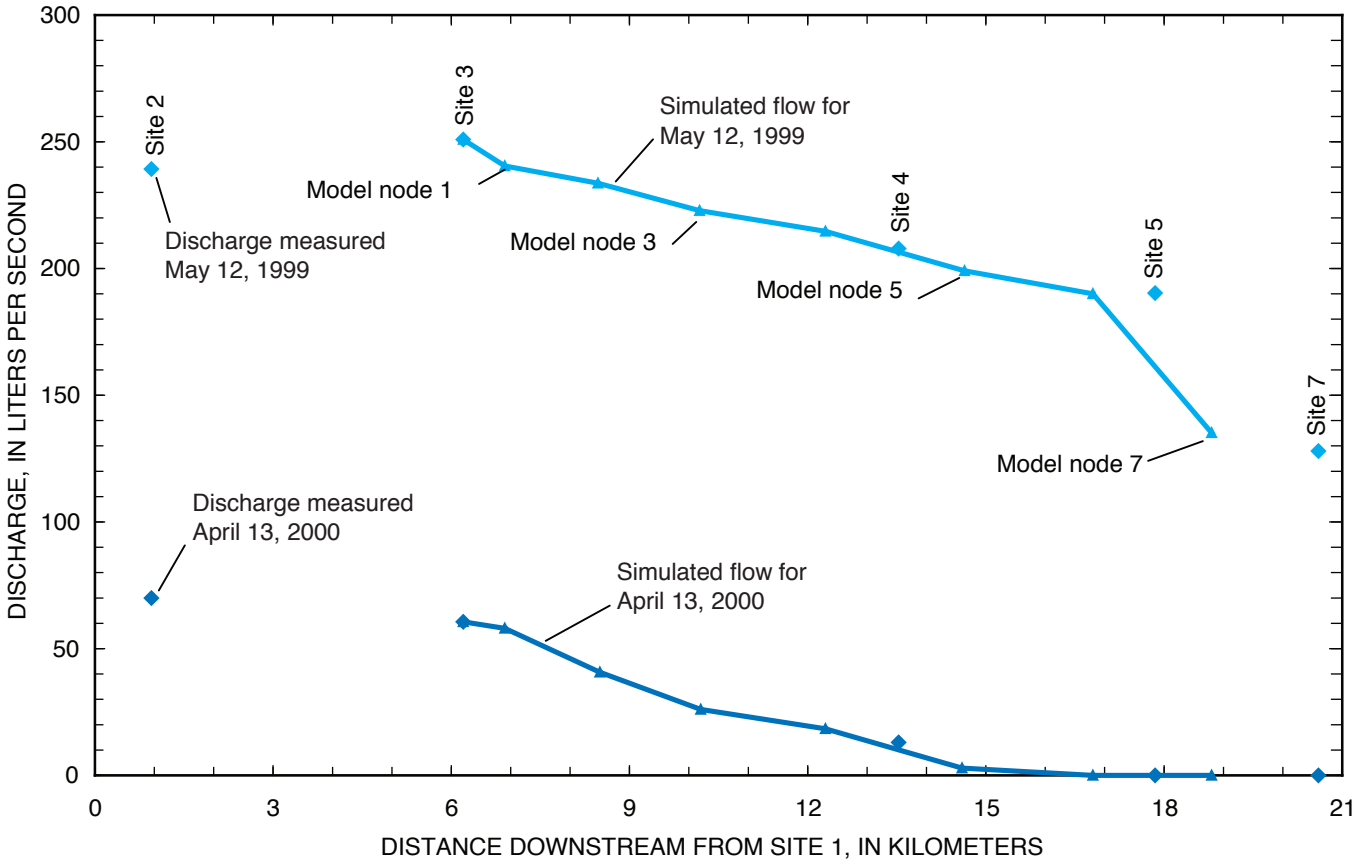

Figure 12. Modeled flows compared with measured discharge along Trout Creek for May 12, 1999 and April 13, 2000. Discharge measurements were made between 7:30 am and noon Pacific Standard Time on May 12, 1999 and between 7:00 am and 9:00 am Pacific Standard Time on April 13, 2000 starting at furthest upstream site on both dates and working downstream. Model simulations are for the same time periods on each date. Location of sites and model nodes are shown on figure 2.

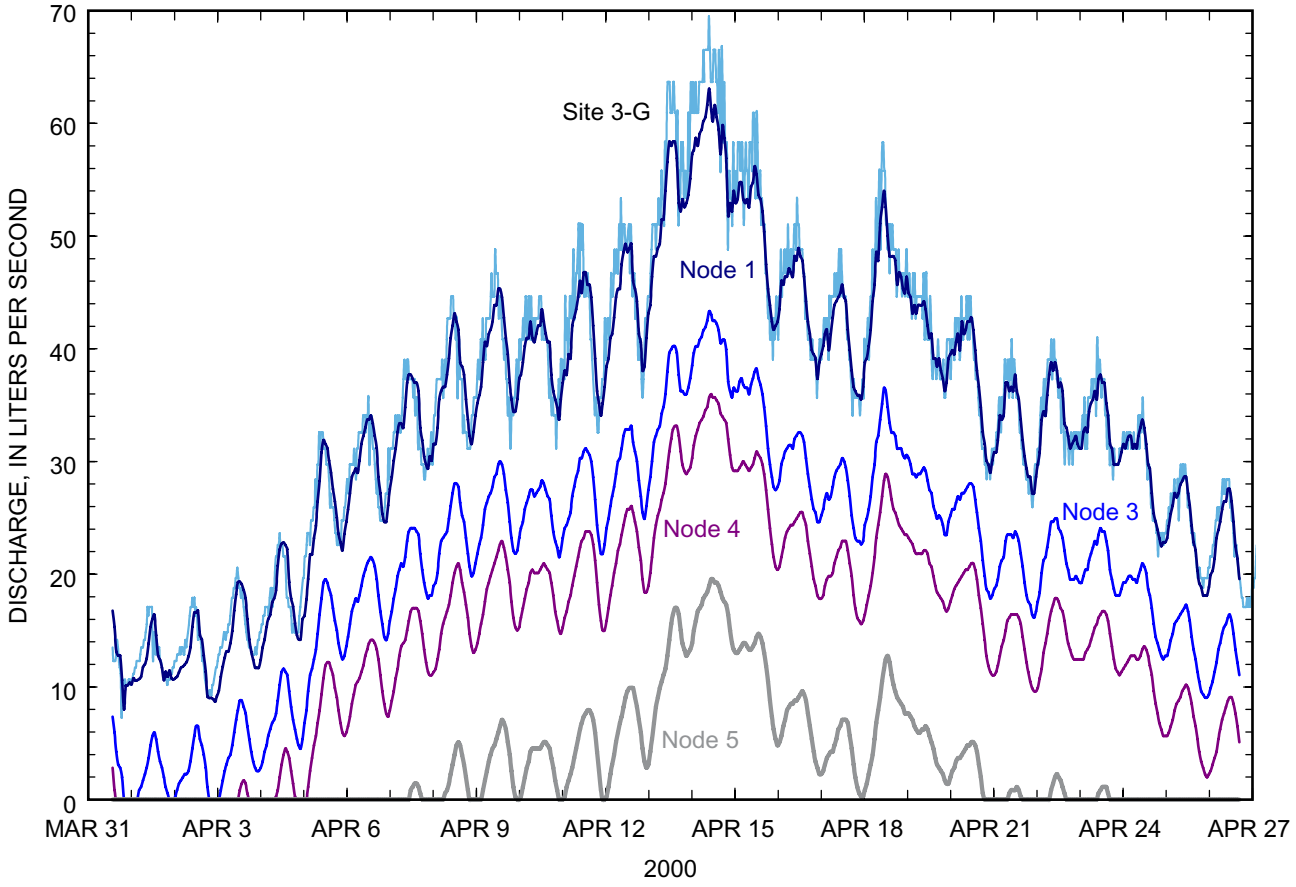

Figure 13. Simulated flow at selected distances along Trout Creek during April 2000. Flow at upper model boundary is estimated discharge at site 3. Locations of site 3 and modeled nodes are shown on figure 2.

Simulated flow during the morning of April 13, 2000 was compared with measured discharges (fig. 12). Simulated flow reasonably matched the measured discharge, indicating that the seepage loss rates determined from stream stage and model calibration at much higher flows worked well at the lower measured discharges during the spring of 2000. The measured discharges in April 13, 2000 are much less than those of May 12, 1999 and result from less accumulation of snow during the winter of 2000 compared with the winter of 1999. The diurnal variation in flow shown in figure 13 is due to increased snowmelt as ambient temperatures increased until mid-day and then decreased as the temperature cooled into the night. The diurnal variation in snowmelt results in a diurnal variation in the point downstream where all the flow seeps into the underlying sediments. Simulated discharges at different places along the channel profile show this diurnal migration of where the flow ceases in the channel. The simulated duration of flow at model node 5 (a distance of 1.1 km downstream of site 4; fig. 2) shows duration of flow similar to that estimated from the surface and subsurface temperatures at site 4 (figs. 8,9 and 10). The simulated flow begins on April 7, slightly earlier than temperature data indicates at site 4 and has brief periods of no flow for several days, consistent with changes in the diurnal surface temperature pattern (fig. 8). The modeled flow is continuous from April 12 through April 19, and becomes discontinuous afterwards. This is also consistent with observations at site 4. In the model simulation, flow does not reach as far as Interstate 80 (site 5), again consistent with surface and subsurface temperature measurements at that site (figs. 9 and 10).

Much of the seepage loss along Trout Creek during the first part of spring runoff in early April was upstream or adjacent to Marigold mine (fig. 14; site 2 to model node 2 on fig. 2). As snowmelt runoff in Trout Creek reached its peak in mid April, a greater percentage of the cumulative seepage loss was transferred downstream. By mid April, about 50 percent of the total loss was on the upper alluvial fan (between model nodes 2 and 4) and about 10 percent was on the middle fan (between model nodes 4 and 6) downstream of Marigold mine even though the duration of flow on the middle fan was only a couple of weeks. Snowmelt runoff during the spring of 2000 was near or below normal on the basis of precipitation records during the fall of 1999 and winter of 2000. This suggests that during years of near normal to above normal precipitation, a substantial part of the seepage loss along Trout Creek is on the alluvial fan below Marigold mine.

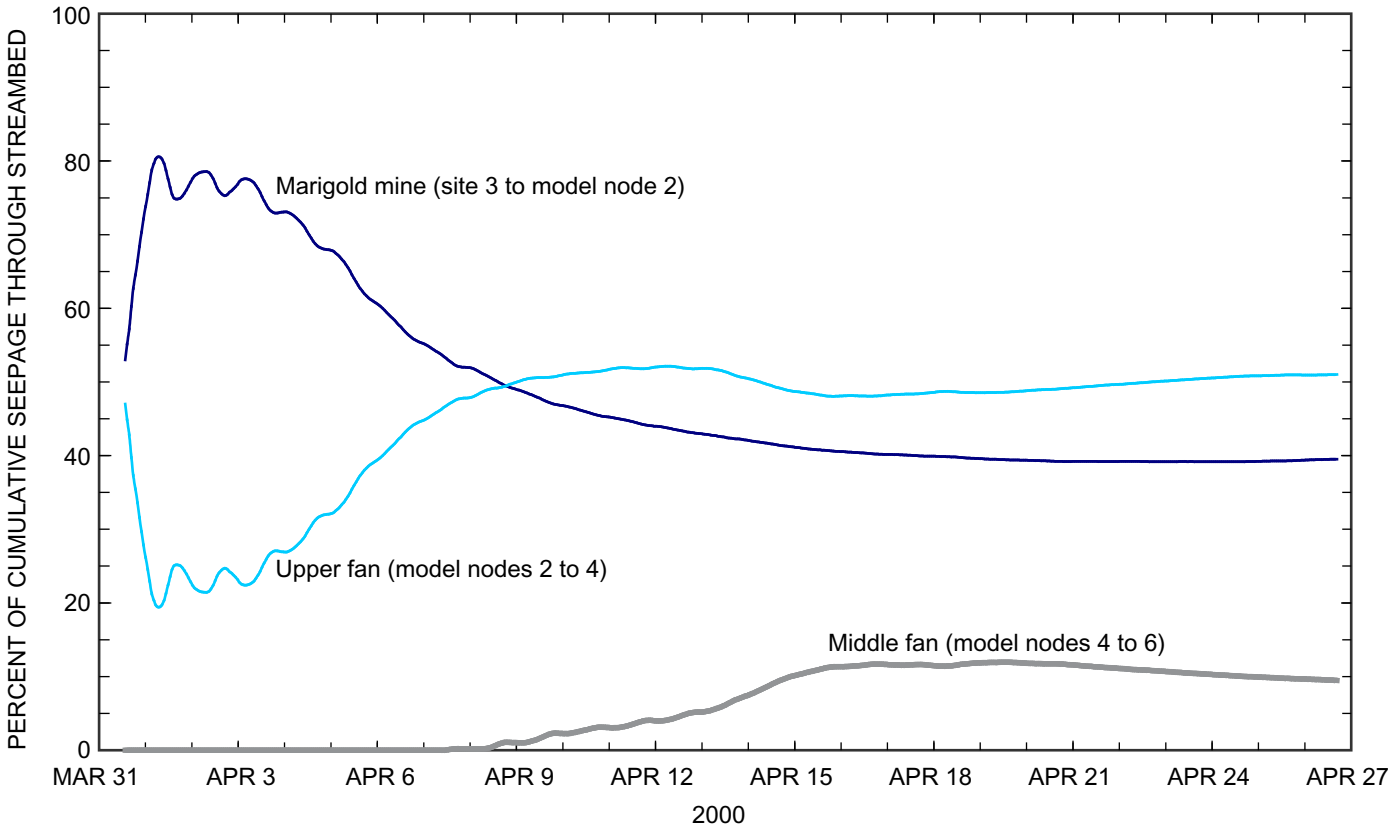

Figure 14. Percentage of cumulative seepage for selected reaches along Trout Creek during April 2000. Locations of site 3 and modeled nodes along stream channel are shown on figure 2.

In summary, estimates of the duration of flow from stream temperature and subsurface temperature profiles were useful in understanding the variability of flow and seepage losses along Trout Creek. However, changing weather conditions, which can create considerable uncertainty, complicates the analyses of stream temperatures to ascertain periods of flow and no flow along the stream channel. Subsurface temperature profiles are useful at detecting when flow starts following extended periods of no flow and also can be used to provide reliable estimates of the seepage loss rates. However, the profiles are questionable in determining a precise time when flow stops because continued drainage through the streambed masks this event. Although not perfect, a simple analysis of comparing differences in daily minimum stream temperatures in the stream to an off-channel temperature sensor provides a reasonable estimate of the total duration of flow along Trout Creek. The method, however, is insensitive to brief periods of no flow during the night as the stream channel remains damp and has a minimum temperature similar to when flow is in the channel. A detailed analysis of the stream temperature along with additional field observations are necessary to determine the brief periods of no flow that occur as a result of decreased snowmelt at night. A channel routing model that incorporates channel seepage losses provided a means for estimating the cumulative volumes of seepage loss along Trout Creek as well as insight to the diurnal variability of flow and seepage losses along the channel.

Appendix A

Determining temperature and thermal properties for heat-based studies of surface-water ground-water interactions

David A. Stonestrom and Kyle W. Blasch

Introduction

Advances in electronics leading to improved sensor technologies, large-scale circuit integration, and attendant miniaturization have created new opportunities to use heat as a tracer of subsurface flow. Because nature provides abundant thermal forcing at the land surface, heat is particularly useful in studying stream-groundwater interactions. This appendix describes methods for obtaining the thermal data needed in heat-based investigations of shallow subsurface flow.

Techniques for measuring temperature have evolved considerably since 1714, when German physicist Gabriel Daniel Fahrenheit introduced the sealed mercury-in-glass thermometer as an improvement over Galileo's alcohol-in-glass thermometer (Star, 1983). The Galilean thermometer, being open to air, also responded to barometric fluctuations. The temperature scale that bears Fahrenheit's name pays tribute to the significance of solving the long-standing problem of creating an accurate, readily transferable unit of temperature. Swedish astronomer Anders Celsius introduced a water-based, power-of-ten scale shortly thereafter that was later adopted by the Swedish Academy of Sciences as the basis of the metric temperature scale (Kant, 1984). On adoption, the Academy wisely reversed Celsius' original assignments of 0 ºC and 100 ºC, respectively, to the boiling and freezing points of water. Development and linkage of the Celsius scale to the thermodynamically based Kelvin scale paved the way for quantitative theories of heat flow and transformation during the 1800's that formalized the concepts of heat capacity and thermal conductivity. Mathematicians, physicists, and engineers who developed the conceptual framework included such notables as Jean Baptiste Joseph Fourier, James Prescott Joule, and William Thompson (Lord Kelvin). Their work spurred scientific investigations into the thermal behavior of matter that continue today (Lienhard and Layton, 1988).

Industry, government, and other technical organizations provide periodic compendia of temperature-measurement techniques (for example, Herzfeld, 1962; Schooley, 1982; ASTM, 1993; CSIRO, 1998). These works include elaborate, special-purpose techniques for specific applications. The focus herein is on practical methods employed in hydrologic investigations. These methods are relatively inexpensive and accurate, and comprise the thermal measurement techniques used in the case studies of this circular.

Types and characteristics of temperature sensors

Applications that use heat as a tracer of subsurface flow usually require multiple measurements of temperature through time at relatively inaccessible locations. This requirement generally limits suitable sensors to those that convert temperature to some form of electronic signal. The sensors most often employed are thermocouples (Constantz and Thomas, 1996) and thermistors (LeCain, Lu, and Kurzmack, 2002). Resistance temperature devices (RTDs) and integrated-circuit (IC) sensors can also be used (Paluch, 2002). Figure 1 shows characteristic responses of these sensors together with advantages and disadvantages of each. Due to their small thermal masses, all of the sensors depicted in Figure 1 respond quickly to changes in temperature.

Thermocouples are the least expensive and most easily deployed sensor (fig. 1A). They can be fabricated as needed from thermocouple cable with little more than a soldering tool and a wire stripper. Thermocouples operate on the principle, discovered by Thomas Seebeck in 1821, that dissimilar metals in a circuit develop a voltage proportional to the temperature difference between their junctions (Finch, 1962). Thermocouples are more stable than thermistors but less stable than RTDs. Being self-powered, they are not subject to self-heating effects like thermistors, RTDs, and IC sensors. Of common thermocouple pairs, type T (copper-Constantan) is well suited for hydrologic applications due to its high sensitivity (relative to other thermocouple types) and corrosion resistance. Thermocouples require linearization and measurement of reference-junction temperatures. Linearization and reference circuitry is often integrated into data-acquisition systems, making thermocouples suitable for multi-point sampling arrays. An important consideration with thermocouples is that their output voltages are small, placing stringent demands on signal-conditioning equipment. A type T thermocouple generates only 0.04 millivolt per ºC temperature difference between reference and measuring junctions, requiring the data-acquisition system to resolve four millionths of a volt (0.000,004 V) to detect a 0.1-ºC change in temperature. Stray currents in poorly configured systems can cause common-mode (error) voltages much larger than this (Horowitz and Hill, 1989; Morrison, 1998). Another consideration stems from the fact that any errors in reference-junction temperatures produce equal errors in indicated subsurface temperatures. Such errors may represent a time-invariant bias common to all measured temperatures, with perhaps little consequence on inferred transport. But if the reference junction is even a few millimeters from the reference-temperature-measurement point,

	A. THERMOCOUPLE	*B.* THERMISTOR	*C.* RTD	*D.* IC SENSOR
	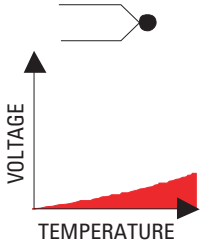	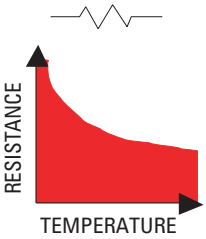	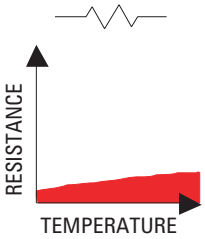	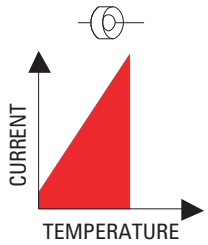
Advantages	• Self-powered • Rugged • Inexpensive • Simplest to install	• High output • High sensitivity • Fast response • Two-conductor lead OK	• Most stable • Most accurate	• Most linear • Highest output • Increasing choices • Two-conductor lead OK
Disadvantages	• Low output • Non linear • Requires reference • Least sensitive	• Non linear • Fragile • Requires current source • Self heating • Least stable	• Most expensive • Low sensitivity • Low resistance • Requires current source • Self heating	• Standards lacking • Requires clean & dry environment • Self heating

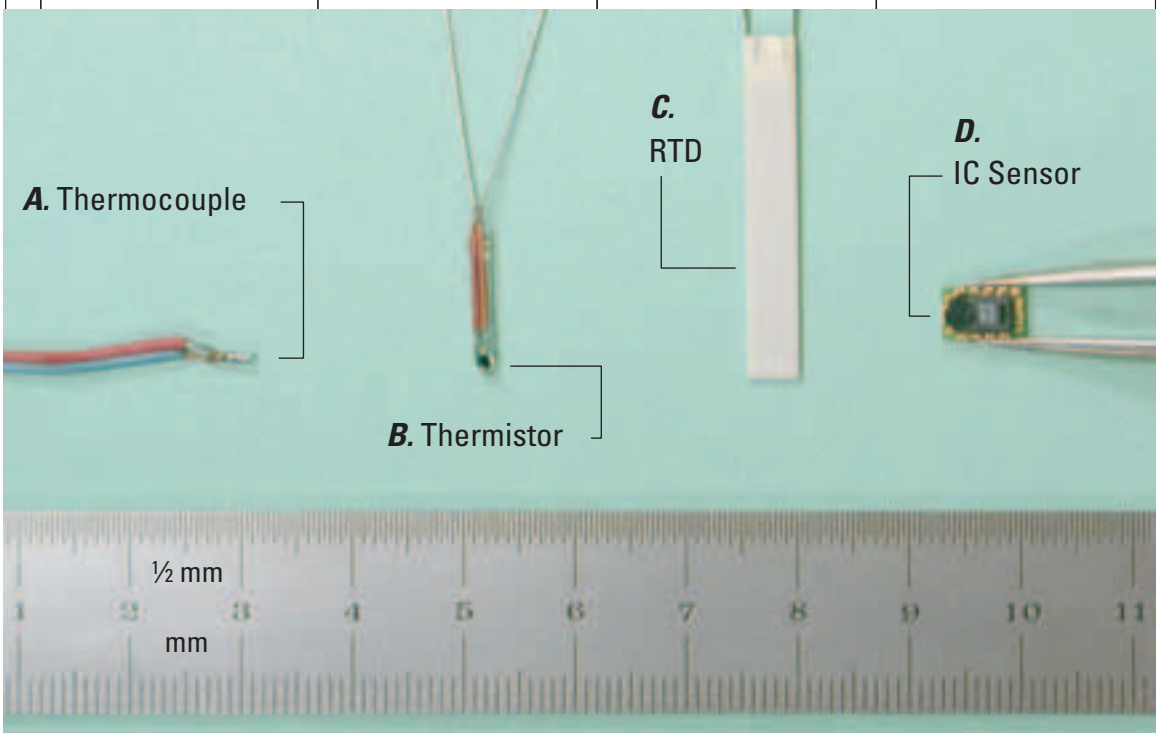

Figure 1. Common electronic temperature sensors with schematic symbols, response characteristics, and advantages and disadvantages of each type (adapted from Hewlett Packard, 1983). RTD and IC are industry acronyms for resistance temperature device and integrated circuit, respectively.

thermal transients in the data-acquisition system can produce time-varying errors that are on the same order of magnitude as the signal of interest. Isolation of the data-acquisition system from thermal transients, usually by insulating and burying it, is essential for avoiding these errors.

The other commonly deployed sensor is the thermistor. Thermistors are temperature-dependent resistors made from transition-metal oxides (Hewlett-Packard, 1983). They have a large base resistance, typically on the order of 2000 ohms at 20 ºC, and a nonlinear sensitivity in the range of -10 to -20 ohms $ºC^{-1}$. Thermistors are usually embedded in glass or other material for chemical protection (fig. 1B). Thermistors can be made to microscopic dimensions, trading off calibration stability for thermal mass. But all thermistors drift with time, requiring periodic calibration (CSIRO, 1998). This becomes a consideration for long-term deployments in inaccessible locations.

Resistance temperature devices (RTDs) have highly stable calibrations even in harsh environments. Figure 1C shows a platinum RTD embedded in a ceramic body. Platinum RTDs are sufficiently stable to serve as calibration-transfer standards in metrology laboratories (Klock and Sullivan, 1962; Morris, 2002). The temperature sensitivity of RTDs is positive, slightly nonlinear, and small relative to thermistors (fig. 1). The relative insensitivity of RTDs, typically 0.04 ohms $ºC^{-1}$ for platinum, limits their use to settings with relatively large thermal gradients. Because of their low base resistance (typically 100 ohms at 0 ºC), RTDs require redundant leads and active compensation for lead-wire resistance. RTDs are also the most expensive of the common sensor types.

IC sensors are based on a semiconductor resistor embedded in an integrated circuit for conversion to a linear electrical output (fig. 1D). Current-output IC sensors require only two wires for connection to data-logging equipment, making them relatively easy to deploy (Sheingold, 1980). Unfortunately, most IC sensors are designed for dry environments and have relatively short times-to failure in moist environments. IC sensors are actively being developed, and may soon emerge as an advantageous choice for field deployments.

Single-channel temperature loggers offer an alternative to multiplexed sensor installations. Available from various manufacturers, these devices contain a thermistor or thermocouple integrated with signal-conditioning circuitry, a real-time clock, a memory unit, and an optical or infrared interface to provide access by computer or portable data shuttle. Figure 2A shows an example of one such device. Response times are slower than the sensors in Figure 1, but fast enough to track most hydrologic signals of interest (fig. 2B). Self-contained devices have the advantage of not needing an external data logger or connecting wires. The user retrieves the devices to acquire collected data.

Specific heat capacity, thermal conductivity, and thermal diffusivity

The thermal properties of soils and sediments can be obtained either from literature values, laboratory analyses of field samples, or field measurements. As explained in Chapter 1,

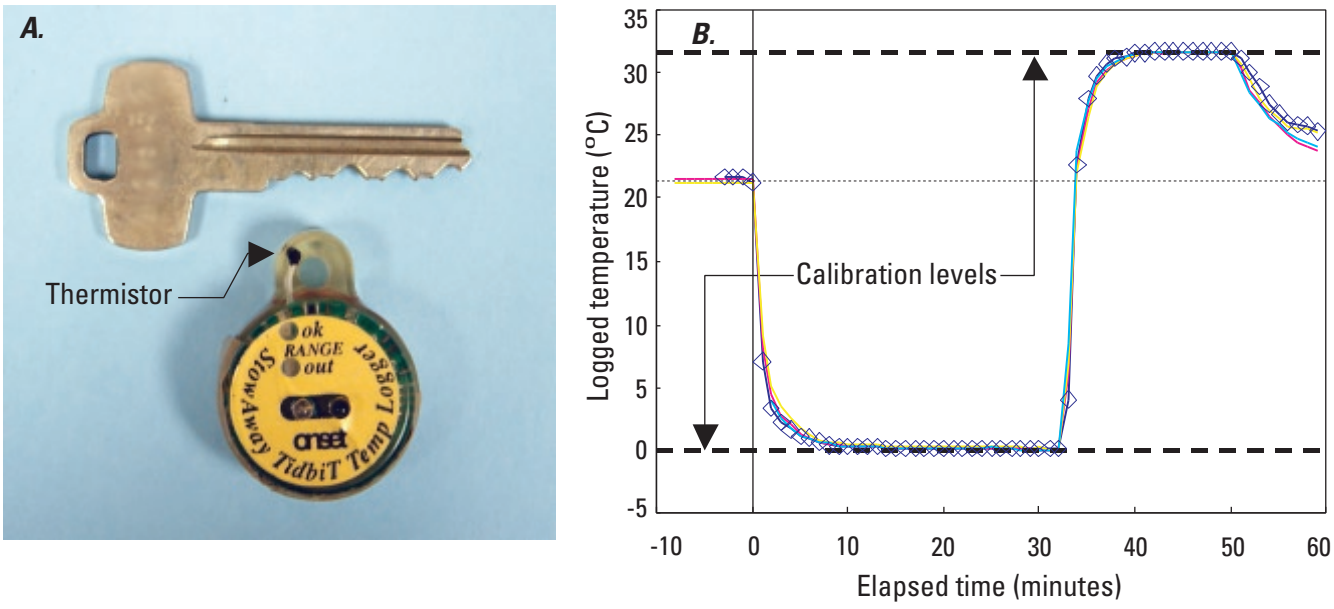

Figure 2. (***A***) Self-contained temperature logger is about 3 cm in diameter. Note thermistor in mounting eyelet. (***B***) Dynamic response of four self-contained temperature loggers during calibration tests. Loggers, initially at room temperature, were immersed in a 0-ºC bath, followed by a 32ºC bath. The average 95% response time of the loggers was about 5 minutes. Data sets are color coded. To avoid clutter, individual data points are shown for only one of the loggers.

thermal properties vary over a much narrower range than do analogous hydraulic properties. Because of this, estimates of water flux are insensitive to errors in thermal properties relative to errors in hydraulic properties. Thermal properties are difficult to measure outside of the laboratory. Thus, temperature is usually the only thermal parameter measured in the field.

Specific heat capacity is the amount of heat absorbed or released per mass of material when the material's temperature increases or decreases by a small increment, operationally defined as one degree Celsius (°C). Multiplying specific heat capacity by density (mass per unit volume) gives volumetric heat capacity, which is the change in heat per volume of material per change in temperature. Units of volumetric heat capacity are joules per cubic meter per degree Celsius ($J\ m^{-3}\ °C^{-1}$). Heat capacities of relevant phases rank in the order: [liquid water] > [organic solids] > [mineral solids] >> [soil gases] (table 1A). Heat capacities of porous materials depend on their composition and bulk density, and vary linearly with water content (table 1B, fig. 3).

Heat capacities of unconsolidated materials can be determined in the laboratory with a calorimeter, which is an insulated chamber equipped with a stirrer and precision thermometer. The method of Taylor and Jackson (1986) determines heat capacity by mixing a slurry made from the porous medium with water at a different temperature. The heat capacity of the sediment is calculated from the masses and temperatures of initial slurry, added water, and final slurry. In practice, heat capacities are often calculated from the volume-weighted sum of heat capacities of constituents making up the material, using literature values (de Vries, 1966). Denoting volume fractions as x and heat capacities as c, the volumetric heat capacity of the bulk material C_b is approximately

$$C_b = x_w c_w + x_o c_o + x_m c_m + x_a c_a,$$

where subscripts w, o, m, and a denote water, organic solids, mineral solids, and air, respectively.

Thermal conductivity, κ, is a measure of a material's ability to conduct heat. It is defined as the amount of heat trans-

Table 1A. Thermal properties of selected materials -- Individual phases

Individual phase	Density (10^6 g/m^3)	Volumetric heat capacity (10^6 J/m^3 °C)	Thermal conductivity (W/m °C)	Thermal diffusivity (10^{-6} m^2/s)
Air[1]	0.001	0.001	0.024	19.
Liquid water[1]	1.0	4.2	0.60	0.14
Ice[2]	0.9	1.9	2.2	1.2
Quartz[3]	2.7	1.9	8.4	4.3
Average, soil minerals[3]	2.7	1.9	2.9	1.5
Average, clay minerals[4]	2.7	2.0	2.9	1.5
Average, soil organic matter[3]	1.3	2.5	0.25	0.10

Table 1B. Thermal properties of selected materials -- Porous media

Porous medium	Bulk Density (10^6 g/m^3)	Porosity (V_{pores}/V_{bulk})	(Liquid) Water content	Volumetric heat capacity (10^6 J/m^3 °C)	Thermal conductivity (W/m °C)	Thermal diffusivity (10^{-6} m^2/s)
Tottori sand[5]	1.83	0.31	saturated	2.6	2.2	0.85
Clarion sandy loam[6]	1.38	0.48	saturated	3.2	1.8	0.55
Harps clay loam[6]	1.21	0.54	saturated	3.2	1.4	0.42
Sandfly Creek sand[7]	1.50	0.43	dry	1.3	0.25	0.18
Yolo silt loam[8]	1.30	0.51	dry	1.1	0.26	0.23
Clarinda clay[7]	1.16	0.56	dry	1.2	0.18	0.15
Snow[9]	0.46	0.50	dry	1.0	0.71	0.68
Snow[9]	0.18	0.80	dry	0.4	0.13	0.36
Snow[9]	0.05	0.95	dry	0.1	0.06	0.60

[1]Carslaw and Jaegger (1959, p. 497); [2]van Wijk and de Vries (1966a, p. 40); [3]van Wijk and de Vries (1966b, p. 105); [4]de Vries (1966, p. 210); [5]Hopmans, Simunek, and Bristow (2002); [6]Ren, Kluitenberg, and Horton (2000); [7]Bristow, Kluitenberg, and Horton (1994); [8]Wierenga, Nielsen, and Hagan (1969); [9]van Wijk and de Vries (1966b, p. 110).

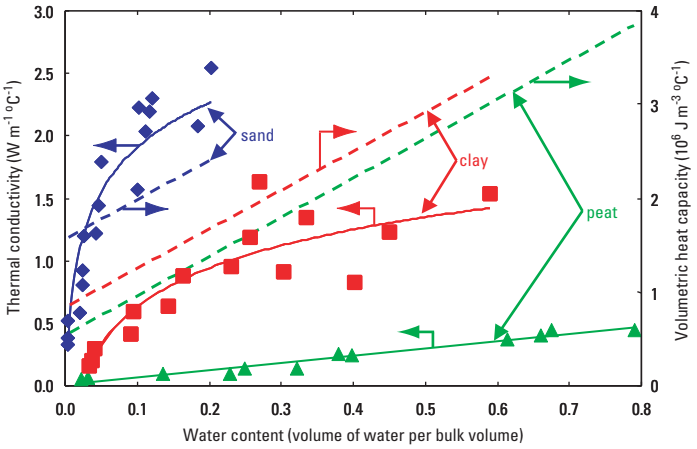

Figure 3. Dependence of volumetric heat capacity and thermal conduction on water-content for selected materials. Dashed lines are volumetric heat capacities calculated as described in the text, using data from table 1A. Points are experimentally determined thermal conductivities, from deVries (1966). Solid curves are empirical fits to the thermal-conductivity data.

mitted per unit time per unit area per unit temperature gradient. Units of thermal conductivity are watts (joules per second) per square meter per degree Celsius per meter (W m^{-1} $^oC^{-1}$). The thermal conductivity of porous materials depends upon the composition and arrangement of the solid phase. Coarse-grained materials generally have higher thermal conductivities than fine-grained materials. Also, because water conducts heat much better than air, thermal conductivity depends strongly on water content (table 1A and B; fig. 3). Due to the complexities of pore geometry, this dependence is non-linear and difficult to predict (Wierenga, Nielsen, and Hagan, 1969). In practice empirical equations are used to fit measured thermal-conductivity data over limited ranges of water content (Hopmans, Simunek, and Bristow, 2002).

Thermal conductivities of porous media can be measured using steady-state or transient-state methods (Jackson and Taylor, 1986). Steady-state methods facilitate testing of Fourier's law, which is almost universally assumed to govern heat conduction (Carslaw and Jaeger, 1959). Maintaining a thermal gradient in moist materials, however, induces fluid flow along temperature and density gradients. Fluid flow complicates the measurement of thermal conductivity because advection (as well as conduction) transfers heat. In partly saturated media, latent heat transfer (that is, heat associated with transitions from vapor to liquid and liquid to vapor) become important. Additionally, water contents in partly saturated media become non-uniform when temperature gradients are maintained. To avoid complications associated with these processes, rapid transient-state methods have been developed for measuring thermal conductivities in moist materials. The pulsed cylindrical-heat-source method (also known as the pulsed thermal-probe method; described below), is the most commonly used transient method for measuring thermal conductivities in both field and laboratory applications (de Vries, 1952; Wierenga, Nielsen, and Hagan, 1969; Jackson and Taylor, 1986; Shiozwa and Campbell, 1990).

Thermal diffusivity is the ratio of thermal conductivity to volumetric heat capacity. The units of thermal diffusivity are meters squared per second (m^2 s^{-1}). Thermal diffusivity is a measure of how quickly an imposed change in temperature is transmitted through the material. Air has a large thermal diffusivity, despite having a low thermal conductivity, because its volumetric heat capacity is small (table 1A). With almost no capacity for storing or releasing heat, temperature signals travel quickly through air.

Jackson and Taylor (1986) described a method for the direct determination of thermal diffusivities of soils and sediments. The method analyzes transient temperatures within a sample as heat is applied to its surface through a copper plate. The method, while relatively simple, is difficult to apply outside the laboratory. Recent advances in the pulsed thermal-probe method have produced field-deployable probes that simultaneously determine various combinations of heat capacity, thermal conductivity, and thermal diffusivity (Campbell, Calissendorff, and Williams, 1991; Bristow, Kluitenberg, and Horton, 1994; Kluitenberg, Bristow, and Das, 1995; Hopmans, Simunek, and Bristow, 2002). These techniques apply heat-pulse theory to cylindrical probes made from hypodermic-needle tubing. One probe contains a heater. Parallel to this probe are one or more auxiliary probes for measuring temperature responses. Pulses of heat induce changes in surrounding temperatures measured by auxiliary probes. Analytical or numerical analyses of temperature histories produce estimates of thermal properties. Pulsed thermal probes have been combined with time-domain-reflectrometry probes for simultaneously measuring thermal properties, water content, and bulk electrical conductivity (Noborio, McInnes, and Heilman, 1996; Ren, Noborio, and Horton, 1999).

Sensor deployment and data acquisition

A pipe driven into loose sediments can provide a temporary casing while sensors are deployed to desired depths. The sediments collapse around the wires as the pipe is withdrawn (fig. 4A, B, and C). To avoid induced preferential flow, intervals between sensors can be grouted with swelling clay (Nielsen and Sara, 1992) or expanding foam (Faybishenko, 2000). These materials are emplaced through the temporary casing as the casing is withdrawn. Proper grouting is required in cohesive soils and sediments. To minimize disruption of sedimentary layers and soil structures, sensors can be installed through holes that slant diagonally beneath the study area or extend horizontally from an adjacent access point (Faybishenko, 2000). Wires connecting streambed sensors to remote data loggers need to be deeper than the maximum depth of scour. Conduit anchored to the streambed can help protect the wires. Deploying a precision temperature reference on the


A


B


C

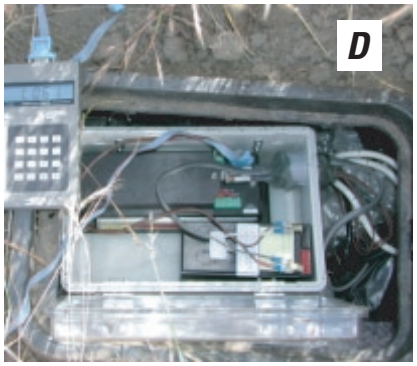
D


E


F


G


H


J

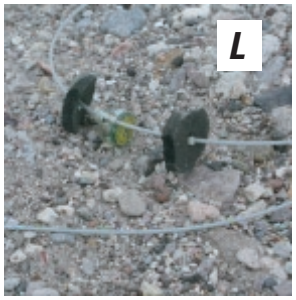
L


I


K

wiring panel reduces reference-junction errors. A thermally conductive strip on the wiring panel minimizes temperature offsets between the reference junction and reference-junction-temperature measurement point. Burial of loggers in water-tight containers that are packed in thermal insulation further reduces errors from temperature transients (fig. 4D and E).

Self-contained temperature loggers can be buried directly in the ground with or without protective housings, or deployed in access tubes. Loggers directly buried in stream channels usually have housings that are tethered to anchors driven into the channel upstream of the measurement point (fig. 4F). Access tubes need to be grouted to prevent preferential flow down the annular space around the tube (figs. 4H-J). Baffles inhibit thermally induced advection (fig. 4L). In addition to the self-contained temperature loggers, figures 4G-L also show external thermocouples on moveable arms that press against surrounding sediments after the access tube is in position. A two-component expanding foam grouts the annular space, locking the arms into position as it hardens (fig. G-J).

Design of temperature-measurement arrays

Success of thermal methods for quantifying surface-water ground-water exchange is dependent on appropriate placement of temperature sensors. Appropriate placement depends on (1) hydraulic and thermal properties of the sediments, (2) climatic conditions, which determine the nature of thermal forcing, (3) anticipated pore-water velocities, and (4) practical considerations, such as depth of scour. Experimental design includes selecting the frequency of data collection. While the overall strategy will be dictated by the purpose of the study, standard principles of experimental design should be incorporated at every stage of planning (Garcia-Diaz and Phillips, 1995). In large-scale projects, formalized data-quality objectives can help produce efficient measurement networks (USEPA, 2000).

Preliminary modeling is useful for selecting measurement locations and frequencies (Constantz, Stonestrom, and others, 2001). Fluid flow modulates the transmission of thermal signals into the profile (van der Kamp and Bachu, 1989; Silliman, Ramirez, and McCabe, 1995). Fluid flow can thus be determined by the departure of temperatures from a purely conductive pattern (Silliman and Booth, 1993; Constantz and Thomas, 1996). To guide sensor placement, theoretical temperature patterns can be calculated from numerical solutions of the coupled transport equations (Appendix B). For simple cases, theoretical temperature patterns can be predicted from analytical solutions. The analytical solution for pure thermal conduction in a deep, uniform profile with sinusoidal heating at the land surface is (Carslaw and Jaeger, 1959)

$$\Delta T(z,t) = A \cdot e^{-z/D} \cdot \sin[(2\pi/P)(t-t_0)-(z/D)],$$

where ΔT is the departure of temperature from the average value, z is depth, t is time, A is the amplitude of temperature at the surface, D is the damping depth, P is the period of surface temperature, and t_0 is the time at which ΔT equals zero. The damping depth D is equal to $(P\alpha/\pi)^{-1/2}$, where α is the thermal diffusivity.

Daily and annual temperature fluctuations imposed at the land surface are quasi-periodic. As periodic thermal waves move into a profile, the storage and release of energy by the conducting medium attenuates the signal as it propagates away from the thermally forced boundary. In consequence, the magnitude of periodic temperature perturbations decreases with depth. The depth below which cyclic surface fluctuations

Figure 4. Field deployment of temperature-measuring equipment. (A,B,C) Installation of thermocouple sensors in a stream channel. (D,E) Data logger for thermocouple installation. (F) Installation of stream-bed sensor. (G) Swing-out thermocouple arm on access tube. (H) Top of access tube prior to grouting. (I) Grouting access tube with two-component foam. (J,K) Access-tube enclosure at channel surface. (L) Single-channel temperature logger on cable for suspension in access tube. Foam baffles on either side of logger prevent advection. See text for additional explanation.

of a given magnitude have no measurable effect depends on the period of the fluctuations, the precision and accuracy of the temperature measurements, and the velocity of subsurface fluid flow. For the purely conductive case, the depth D at which daily temperature fluctuations are damped 63% (= $1 - e^{-1}$) is approximately 0.08 m in dry sand and 0.14 m in wet sand (van Wijk and de Vries, 1966b). Damping depths change in direct proportion to the square root of the period of fluctuations. Annual fluctuations thus have damping depths that are roughly 19 times (= $365^{-1/2}$) greater than their diurnal equivalents. Damping depths for annual fluctuations (in the absence of fluid flow) are about 1.5 m in dry sand and 2.7 m in wet sand. Downward movement of water increases the apparent damping depth; similarly, upward movement decreases it. Instruments used for recording temperatures in field installations typically have resolutions ≥0.01 ºC and accuracies ≥0.1ºC. The maximum depth to which annual temperature cycles are resolvable is thus usually about 10-15 meters.

Temperature sensors need to be located within the thermally active zone for studies of surface water-ground water interactions. Depending on the requirements of the study, sensors can be placed at uniform-depth increments, exponentially increasing increments, or according to stratigraphy or other hydrogeologic feature. Multi-dimensional arrays of sensors allow assessment of heterogeneity and lateral flow. Multiple sensors at the same location, possibly of different types, reduce (or expose) uncertainty and provide insurance against sensor failure.

An increasing number of techniques can measure temperature and even thermal properties in field settings. These techniques facilitate the use of heat as a tracer of exchanges between surface water and ground water. As new sensors and data-acquisition systems come onto the market, costs should decrease further while accuracy improves and the variety of instrumental options expands. Thermal techniques will continue to improve understanding of surface water-ground water interactions and other hydrologic processes as well.

Appendix B

Modeling heat as a tracer to estimate streambed seepage and hydraulic conductivity

Richard G. Niswonger and David E. Prudic

Introduction

This appendix focuses on estimating streambed seepage and hydraulic conductivity using numerical model techniques and presents the steps that are normally used in making the estimates. The first part describes several conceptual frameworks for which heat as a tracer has been used to estimate streambed seepage and hydraulic conductivity; the second discusses published U.S. Geological Survey (USGS) numerical models commonly used to model heat as a tracer; the third outlines several approaches for modeling; the fourth describes the importance of observational data in assessing model results; the fifth presents guidelines for model calibration; and the last discusses methods for performing sensitivity analyses and estimating uncertainty.

Numerical models (for example models by Voss, 1984, Kipp, 1987, and Healy and Ronan, 1996) have been developed that solve the equations governing the flow of water and heat through sediments (Stallman, 1965). These models can be used for both gaining and losing streams to estimate streambed seepage and hydraulic conductivity.

Conceptual framework

A conceptual framework is necessary to construct a model for estimating streambed seepage and hydraulic conductivity using temperature data in the stream and in the sediments surrounding the stream. Streambed refers to the sediments that exhibit changes in temperature due to variations in the thermal energy in the stream and the streambed thickness will differ among streams. The application of heat as a tracer provides estimates over a finite volume of space. In all cases, simplifications and assumptions will be made in order to estimate seepage and hydraulic conductivity from temperature measurements. The conceptual framework of water exchange through the streambed will differ depending on the direction of ground-water flow. Surface water usually has greater variations in temperature compared with water in the underlying sediments and consequently, changes in temperature in the streambed are greater for losing streams (Lapham, 1989). Using streambed temperatures beneath gaining streams may require an analysis of other thermal inputs to the stream in addition to the contribution from ground water. Three examples are presented to illustrate common water exchange through the streambed. These examples are differentiated by the dominant direction of flow through the streambed.

Development of a conceptual framework requires a combination of hydrologic intuition and data interpretation. The application of heat as a tracer begins with an initial assessment of the stream and its relation to ground water. A relation can be determined by comparing the elevation of water levels in nearby wells with the elevation of the stream surface (stream stage) and the relation between stream temperatures with temperatures in the streambed. Shallow wells can be installed into or near the streambed to estimate the direction of water exchange across the streambed. Because the stream surface and ground-water elevations may change over short periods of time, measurements of stream surface and ground-water elevations are important during the period when temperatures are being measured.

The first example considers one-dimensional (1d) downward flow through the streambed (fig. 1). Downward flow (or nearly downward flow) through the streambed occurs when the water table is well below the stream and the streambed sediments are not completely saturated or the sediments are saturated but water pressures in the sediments are at or near zero. For streambed sediments that are unsaturated, a downward hydraulic gradient of one can be assumed. However, measuring the water content of the streambed is important. If the ground-water elevation is near the streambed elevation,

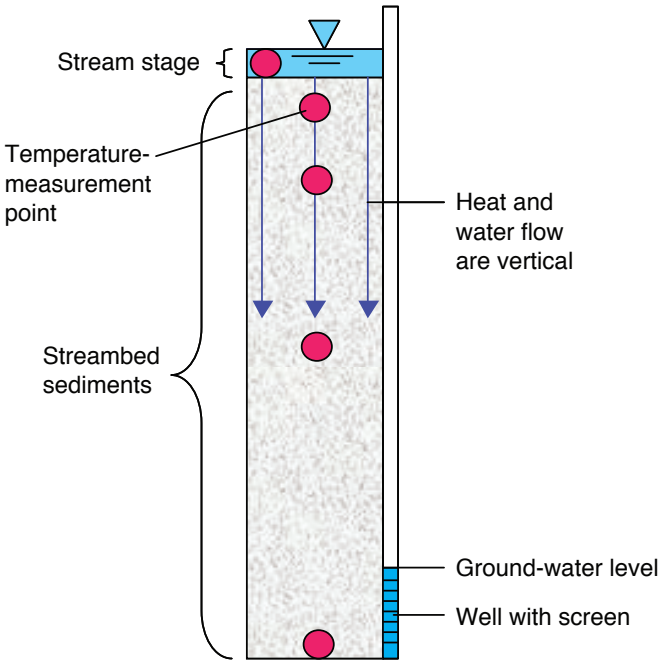

Figure 1. Conceptual framework when flow through streambed is downward.

seepage across the streambed may be mostly downward but the downward hydraulic gradient will need to be determined by measuring the water-level difference between the stream and a well installed beneath the stream.

A numerical model can be used with measured streambed temperatures to test the assumption of downward seepage beneath streams. If the streambed seepage is not downward, then a simple model that assumes only downward flow will not be able to match the measured streambed temperatures and a more complicated conceptual framework will be required.

The second example considers two-dimensional (2d) flow through the streambed that is both outward and downward (fig. 2). This example is used when ground-water levels are near the top of the streambed and hydraulic gradients have both a downward and outward component. Water-level measurements made in shallow wells beneath the stream and along the stream banks can be used to determine the direction of the hydraulic gradient. Seepage may occur in 2d for unsaturated streambeds that have a variety of sediments, which have different water and heat transmitting properties. For this case, it is usually necessary to measure streambed sediment water content or water pressure (negative when unsaturated) to estimate the streambed seepage and hydraulic conductivity.

The third example considers 2d flow through the streambed that is both parallel to the stream and vertically downward (fig. 3). This conceptual framework is used when ground-water levels are near the top of the streambed and the stream is losing flow along its upper reach while gaining flow along its lower reach. This situation occurs commonly in streams from scales of a few meters (for example—between pools and riffles) to many kilometers (for example—where changes in sediment properties or stream gradients force ground water to discharge into the stream).

Streambed seepage and hydraulic conductivity normally are not estimated with three-dimensional (3d) models because available data are not sufficient to refine estimates beyond what can be determined from 1d or 2d models. Public-domain models such as HST3D (Kipp, 1987) are readily available for simulating 3d systems. Three-dimensional flow and transport models have not been used because data collection costs increase exponentially and conceptualization of the flow system becomes much more difficult.

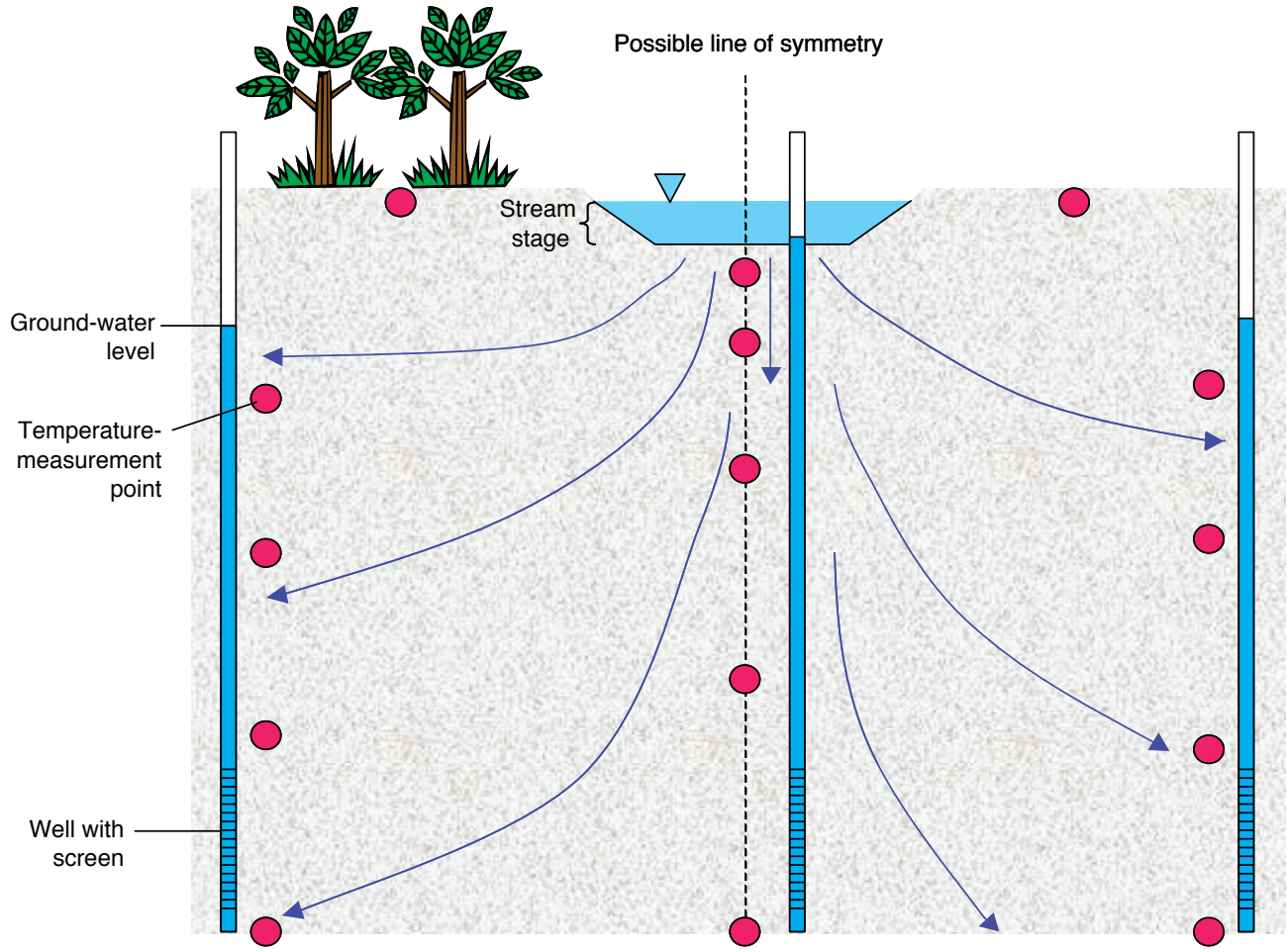

Figure 2. Conceptual framework when flow through streambed is downward and outward.

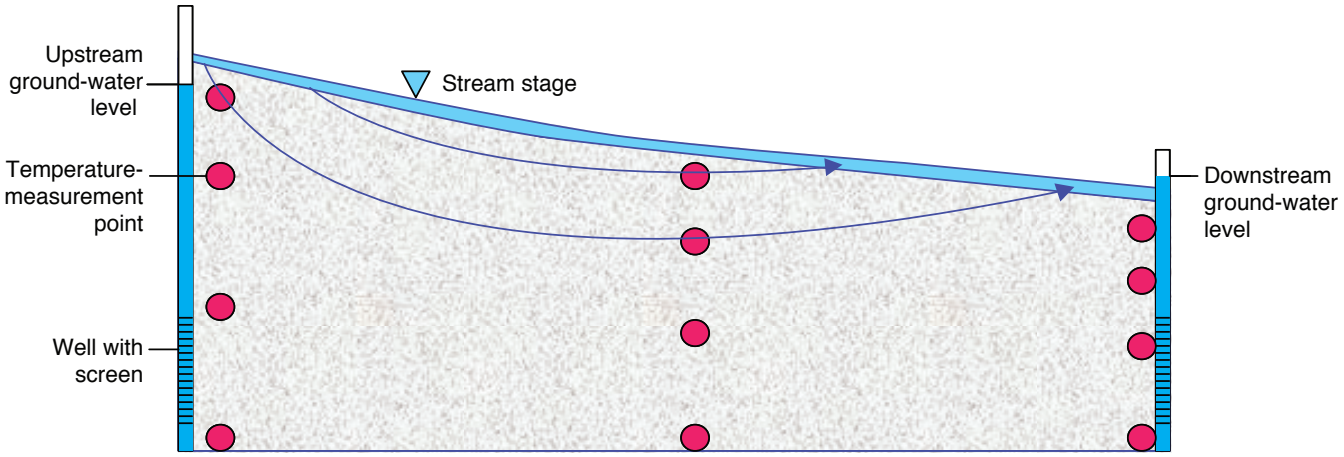

Figure 3. Conceptual framework when seepage through the streambed parallels stream profile.

Model descriptions

Common to all models used for applying heat as a tracer are the governing equations that are solved. These equations include some form of the variably saturated or strictly saturated ground-water flow equation coupled with an energy and/or solute transport equation. Short descriptions of the USGS models VS2DH (Healy and Ronan, 1996) and SUTRA (Voss, 1984), which have been used to estimate streambed seepage and hydraulic conductivity with temperature data, are presented in this section. Each model has detailed documentation that explains how the model can be used to simulate the transport of heat through ground water. All of the models are available free and can be downloaded from the USGS website (http://water.usgs/nrp/gwsoftware/). When using heat as a tracer, the most commonly used model within the USGS is VS2DH. Examples of how heat as a tracer was used with VS2DH are presented by Ronan and others (1998) and Bartolino and Niswonger (2000).

Other ground-water flow and heat transport models may be useful, and warrant consideration, as well. Model selection is based on the desired criteria of interest. For example, if the influence of temperature on streambed biologic activity were a criterion of interest, then an alternative model that has the necessary equations embedded into it would be preferred.

VS2DH

VS2DH is a 2d variably saturated ground-water flow model that was modified to simulate heat transport by advection and conduction (Healy and Ronan, 1996). VS2DH uses an energy transport approach via the advective-dispersion equation (Healy 1990) for simulating heat transport. A Windows-based graphical user interface was developed for VS2DH, called VS2DI (Hsieh and others, 2000). This interface allows the user to quickly develop a model using dialogue boxes and a point and click approach for creating all the needed input information for VS2DH. The post-processing component of VS2DI allows the user to visualize model output for evaluating results. The process of adjusting the hydraulic conductivity until measured and simulated temperatures are in close agreement requires the post processing of model results outside of the VS2DHI environment.

SUTRA

SUTRA is a 2d model that solves the variably saturated fluid density-dependent ground-water flow equation (Voss, 1984). In addition, SUTRA simulates either heat or single species chemically reactive transport. Because of its finite-element construction, SUTRA offers more flexibility than finite difference models. This may be a useful attribute for incorporating variability in streambed surfaces as well as heterogeneity in hydraulic parameters of the subsurface. SUTRA's ability to simulate density-dependent flow makes it a useful model when simulating systems where buoyancy effects are important, such as for large solute or heat gradients. SUTRA, along with a Windows-based graphical user interface and post-processor, can be downloaded from the USGS website.

Building the model

Creating a numerical model of a stream and its streambed involves converting the conceptual framework into input that can be used by the selected model. The input requirement for each model is specific and only general details are provided in this section. The model domain and boundaries for the conceptual frameworks described in figures 1 and 2 are shown in figure 4. The model domain and boundary conditions corresponding to the conceptual framework presented in figure 3 are shown in figure 5.

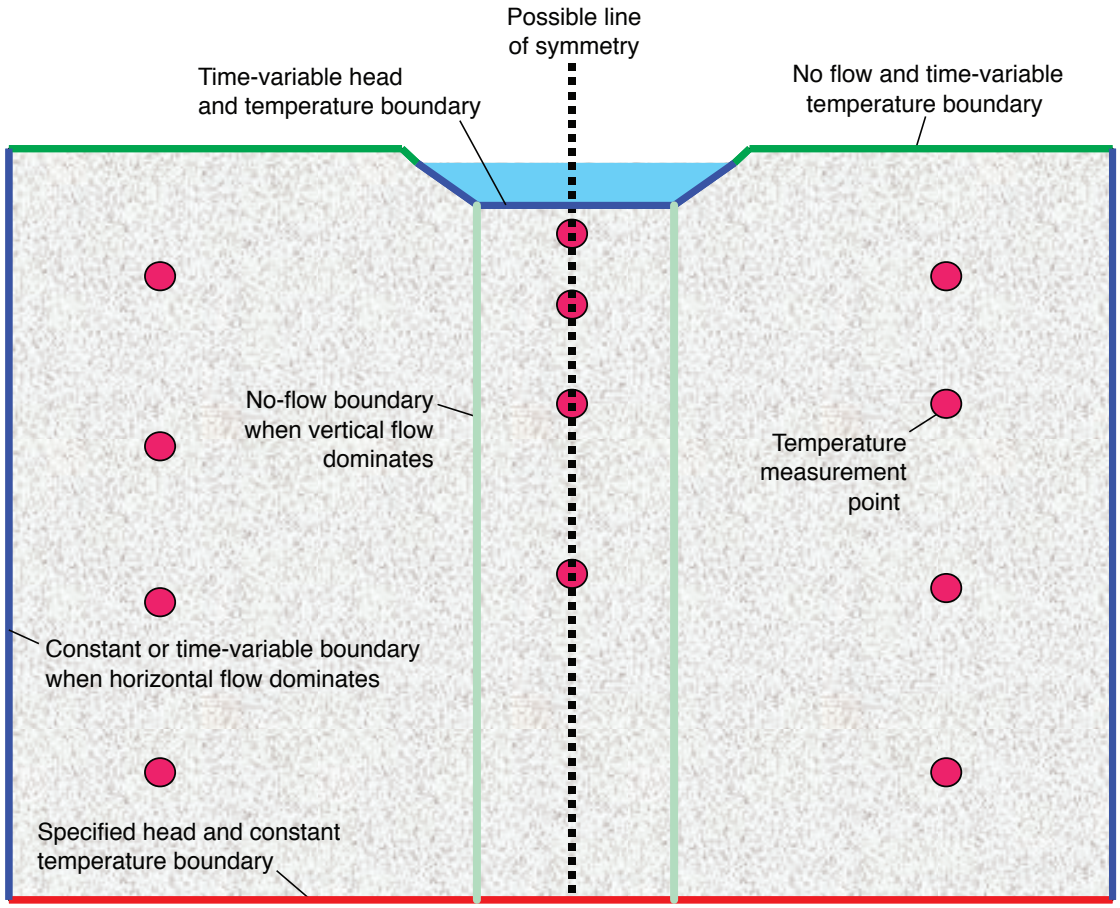

Figure 4. Model domain showing boundary conditions generalized for models of downward and outward flow through the streambed.

Surface boundary

Surface boundary conditions account for heat and water exchange between the stream and streambed. The hydrostatic pressure exerted by the stream on the streambed is represented by a total or pressure head boundary condition. Heat exchange into and out of the stream is modeled by setting the temperature boundary equal to the measured stream-water temperature. In general, surface boundary conditions of the stream will be time varying because both stream temperature and stream stage often vary on an hourly basis.

Surface boundary conditions depend on the dimensionality of the conceptual framework. A 1d model will have only one node that represents the stream boundary condition; however, a 2d model that is perpendicular to the stream (fig. 4) will have several nodes that represent the stream and several nodes that represent the stream bank above the stream stage. Ephemeral streams that lose all their water to the streambed may be dry for part of the simulation period. For sections of the stream that are dry, only a conductive temperature boundary condition is defined equal to the measured temperatures of the dry streambed.

When performing 2d modeling of a stream with fluctuating stream stage, all model nodes that lie below the highest stream stage should be set as a time-dependent total head boundary. This approach avoids activating and deactivating stream boundary nodes every time the water level rises and falls. If the total head applied to a node is less than the elevation of the node, the node will have a negative water pressure, as would be the case for a draining stream bank. Stream bank temperature measurements are used to define the boundary condition along the surface of the model above the stream stage.

Finally, a 2d model that is parallel to the stream (fig. 5) will have several nodes that represent the stream in profile. Each node along the stream profile is represented by a stream stage and temperature boundary. Normally, measured stream stage and water temperature are used to define the boundary conditions at all nodes.

Subsurface boundary conditions

Subsurface boundary conditions also vary depending on the dimensionality of the conceptual framework. A 1d model will have a single node to represent water and heat exchange across the bottom of the model, whereas a 2d model will have a series of nodes (figs. 4 and 5). For the case when the water

table is below the top of the streambed, the bottom of the model can be represented by a zero pressure head boundary and specified temperature equal to the measured temperature at the water table. For the case when the water table is at or near the top of the streambed, the bottom boundary can be set equal to the measured water levels and temperatures in wells. If water flow through the streambed in both 2d models is horizontal, then the bottom boundary can be assigned as no water and heat flow.

The sides of a 1d model are always set for no water or heat flow (fig. 4). Side boundaries of a 2d model are dependent on the hydraulic gradient through the streambed. When the water table is below the top of the streambed, the lateral boundaries for a 2d model perpendicular to the stream (fig. 4) are placed far enough away from the stream so they have no influence on the infiltrating water. The lateral boundaries for a 2d model parallel to the stream are set equal as either water and heat flow or as a specified head and temperature, provided pressure and temperature data are available in the streambed above the water table. When the water table is at or near the top of the streambed, the side boundaries for both 2d models (fig. 4 and 5) are assigned measured water levels and temperatures from wells placed at different depths.

Initial conditions

Initial estimates of head and temperature are needed for every active node inside of the model boundaries. There are two common ways of defining heads and temperatures at all the active nodes: spatial interpolation and simulation.

Point measurements of head and temperature are interpolated to all the nodes in the model spatially. This approach works relatively well if there are enough measurements to define the temperature distribution throughout the model domain. However, this approach can introduce bias into the model results, particularly early in the simulation period. The bias can be explained by comparing the elapsed simulation time to rates of change in simulated temperatures. If the simulation begins with a temperature distribution that matches measured data, then as time passes, the simulated temperatures will continue to be similar to the initial temperatures (called an initial value problem) until the effects of heads and temperatures along the boundaries have propagated throughout the model domain (called a boundary value problem). Consequently, a sufficient time period (a few days for small models and longer for larger models) is needed to estimate the streambed seepage and hydraulic conductivity.

A second approach uses simulated heads and temperatures for defining initial conditions. This approach uses heads and temperatures generated from a model whereby the distribution of heads and temperatures are allowed to come to equilibrium with the model boundaries. The time needed to establish the initial distribution of heads and temperature within the model domain is on the order of the residence time of a packet of water to move through the model. Similar to the first approach, this approach amounts to matching observation data with the model corresponding to times later in the simulation period.

Model parameter data

Modeling water and heat movement through a streambed requires several model parameter values that are specific to the site being analyzed. These parameters are listed in table 1 along with an expected range for stream sediments based on available literature. The most important parameters to estimate accurately before model calibration are the heat capacity and thermal conductivity of the stream sediments. Both of these parameters are a function of the sediment water content.

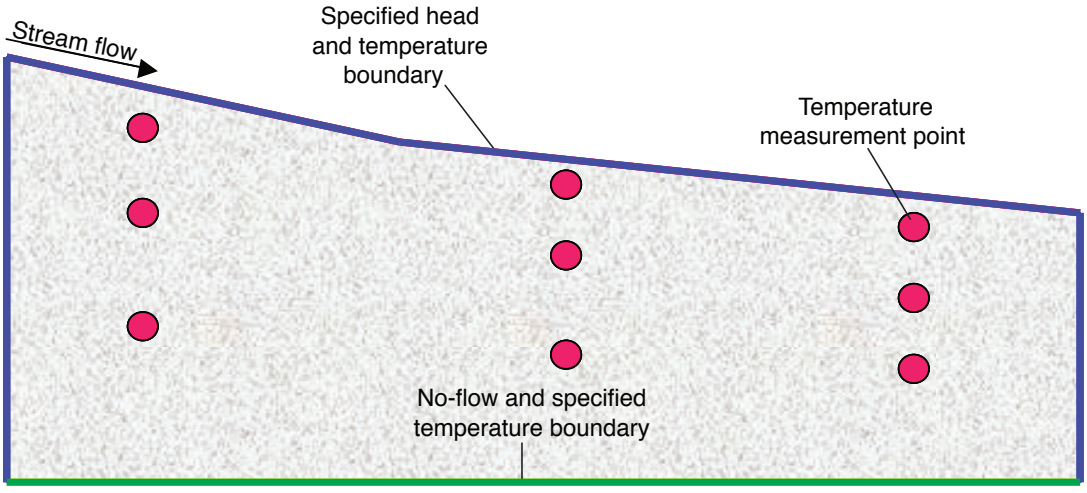

Figure 5. Model domain showing boundary conditions generalized for models of flow through streambeds along a stream profile.

The function that relates the heat capacity to water content can be established using a volume-weighted sum of the heat capacity of water and the dry sediments. Heat capacity of water is a well-known quantity and heat capacity of the dry sediments can be determined based on bulk density and texture of the sediment.

Thermal conductivity is a linear function of water content when sediments are near saturation; however, thermal conductivity is not linear at low water content. Because streambeds often are near saturation for flowing streams, VS2DH assumes a linear relation and requires values for sediment thermal conductivity at residual and saturated water content only. These values can be estimated from the literature based on sediment bulk density and texture. When modeling flow through streambeds with low water content, the thermal conductivity for a range in water content may be determined in the laboratory using core samples.

When monitoring ephemeral streams, temperature measurements often are collected when stream flow is absent. In this case, heat conduction is the dominant process and the sediment thermal parameters can be estimated using automated inverse procedures of conduction only. The automated inverse procedure requires knowledge of the sediment moisture content at the time the temperature measurements were made and only provides a value of the thermal properties of the streambed sediments at the observed water content.

Table 1. Parameters used in VS2DH to model heat as a tracer through fluvial sediments

Parameter	Sensitivity	Range in values
Parameters for saturated flow through fluvial sediments		
Saturated hydraulic conductivity[1] (m/s)	High	10^{-7} to 10^{0}
Horizontal and vertical hydraulic conductivity ratio[1]	High	3 to 100
Porosity[1] (m^3/m^3)	Moderate	0.25 to 0.5
Dispersivity[2] (m)	Moderate	0.01 to 1
Heat capacity of dry sediments[3] ($J/m^3\ ^oC$)	Moderate	1.1×10^6 to 1.3×10^6
Thermal conductivity of saturated sediments ($W/m\ ^oC$)[3]	Moderate	1.4 to 2.2
Heat capacity of water at 20 ^oC [4] ($J/m^3\ ^oC$)	Low	4.2×10^6
Additional parameters for variably saturated flow through fluvial sediments		
Unsaturated hydraulic conductivity parameters in van Genuchten retention model[5]		
α (per meter)	Moderate	1 to 500
n (dimensionless exponent)	Moderate	1.1 to 2.8
Thermal conductivity at residual water content[3] ($W/m\ ^oC$)	Moderate	0.18 to 0.26
Residual water content[5] (m^3/m^3)	Low	0.00 to 0.10

[1] Values are from Freeze and Cherry (1979, p. 29, 32–34, and 37) for silty sand, clean sand and gravel.
[2] Thermal dispersivity is assumed analagous to solute dispersivity. Solute dispersities are from Fetter (1993, p. 71–77) for observation scales between 1 and 10 m.
[3] Values are for sandy, loamy, and clayey soils – see Appendix A, table 1B.
[4] See Appendix A, table 1A.
[5] Values are from Kosugi and others (2002, p. 743) for soils, and from Fayer and others (1992, p. 693) for gravel.

All other model parameters required for using heat as a tracer usually can be estimated based on available literature values such as those listed in table 1 and information on sediment texture. The hydraulic conductivity does not need to be estimated accurately before modeling because it is estimated in the modeling procedure. The modeler needs only to provide the model with an initial guess of the hydraulic conductivity that will be refined in the modeling process based on observation data.

Observation data

For observation data to be used for estimating streambed seepage and hydraulic conductivity, three requirements must be met. First, the observation data (head for saturated streambeds, water content for unsaturated streambeds and streambed temperature) should have small uncertainty. Second, the coordinates of the observation data relative to the stream and other observations and the time of the observations should be known accurately. Third, temperature data should exhibit some spectrum of variation. For the solution to be unique, two aspects of temperature variation need to be simulated, the attenuation of the temperature signal's amplitude and the shift in the temperature signal's phase in the direction of groundwater movement.

Model calibration

The first calibration method is based on trial and error and is most appropriate for simple problems such as homogeneous and isotropic 1d or 2d models. The second method utilizes an automated inverse procedure and is most useful for complex anisotropic and heterogeneous 2d or 3d models. Model calibration in the context of using heat as a tracer usually requires the adjustment of the hydraulic conductivity in such a manner that simulated temperatures in the model match corresponding measured temperatures. Modeling saturated streambeds with fluctuating stream stage and heads may require adjustment of the aquifer specific storage to get a better match between simulated and measured heads.

Obtaining a good match to both the measured head and temperature data (water content for unsaturated streambeds) is necessary for obtaining a reliable estimate of streambed seepage and hydraulic conductivity. Even if the simulated and measured temperatures agree well, any disagreement between the simulated and measured heads (water content) will be compensated by errors in the hydraulic conductivity.

Trial and error modeling

Trial and error calibration consists of making repeated simulations while adjusting the hydraulic conductivity until simulated heads (water content) and temperature match measured heads (water content) and temperatures. An initial streambed hydraulic conductivity is assigned. Following the initial guess, the hydraulic conductivity is adjusted higher or lower depending on the difference between simulated and measured temperatures. If the hydraulic conductivity is too high, the simulated temperature signal will have higher amplitude and a phase that is shifted back in time as compared to the measured temperatures (fig. 6A). If the hydraulic conductivity is too low, the simulated amplitude will be too small and the phase will be shifted forward in time as compared to the measured temperatures (fig. 6B). Figure 6 is for a simple conceptualization of vertical downward flow through homogeneous and isotropic sediments beneath an ephemeral stream (Trout Creek, Nevada; Chapter 8). The best-fit estimate of streambed hydraulic conductivity is 0.42 m/d (fig. 6C) and the good agreement between the measured and simulated temperatures supports the concept of dominantly vertical flow beneath the channel. However, even the best-fit simulation is not perfect as indicated by the less than perfect match in the amplitude and phase of the temperature variations at the 50 cm depth beneath the stream. This error likely results from sediments beneath the channel not being completely homogeneous and isotropic.

Automated inverse procedure

Complex systems require an automated approach because of the large number of different combinations of parameters that could be used to calibrate the model to measured heads (water content) and temperatures. For such systems, a trial and error approach is impractical. The automated inverse procedure adjusts the different parameters through repeated simulations until the process finds the best solution to the observation data. Several computer programs are available that can be used with any models that simulate flow and heat transport. The concepts associated with using automated inverse procedures are basically the same for all programs. The USGS offers a free model independent inverse program called UCODE (Poeter and Hill, 1998) and it can be downloaded from the USGS web page (http://water.usgs/nrp/gwsoftware/). Another commonly used inverse program is called PEST (Doherty, 2002). Both of these inverse programs use an objective function to find the best combination of model parameters by minimizing the sum of the squared deviations between simulated and measured observations as follows:

$$Min\ \varphi = \sum_i \left(Y_i^m - Y_i^o \right)^2$$

where φ is the value of the objective function; Y^m is the measured temperatures or heads; Y^o is the simulated temperatures or heads; and i is a subscript designating the observation number.

Model uncertainty

After streambed seepage and hydraulic conductivity have been estimated, the final step is determining how much uncertainty exists in the estimates. Uncertainty results from all

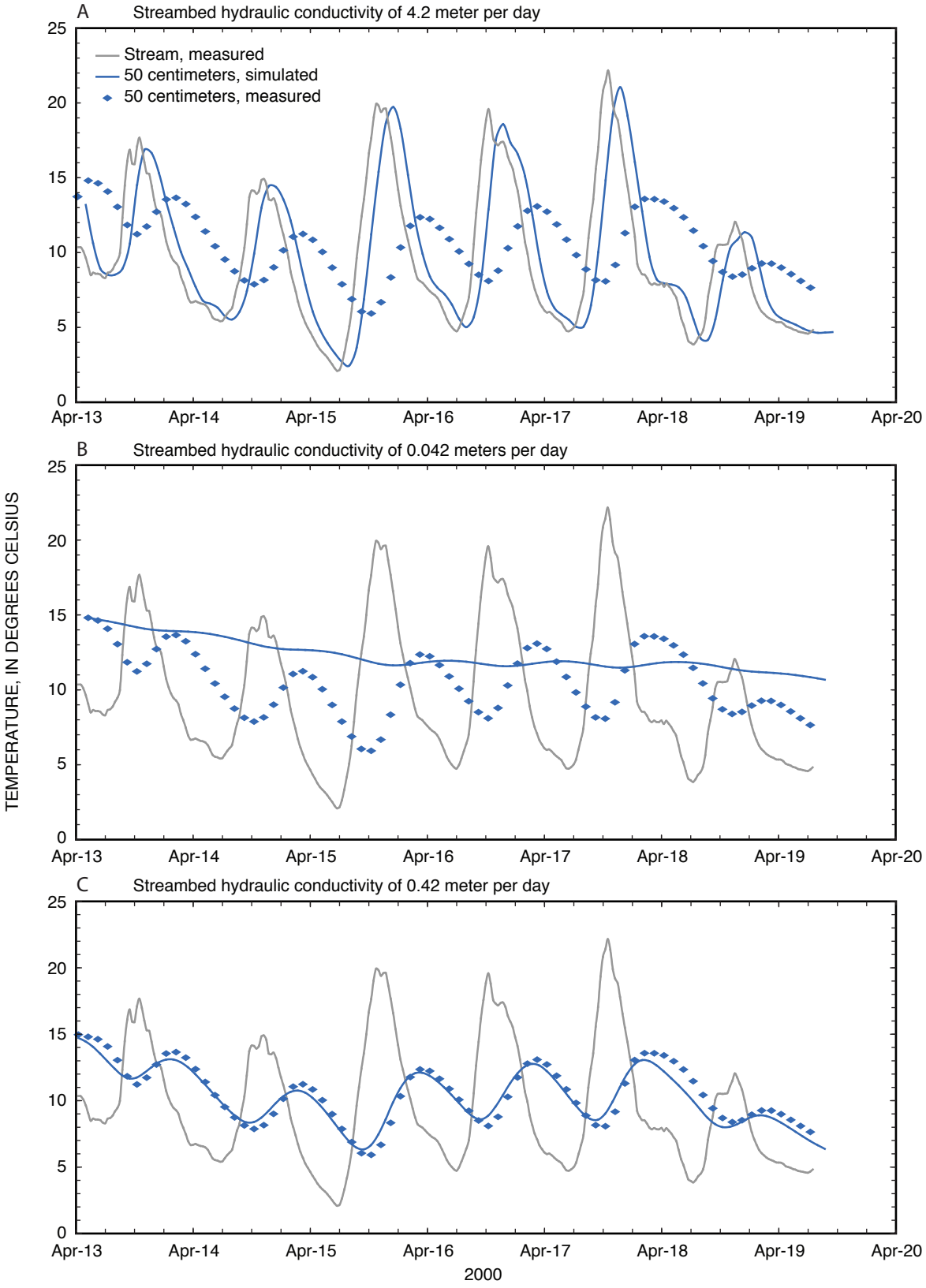

Figure 6. Comparisons of simulated and measured temperatures assuming flow through streambed is downward and the streambed consists of uniform sediments (example is from Trout Creek, Nevada described in Chapter 8). Comparison when: (A) hydraulic conductivity is too high; (B) hydraulic conductivity is too low; and (C) hydraulic conductivity is the best fit to measured data.

the various sources of error that arise in the model formulation of the system being analyzed. The error that is addressed here comes from the uncertainty in all other model parameters other than the parameters being estimated in the model inversion.

The uncertainty that arises due to model input parameters varies depending on the parameter and the system under investigation. Uncertainty in some parameters will have a negligible effect on the solution, whereas others will have a significant effect. Table 1 provides a list of the required parameters for modeling heat as a tracer along with a qualitative description of the impact (low, moderate, or high) each parameter has on modeling results. In general, the most important parameters with respect to uncertainty are the sediment hydraulic parameters. However, the parameters providing the most uncertainty and the magnitude of the uncertainty depend on the system being analyzed and the dynamics of this system. Consequentially, an uncertainty analysis is desirable when using heat as a tracer.

A sensitivity analysis is the simplest method for estimating uncertainty. Model simulations using the maximum and minimum values for each of the input model parameters provide a range in the estimated streambed seepage and hydraulic conductivity. If the range in the hydraulic conductivity and seepage resulting from this exercise is too high, more accurate estimates of, for example, the thermal parameters are required. This type of sensitivity analysis provides a rough estimate of uncertainty and considers uncertainty for each parameter independently.

For complex problems that require more accurate predictions of model uncertainty, a Monte Carlo approach can be used. This approach requires a detailed explanation that is beyond the scope of this paper. A good explanation of the Monte Carlo method is described by de Marsily (1986) and an example of this method being applied to determine uncertainty in inverse solutions using heat as a tracer is presented by Niswonger and Rupp (2000). A list of available documentation for USGS ground-water models, along with compiled models, may be retrieved from http://water.usgs.gov/nrp/gwsoftware.

References

Anderholm, S.K., 1997, Water-quality assessment of the Rio Grande valley, Colorado, New Mexico, and Texas—shallow ground-water quality and land use in the Albuquerque area, central New Mexico, 1993: U.S. Geological Survey Water-Resources Investigations Report 97-4067, 73 p.

Anderson, S.R., 1987, Cenozoic stratigraphy and geologic history of the Tucson basin, Pima County, Arizona: U.S. Geological Survey Water-Resources Investigations Report 87-4190, 20 p.

ASTM, 1993, Annual book of ASTM standards, vol. 14.03—temperature measurement: West Conshohocken, Pa., American Society for Testing and Materials, 502 p.

Bailey, M.A., Ferre, P.A., and Hoffmann, J.P., 2000a, Numerical simulation of measured streambed-temperature profiles and soil hydraulic properties to quantify infiltration in an ephemeral stream [abs.]: EOS, Transactions, American Geophyical Union, v. 81, p. F501–F502.

Bailey, M.A., Hoffmann, J.P., and Ferre, P.A., 2000b, Investigation of subsurface variations to quantify infiltration in an ephemeral stream, Tucson, Arizona [abs.]: Geological Society of America Abstracts with Programs, v. 32, p. A-185.

Bartolino, J.R., and Cole, J.C., eds., 2002, Ground-water resources of the Middle Rio Grande Basin, New Mexico: U.S. Geological Survey Circular 1222, 132 p.

Bartolino, J.R., and Constantz, J., 2002, How mountain-front recharge is studied, *in* Bartolino, J.R., and Cole, J.C., eds., Ground-water resources of the Middle Rio Grande Basin, New Mexico: U.S. Geological Survey Circular 1222, p. 74–75.

Bartolino, J.R., and Niswonger, R.G., 1999, Numerical simulation of vertical ground-water flux of the Rio Grande from ground-water temperature profiles, central New Mexico: U.S. Geological Survey Water-Resources Investigations Report 99-4212, 34 p.

Bartolino, J.R., 2002, How we have examined ground-water/surface-water interaction of the Rio Grande, *in* Bartolino, J.R., and Cole, J.C., eds., Ground-water resources of the Middle Rio Grande Basin, New Mexico: U.S. Geological Survey Circular 1222, p. 78–79.

Bencala, K.E., Kennedy, V.C., Zellweger, G.W., Jackman, A.P., and Avanzino, R.J., 1984, Interaction of solutes and streambed sediments, 1 An experimental analysis of cation and anion transport in a mountain stream: Water Resources Research, v. 20, p. 1797–1803.

Blasch, K.W., Fleming, J.B., Ferre, P.A., and Hoffmann, J.P., 2000, One- and two-dimensional temperature and moisture-content profiling of an ephemeral stream channel in a semiarid watershed [abs]: EOS, Transactions, American Geophyical Union, v. 81, p. F502.

Bristow, K.L., Kluitenberg, G.J., and Horton, R., 1994, Measurement of soil thermal properties with a dual-probe heat-pulse technique: Soil Science Society of America Journal, v. 58, p. 1288–1294.

Bouyoucos, G., 1915, Effects of temperature on some of the most important physical process in soils: Mich. Coll. Ag. Tech. Bull. 24, 63 p.

Bredehoeft, J.D., and Papadopulos, I.S., 1965, Rates of vertical groundwater movement estimated from earth's thermal profile: Water Resources Research, v. 1, p. 325–328.

Buckingham, E., 1907, Studies on the movement of soil moisture: U.S. Department of Agriculture Bureau of Soils Bull. No. 38, 61 p.

Bullard, T.F., and Wells, S.G., 1992, Hydrology of the Middle Rio Grande from Velarde to Elephant Butte Reservoir, New Mexico: U.S. Department of the Interior Fish and Wildlife Service Resource Publication 179, 51 p.

Burkham, D.E., 1970, Depletion of streamflow by infiltration in the main channels of the Tucson basin, southeastern Arizona: U.S. Geological Survey Water-Supply Paper 1939-B, 36 p.

Byron, E.R., and Goldman, C.R., 1989, Land-use and water quality in tributary streams of Lake Tahoe, California-Nevada: Journal of Environmental Quality, v. 18, p. 84–88.

Campbell, G.S., Calissendorff, K., and Williams, J.H., 1991, Probe for measuring soil specific heat using a heat-pulse method: Soil Science Society of America Journal, v. 55, p. 291–293.

Carslaw, H.S., and Jaeger, J.C., 1959, Conduction of Heat in Solids (2nd ed.): New York, Oxford University Press, 510 p.

Cartwright, K., 1974, Tracing shallow groundwater systems by soil temperature: Water Resources Research, v. 10, p. 847–855.

City of Albuquerque Public Works Department, 1997, City of Albuquerque water resources management strategy: Albuquerque, N. Mex., City of Albuquerque Public Works Department, Water Resources, 38 p.

Constantz, J., 1982, Temperature dependence of unsaturated hydraulic conductivity of two soils: Soil Science Society of America Journal, v. 26, p. 466–470.

Constantz, J., 1983, Laboratory analysis of water retention in unsaturated zone materials at high temperatures, *in* Mercer, ed., The role of the unsaturated zone in radioactive and hazardous waste disposal: Ann Arbor, Mich., Ann Arbor Press, p. 147–164.

Constantz, J., 1998, Interaction between stream temperature, streamflow, and groundwater exchanges in alpine streams: Water Resources Research, v. 34, p. 1609–1616.

Constantz, J., Cox, M., Sarma, L., and Mendez, G., 2000, Comparison of heat and bromide as tracers of stream/groundwater exchanges during a surfacewater bromide injections [abs.]: Geological Society of America Abstracts with Programs, v. 32, p. A-405.

Constantz, J., Herkelrath, W.N., and Murphy, F., 1988, Air encapsulation during infiltration: Soil Science Society of America Journal, v. 52, p. 10–16.

Constantz, J., and Murphy, F., 1991, Temperature dependence of ponded infiltration under isothermal conditions: Journal of Hydrology, v. 122, 119–128.

Constantz, J., Stonestrom, D.A., Stewart, A.E., Niswonger, R.G., and Smith, T.R., 2001, Analysis of streambed temperatures in ephemeral channels to determine streamflow frequency and duration: Water Resources Research, v. 37, p. 317–328.

Constantz, J., and Thomas, C.L., 1996, The use of streambed temperature profiles to estimate the depth, duration, and rate of percolation beneath arroyos: Water Resources Research, v. 32, p. 3597–3602.

Constantz, J., and Thomas, C.L., 1997, Streambed temperature profiles as indicators of percolation characteristics beneath arroyos in the Middle Rio Grande Basin, USA: Hydrological Processes, v. 11, p. 1621–1634.

Constantz, J., Thomas, C.L., and Zellweger, G., 1994, Influence of diurnal variations in stream temperature on streamflow loss and groundwater recharge: Water Resources Research, v. 30, p. 3253–3264.

CSIRO, 1998, Handbook of Temperature Measurement: New York, Springer Verlag, 3 vol., 400 p.

Davidson, E.S., 1973, Geohydrology and water resources of the Tucson basin, Arizona: U.S. Geological Survey Water-Supply Paper 1939-E, 81 p.

de Marsily, Ghislain, 1986, Quantitative Hydrogeology: New York, Academic Press Inc., 440 p.

de Vries, D.A., 1952, A non-stationary method for determining thermal conductivity of soil in situ: Soil Science, v. 73, p. 83–89.

_____1966, Thermal properties of soils, *in* van Wijk, W.R., ed., Physics of plant environment (2nd ed.): Amsterdam, North-Holland Publishing Co., p. 210–235.

Doherty, John, 2002, Manual for PEST (5th ed): Brisbane, Australia, downloadable from www.sspa.com/pest.

Faybishenko, B., 2000, Vadose zone characterization and monitoring, *in* Looney, B.B., and Falta, R.W., eds., Vadose zone science and technology solutions: Columbus, Ohio, Battelle Press, p. 133–395.

Fayer, M.J., Rockhold, M.L., and Campbell, M.D., 1992, Hydrologic modeling of protective barriers—comparison of field data and simulation results: Soil Science Society of America Journal, v. 56, p. 690–700.

Fetter, C.W., 1993, Contaminant hydrogeology: New York, Macmillan Publishing Company, 458 p.

Finch, D.I., 1962, General principles of thermoelectric thermometry, *in* Herzfeld, C.M., ed., Temperature, its measurement and control in science and industry: New York, Reinhold Pub. Corp. (joint publication of the American Institute of Physics, Instrument Society of America, and National Bureau of Standards), p. 3–32.

Freeze, R.A., and Cherry, J.A., 1979, Groundwater: Englewood Cliffs, N.J., Prentice-Hall, 604 p.

Garcia-Diaz, A., and Phillips, D.T., 1995, Principles of experimental design and analysis: London, Chapman & Hall, 409 p.

Goldman, C.R., 1988, Primary productivity, nutrients, and transparency during the early onset of eutrophication in ultra-oligotrophic Lake Tahoe, California-Nevada: Limnology and Oceanography, v. 33, p. 1321–1333.

Goldman, C.R., and Byron, E.R., 1986, Changing water quality at Lake Tahoe—The first five years of the Lake Tahoe Interagency Monitoring Program: Davis, Calif., Tahoe Research Group, University of California, Davis, 12 p.

Halupka, K.C., Bryant, M.D., Willson, M.F., and Everest, F.H., 2000, Biological characteristics and population status of anadromous salmon in southeast Alaska: Portland, Oreg., U.S. Department of Agriculture, Forest Service, Pacific Northwest Research Station, General Technical Report PNW-GTR-468, 265 p.

Hanson, R.T., and Benedict, J.F., 1994, Simulation of groundwater flow and potential land subsidence, upper Santa Cruz basin, Arizona: U.S. Geological Survey Water-Resources Investigations Report 93-4196, 47 p.

Healy, R.W., 1990, Simulation of solute transport in variably saturated porous media with supplemental information on modification of the U.S. Geological Survey's computer program VS2D: U.S. Geological Survey Water-Resources Investigations Report 90-4025, 125 p.

Healy, R.W., and Ronan, A.D., 1996, Documentation of the Computer Program VS2DH for Simulation of Energy Transport in Variably Saturated Porous Media—Modification of the U.S. Geological Survey's Computer Program VS2DT: U.S. Geological Survey Water-Resources Investigation Report 96-4230, 36 p.

Herzfeld, C.M., 1962, Temperature, its measurement and control in science and industry: New York, Reinhold Pub. Corp. (Joint publication of the American Institute of Physics, Instrument Society of America, and National Bureau of Standards), 3 volumes, variously paginated.

Hewlett-Packard, 1983, Practical temperature measurements—application note 290: Palo Alto, Calif., Agilent Technologies, Inc., 32 p.

Hopmans, J.W., Simunek, J., and Bristow, K.L., 2002, Indirect estimation of soil thermal properties and water flux using heat pulse probe measurements—Geometry and dispersion effects: Water Resources Research, v. 38, p. 7-1 to 7-14.

Horowitz, P., and Hill, W., 1989, The art of electronics (2nd ed.): New York, Cambridge University Press, 1125 p.

Hsieh, P.A., Wingle, W., and Healy, R.W., 2000, VS2DI—A graphical software package for simulating fluid flow and solute or energy transport through variably saturated porous media: U.S. Geological Survey Water-Resources Investigations Report 99-4130, 16 p.

Jackson, R.D., and Taylor, S.A., 1986, Thermal conductivity and diffusivity, *in* Black, C.A., ed., Methods of soil analysis, part 1 physical and mineralogical methods (2nd ed.): Madison, Wis., American Society of Agronomy, p. 945–956.

Jaynes, D.B., 1990, Temperature variations effects on field measured infiltration: Soil Science Society of America Journal, v. 54, p. 305–312.

Jury, W.A., Gardner, W.R., and Gardner, W.H., 1991, Soil physics (5th ed.): New York, J. Wiley, 328 p.

Kalin, R.M., 1994, The hydrogeochemical evolution of the groundwater of the Tucson basin with application to 3 dimensional groundwater flow modeling: Tucson, Ariz., University of Arizona, Ph.D. dissertation, 510 p.

Kant, H., 1984, Gabriel Daniel Fahrenheit, Renâe-Antoine Ferchault de Râeaumur, Anders Celsius: Leipzig, B.G. Teubner, 133 p.

Katz, L.T., 1987, Steady state infiltration processes along the Santa Cruz and Rillito Rivers: Tucson, Ariz., University of Arizona, unpublished M.S. thesis, 119 p.

Kernodle, J.M., McAda, D.P., and Thorn, C.R., 1995, Simulation of ground-water flow in the Albuquerque Basin, central New Mexico, 1901–1994, with projections to 2020: U.S. Geological Survey Water-Resources Investigations Report 94-4251, 114 p.

Kipp, K.L., 1987, HST3D—A computer code for simulation of heat and solute transport in three-dimensional groundwater systems: U.S. Geological Survey Water Resources Investigations Report 86-4095, 517 p.

Klock, F.G.J., and Sullivan, J.J., 1962, Precision resistance thermometers as calibration standards, *in* Herzfeld, C.M., ed., Temperature, its measurement and control in science and industry: New York, Reinhold Pub. Corp., p. 329–335.

Kluitenberg, G.J., Bristow, K.L., and Das, B.S., 1995, Error analysis of heat pulse method for measuring soil heat capacity, diffusivity, and conductivity: Soil Science Society of America Journal, v. 59, p. 719–726.

Kosugi, K., Hopmans, J.W., and Dane, J.H., 2002, Parametric models, *in* Dane, J.H., and Topp, G.C., eds., Methods of soil analysis, part 4, physical methods: Madison, Wis., Soil Science Society of America, Inc., p. 739–757.

Lane, L.J., 1983, Transmission losses, sec. 4, chap. 19 of National engineering handbook, U.S. Department of Agriculture, Soil Conservation Service, 21 p.

Lapham, W.W., 1988, Conductive and convective heat transfer in sediments near streams: Tucson, Ariz., University of Arizona, Ph.D. dissertation, 315 p.

Lapham, W.W., 1989, Use of temperature profiles beneath streams to determine rates of vertical ground-water flow and vertical hydraulic conductivity: U.S. Geological Survey Water-Supply Paper 2337, 35 p.

LeCain, G.D., Lu, N., and Kurzmack, M., 2002, Use of temperature, pressure, and water potential data to estimate infiltration and monitor percolation in Pagany Wash associated with the winter of 1997-98 El Nino precipitation, Yucca Mountain, Nevada: U.S. Geological Survey Water-Resources Investigations Report 02-4035, 25 p.

Lee, D.R., and Cherry, J.A., 1978, A field exercise on groundwater flow using seepage meters and mini-piezometers: Journal of Geological Education, v. 27, p. 6–10.

Lewis, A.C., 2000, Seepage study for the Santa Fe River: Santa Fe, N. Mex., Sangre de Cristo Water Division, Miscellaneous Report Series, 4 p.

Lienhard, J.H., and Layton, E.T., 1988, History of heat transfer—essays in honor of the 50th anniversary of the ASME Heat Transfer Division: New York, American Society of Mechanical Engineers, 260 p.

Matlock, W.G., and Davis, P.R., 1972, Groundwater in the Santa Cruz Valley, Arizona: Tucson, Ariz., University of Arizona Agricultural Experiment Station Technical Bulletin 232, 59 p.

Morris, B., 2002, Temperature calibration is critical to product quality, regulatory compliance: Control Solutions, v. 75, no. 6, p. 22–24.

Morrison, R., 1998, Grounding and shielding techniques (4th ed.): New York, John Wiley and Sons, Inc., 201 p.

Nielsen, D., and Sara, M.N., 1992, Current practices in ground water and vadose zone investigations: Philadelphia, American Society of Testing and Materials (ASTM), 431 p.

Nightingale, H.I., 1975, Groundwater recharge rates from thermometry: Ground Water, v. 18, p. 340–344.

Nimmo, J.R., and Miller, E.E., 1986, The temperature dependence of isothermal moisture-vs.-potential characteristics of soils: Soil Science Society of America Journal, v. 50, p. 1105–1113.

Niswonger, R.G., 2001, Assessing streamflow processes in mountain front streams using surface/groundwater modeling: Reno, Nev., University of Nevada, Reno, unpublished M.S. thesis, 91 p.

Niswonger, R.G., and Constantz, J., 2001, Determination of streamflow loss to estimate mountain-front recharge at Bear Canyon, New Mexico, *in* Cole, J.C., ed., U.S. Geological Survey Middle Rio Grande Basin Study—Proceedings of the Fourth Annual Workshop, Albuquerque, New Mexico, February 15–16, 2000: U.S. Geological Survey Open-File Report 00-488, p. 38–40.

Niswonger, R.G., and Rupp, J.L., 2000, Monte Carlo analysis of streambed seepage rates, *in* Wigington, P.J., and Beschta, R.C., eds., International Conference on Riparian Ecology and Management in Multi-land Use Watersheds, Portland, Oreg., August 2000, Proceedings: Middleburg, Va., American Water Resources Association, p. 161–166.

Noborio, K., McInnes, K.J., and Heilman, J.L., 1996, Measurements of soil water content, heat capacity, and thermal conductivity with a single TDR probe: Soil Science, v. 161, p. 22–28.

Paluch, R., 2002, Field installation of thermocouple and RTD temperature sensor assemblies: Sensors, v. 19, no. 8, p. 18–27.

Phillips, J.R., and D.A. deVries, 1956, Moisture movement in porous materials under temperature gradients, EOS, Transactions, American Geophysical Union, v. 38, p. 222–232.

Poeter, E.P., and Hill, M.C., 1998, Documentation of UCODE, a computer code for universal inverse modeling: U.S. Geological Survey Water-Resources Investigations Report 98-4080, p. 116.

Pruess, K., Oldenburg, C., and Moridis, G., 1999, TOUGH2 User's Guide, Version 2.0: Berkeley, Calif., Lawrence Berkeley National Laboratory Report LBNL-43134, 196 p.

Ren, T., Kluitenberg, G.J., and Horton, R., 2000, Determining soil water flux and pore water velocity by a heat pulse technique: Soil Science Society of America Journal, v. 64, p. 552–560.

Ren, T., Noborio, K., and Horton, R., 1999, Measuring soil water content , electrical conductivity and thermal properties with a thermo-TDR probe: Soil Science Society of America Journal, v. 63, p. 450–457.

Reuter, J.E., Jassby, A.D., Marjanovic, P., Heyvaert, A.C., and Goldman C.R., 1998, Preliminary phosphorus and nitrogen budgets for Lake Tahoe, annual progress report-1998—lake clarity and watershed modeling, presidential deliverable: Davis, Calif., Tahoe Research Group, John Muir Institute for the Environment, Department of Civil and Environmental Engineering, University of California, Davis, 28 p.

Reuter, J.E., and Miller, W.W., 2000, Aquatic resources, water quality, and limnology of Lake Tahoe and its upland watershed, chap. 4 *of* Lake Tahoe watershed assessment: U.S. Department of Agriculture, Forest Service General Technical Report PSW-GTR-175, 735 p.

Richards, L.A., 1931, Capillary conduction of liquids through porous mediums: Physics, v. 1, p. 318–333.

Riggs, H.C., 1972, Low-flow investigations: U.S. Geological Survey Techniques of Water-Resources Investigations, book 4, chap. B1, 18 p.

Ronan, A.D., Prudic, D.E., Thodal, C.E., and Constantz, J., 1998, Field study and simulation of diurnal temperature effects on infiltration and variably saturated flow beneath an ephemeral stream: Water Resources Research, v. 34, no. 9, p. 2137–2152.

Rorabaugh, M.I., 1954, Streambed percolation in development of water supplies, U.S. Geological Survey Groundwater Notes on Hydraulics No. 25, 13 p.

Rowe, T.G., Saleh, D.K., Watkins, S.A., and Kratzer, C.R., 2002, Streamflow and water-quality data for selected watersheds in the Lake Tahoe Basin, California and Nevada, through September 1998: U.S. Geological Survey Water-Resources Investigations Report 02-4030, 118 p.

Samuels, E.A., 1968, Convective flow and its effect on temperature logging in small-diameter wells: Geophysics, v. 33, p. 1004–1012.

Scanlon, B.R., and Milly, P.C.D., 1994, Water and heat fluxes in desert soils, 2, numerical simulations: Water Resources Reserach, v. 30, p. 721–733.

Schooley, J.F., ed., 1982, Temperature, its measurement and control in science and industry: New York, American Institute of Physics, 1395 p.

Scurlock, D., 1998, An environmental history of the Middle Rio Grande Basin: Fort Collins, Colorado, U.S. Department of Agriculture Forest Service General Technical Report RMRS-GTR-5, 440 p.

Sheingold, D.H., 1980, Transducer Interfacing Handbook: Norwood, Massachusetts, Analog Devices, Inc., 231 p.

Shiozwa, S., and Campbell, G.S., 1990, Soil thermal conductivity: Remote Sensing Reviews, v. 5, p. 301–310.

Silliman, S.E., and Booth, D.F., 1993, Analysis of time-series measurements of sediment temperature for identification of gaining vs. losing portions of Juday Creek, Indiana: Journal of Hydrology, v. 146, p. 131–148.

Silliman, S.E., Ramirez, J., and McCabe, R.L., 1995, Quantifying downflow through creek sediments using temperature time series; one-dimensional solution incorporating measured surface temperature: Journal of Hydrology, v. 167, p. 99–119.

Sorey, M.L., 1971, Measurement of vertical groundwater velocity from temperature profiles in a well: Water Recources Research, v. 7, p. 963–970.

Stallman, R.W., 1963, Methods of collecting and interpreting ground-water data, U.S. Geolological Survey Water-Supply Paper 1544-H, p. 36–46.

Stallman, R.W., 1965, Steady one-dimensional fluid flow in a semi-infinite porous medium with sinusoidal surface temperature, Journal of Geophysical Research, v. 70, p. 2821–2827.

Star, P.v.d., 1983, Fahrenheit's letters to Leibniz and Boerhaave: Leiden, Netherlands, Museum Boerhaave, 195 p.

Stewart, A.E., and Constantz, J., 2001, Determination of streamflow patterns to estimate stream loss along Abo Arroyo, New Mexico, *in* Cole, J.C., ed., U.S. Geological Survey Middle Rio Grande Basin Study—Proceedings of the Fourth Annual Workshop, Albuquerque, New Mexico, February 15-16, 2000: U.S. Geological Survey Open-File Report 00-488, p. 35–37.

Stonestrom, D.A., and Rubin, J., 1989, Air permeability and trapped-air content in two soils: Water Resources Research, v. 25, p. 1959–1969.

Suzuki, S., 1960, Percolation measurements based on heat flow through soil with special reference to paddy fields: Journal of Geophysical Research, v. 65, p. 2883–2885.

Tahoe Regional Planning Agency, 2002, Mission statement, accessed December 12, 2002, at URL http://www.trpa.org/Mission.htm/

Tahoe Regional Planning Agency, and U.S. Forest Service, 1971, Geology and geomorphology of the Lake Tahoe region—A guide for planning: South Lake Tahoe, Calif., 59 p.

Taylor, S.A., and Jackson, R.D., 1986, Heat capacity and specific heat, *in* Black, C.A., ed., Methods of soil analysis, part 1 physical and mineralogical methods (2nd ed.): Madison, Wis., American Society of Agronomy, p. 941–944.

Thomas, C.L., Stewart, A.E., and Constantz, J., 2000, Comparison of methods to determine infiltration rates along a reach of the Santa Fe River near La Bajada, New Mexico: U.S. Geological Survey Water-Resources Investigation Report 00-4141, 65 p.

USEPA, 2000, Guidance for Data Quality Assessment: U.S. Environmental Protection Agency Office of Environmental Information, 219 p.

van der Kamp, G., and Bachu, S., 1989, Use of dimensional analysis in the study of thermal effects of various hydrogeological regimes, *in* Garven, G., Stegena, L., and Beck, A.E., eds., Hydrogeological regimes and their subsurface thermal effects (Geophysical Monograph No. 47): Washington, D.C., American Geophysical Union, p. 23–28.

Van Duin, R.H.A., 1963, The influence of management on the temperature wave near the surface: Wageningen, Netherlands, Wageningen Institute of Land and Water Management, Technical Bulletin No. 29, 21 p.

van Wijk, W.R., and de Vries, D.A., 1966a, The atmosphere and the soil, *in* van Wijk, W.R., ed., Physics of plant environment (2nd ed.): Amsterdam, North-Holland Publishing Co., p. 17–61.

_____1966b, Periodic temperature variations, *in* van Wijk, W.R., ed., Physics of plant environment (2nd ed.): Amsterdam, North-Holland Publishing Co., p. 102–143.

Voss, C.I., 1984, A finite-element simulation model for saturated-unsaturated, fluid-density-dependent ground-water flow with energy transport or chemically-reactive single-species solute transport: U.S. Geological Survey Water-Resources Investigations Report 84-4369, 409 p.

Watermark Numerical Computing, 1998, PEST—Model independent parameter estimation, version Pest98: Brisbane, Australia.

Wierenga, P.J., Nielsen, D.R., and Hagan, R.M., 1969, Thermal properties of a soil based upon field and laboratory measurements: Soil Science Society of America Proceedings, v. 33, p. 354–360.

Willden, R., 1964, Geology and mineral deposits of Humboldt County, Nevada: Reno, Nev., Nevada Bureau of Mines and Geology Bulletin 59, 154 p.

Winter, T. C., Harvey, J.W., Franke, O.L., and Alley, W.M., 1998, Ground water and surface water, a single resource, U.S. Geological Survey Circular 1139, 79 p.

USGS

Heat as a tool for studying the movement of ground water near streams

Printed on recycled paper

ISBN = 0-607-94071-9